

# Electric Pulse Aided Bending: An Experimental Study

Sachin Kumar

A Thesis Submitted to  
Indian Institute of Technology Hyderabad  
In Partial Fulfillment of the Requirements for  
The Degree of Master of Technology



भारतीय प्रौद्योगिकी संस्थान हैदराबाद  
Indian Institute of Technology Hyderabad

Department of Mechanical and Aerospace Engineering

July 2017

## Declaration

I declare that this written submission represents my ideas in my own words, and where ideas or words of others have been included, I have adequately cited and referenced the original sources. I also declare that I have adhered to all principles of academic honesty and integrity and have not misrepresented or fabricated or falsified any idea/data/fact/source in my submission. I understand that any violation of the above will be a cause for disciplinary action by the Institute and can also evoke penal action from the sources that have thus not been properly cited, or from whom proper permission has not been taken when needed.

Sachin

(Signature)

July, 19, 2017

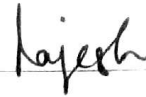
(Sachin Kumar)

ME15MTECH11014

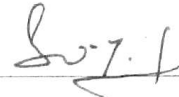
(Roll No.)

## Approval Sheet

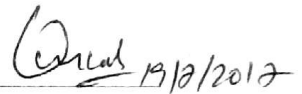
This Thesis entitled Electric Pulse Aided Bending: An Experimental Study by Sachin Kumar is approved for the degree of Master of Technology from IIT Hyderabad.



(Dr. Rajesh Korla) Examiner  
Dept. of Materials Science and Metallurgical Engineering  
IITH



(Dr. S. Suryakumar) Examiner  
Dept. Mechanical and Aerospace Engineering  
IITH



(Dr. N. Venkata Reddy) Adviser  
Dept. of Mechanical and Aerospace Engineering  
IITH

## Acknowledgements

I would like to express my sincere gratitude to my advisor Prof. N. Venkata Reddy for his continuous support, motivation while my M.Tech. study and project work. His guidance helped me during my project work and writing of this thesis report. I am indebted to him for his technical and professional advice.

Besides my advisor, I would like to thank Mr. Ramu G, Technical Superintendent at central workshop, for coming up with idea of bend fixture design and conducting the fabrication process in workshop. I would also like to thank Mr. Ramesh, project staff at central workshop as well as other staff members of workshop for helping me in fabrication of the bend fixture. I would like to thank K.Basveshwara, Project Staff at Manufacturing Science Lab, for his help and assistance while performing the experiments.

I would like to thank Rakesh Lingam Ph.D. scholar for his valuable advises and technical support. I would to thank Adabala Subrahmanyam and Praveen Konka Ph.D. scholars for their help and valuable advises while performing experiments. I would also like to Kale Rakesh Shridhar Ph.D. scholar for providing his help to create image processing code in Matlab. I personally thank my mate Upendra Singh for his suggestions and support during project work and while preparation of this document and proofreading.

This work is done in the project funded by Uchchatar Avishkar Yojana (UAY), Government of India. I am thankful to Ministry of Human Resource Development (MHRD) Government of India, Ministry of Heavy Industries and Public Enterprises Government of India, and TATA Steel for supporting through UAY.

At last, I would like to thank my family: my parents, for providing me moral and spiritual support throughout my life.

**Sachin Kumar**



# Abstract

Sheet Metal Forming is used in major manufacturing like Automotive and Aerospace industries for producing various parts. Materials with low forming limit and high springback cannot be formed using this process without inducing failure and geometrical inaccuracies into the parts. Whereas materials with higher formability can be deformed to a larger extent before failure as compared to lower formability materials. The elastic recovery of the sheet metal after the forming process commonly known as springback which causes geometrical inaccuracies. Materials like Ti-alloys, with higher strength possess low formability and higher springback but also they provide advantage of higher strength to weight ratio over ferrous alloys. Many researchers are trying to develop new forming techniques to form these materials.

A new approach to improve formability and reduce springback of materials using electrical current has been studied and is found to provide greater advantage over the conventional sheet metal forming processes. Reduction in flow stress due to electric current flow during deformation process is defined as Electroplastic Effect. This effect is related to the interaction between flowing electrons and moving dislocations. It was observed that decrease in force required for plastic deformation is directly proportional to the difference between drift speed (electron flow speed in particular material) and dislocation motion speed.

Sheet metal bending experiments are conducted and the effect of electric current on springback is observed. To conduct bending experiments bend fixture is designed. Proper electrical insulation is included in design to ensure safe operation and to prevent electric flow in machine. Material selection is done on the basis of maximum stress developed in deformable tool and die in Finite Element Analysis results. Material is selected in such a way that the yield strength (including factor of safety '3') of the material must always be greater than produced maximum stress in FE analysis. After finalizing design and material for each part of the bend fixture, fabrication is done.

FE analysis is carried out for sheet metal bending process and results are compared with published results to validate FE model. After validation, FE model is used with provided material (HSQ steel) properties to compare simulation and experimental results. It is observed that FE model is predicting springback close to experimental results.

Sheet metal bending experiments on HSQ (High Strength Quenched) steel (provided by TATA Steel) are performed. Electric current, pulse frequency, duty cycle, tool radius, feed rate and dwell time are considered as factors for electroplasticity

experiments. Full factorial design of experiments with 2-levels is carried out to see complete effect. Total 64 experiments are carried out to analyse complete design of experiments. Whole sheet bending process is recorded using a digital camera. From recorded video, images are extracted at the end of deformation and after unloading. For springback measurement, radius of curvature in bend region is calculated using points traced from both the images and the difference between radius of curvature before unloading and after unloading is defined as springback. This methodology is used to eliminate the error induced due to initial curvature present in sheet specimens. Because of initial curvature, it is observed that measuring bend angle after springback is not accurate method.

It is observed from electroplastic bending experiments that springback and punch force are decreased compared to conventional bending process. From DOE analysis it is concluded that the parameters which are affecting springback are mainly current, pulse frequency and tool radius. Temperature measurement is also carried out and maximum temperature reached during each experiment are noted down. It is concluded that increase in temperature ( $200^{\circ}$  C) is not significant enough to cause any change in grain structure levels.

# Contents

Declaration . . . . .	ii
Approval Sheet . . . . .	iii
Acknowledgements . . . . .	iv
Abstract . . . . .	v
<b>Nomenclature</b>	<b>viii</b>
<b>1 Introduction and Literature Review</b>	<b>1</b>
1.1 Electricity Assisted Forming . . . . .	1
1.2 Sheet Metal Bending . . . . .	2
1.3 Electricity Assisted Bending . . . . .	2
1.3.1 Background and Motivation . . . . .	3
1.3.2 Literature Review . . . . .	4
1.4 Scope and Objective of Present Work . . . . .	17
1.5 Organization of Thesis . . . . .	17
<b>2 Design and Fabrication of Bend Fixture</b>	<b>18</b>
2.1 Material Selection . . . . .	18
2.2 Drawings of Bend Fixture Parts . . . . .	19
2.2.1 Base Plate . . . . .	19
2.2.2 Die Holder . . . . .	20
2.2.3 Die . . . . .	20
2.2.4 Bottom Tool . . . . .	22
2.2.5 Top Fixing Plate . . . . .	22
2.2.6 Top Tool Holder . . . . .	23
2.2.7 Top Tool . . . . .	23
2.2.8 Other Parts to Fix Bend Fixture on CNC Machine . . . . .	25
2.3 Assembly of all Bend Fixture Parts . . . . .	26
2.4 Fabrication of Fixture Parts . . . . .	26

<b>3</b>	<b>Finite Element Analysis of V-bending Experiments</b>	<b>28</b>
3.1	Validation of Finite Element Analysis . . . . .	28
3.1.1	NUMISHEET Benchmark 2002 problem . . . . .	28
3.1.2	Results and Comparison . . . . .	31
3.1.3	Shell model analysis . . . . .	37
3.1.4	Solid Model Analysis . . . . .	39
3.2	Shell and Solid Analysis Comparison for FEA Models . . . . .	41
3.3	FEA Analysis for Material Selection of Bend Fixture . . . . .	42
3.3.1	Stresses Generated During Bending Process . . . . .	44
3.4	Finite Element Analysis for IFHS 350 and HSQ 440 Steel U-die Bending Process . . . . .	44
3.4.1	Results and Discussion . . . . .	47
3.5	Finite Element Analysis for HSQ steel V-bending Process . . . . .	48
3.5.1	Results and Discussion . . . . .	52
<b>4</b>	<b>Experimental Investigation of Electroplasticity on HSQ steel</b>	<b>55</b>
4.1	Experimental Planning . . . . .	55
4.1.1	Width effect . . . . .	55
4.2	Electric Assisted Bending Experiments for HSQ Steel . . . . .	57
4.2.1	Experimental Setup and Procedure . . . . .	58
4.3	Process Parameters . . . . .	58
4.4	Results and Discussion . . . . .	61
4.4.1	Process parameters effect on springback . . . . .	61
4.4.2	Effect of parameters on bend profile . . . . .	65
<b>5</b>	<b>Conclusions and Scope for Future Work</b>	<b>71</b>
5.1	Scope for Future Work . . . . .	71
	<b>Appendices</b>	<b>72</b>
	<b>Investigation of Electroplastic Effect in Bending for Various Materials</b>	<b>73</b>
	<b>References</b>	<b>78</b>

# List of Figures

1.1	Sheet metal air bending . . . . .	2
1.2	Sheet metal U-die bending . . . . .	3
1.3	Schematic diagram of Electric Assisted Bending . . . . .	3
1.4	Effect of frequency on stress relaxation for (1) 200 gf, (3) 300 gf, and 400 gf [2]. . . . .	4
1.5	Effect of current pulses at different strain values [3]. . . . .	5
1.6	Effect of current pulses on different crystal structures [3]. . . . .	6
1.7	Deformation in creep at pulse duration of (1) 5 min, (2) 1 min and (3) 30 sec. Top inset figure showing (I) Creep without current, (II) Creep with equivalent heating and (III) Creep with pulse current with different duration. Bottom inset figure shows the logarithmic dependence of the delay time $t_d$ of the appearance of $\Delta\epsilon$ on loading $\Delta\tau$ [4]. . . . .	7
1.8	Drawing stress at different extruded wire diameters [7]. . . . .	8
1.9	Grain refinement for cold worked brass by various methods (a) annealing at 500°C, (b) annealing at 650°C and (c) grain refinement by using high-density electric current [8]. . . . .	8
1.10	Dislocation density comparison for brass material when (a) annealed at 650°C and (b) treatment with high-density electric current [8]. . . . .	9
1.11	Electric assisted open die forging for various metals [9]. . . . .	10
1.12	Effect of two different current amplitudes but same current density [9]. . . . .	10
1.13	Incremental Sheet Metal Forming with the assistance of DC pulsed current [10]. . . . .	11
1.14	Effect of isothermal heating in compression test [11]. . . . .	11
1.15	(a) Tensile test and (b) Compression tests results at different current densities [11]. . . . .	12
1.16	Instantaneous reduction of stress value when switching on current [11]. . . . .	12
1.17	Effect of pulsed DC current in compression and tension tests [11]. . . . .	13

1.18	Flow of electric current (a) Across specimen (b) Through the tool to the common ground [12]. . . . .	13
1.19	Effect of (a) Electric current and (b) Polarity of electric current on forces for stretch forming process at current density 20 A/mm <sup>2</sup> , pulse duration 1 s and pulse period 60s, [12]. . . . .	14
1.20	A simplified model for bending force analysis in air bending [13]. . . . .	14
1.21	Effect of die corner radius on electrically assisted bending [13]. . . . .	15
1.22	Effect of electric current density during compression test for (a) 304 Stainless steel and (b) Ti-6Al-4V [14]. . . . .	16
1.23	Effect of sheet springback on normal tool configuration [15]. . . . .	16
2.1	Base plate drawing (dimensions are in mm) . . . . .	20
2.2	Die holder drawing (dimensions are in mm) . . . . .	21
2.3	Die drawing (dimensions are in mm) . . . . .	21
2.4	Bottom Tool with various parts(dimensions are in mm) . . . . .	22
2.5	Top plate for fixing bend fixture in AMINO Press (dimensions are in mm) . . . . .	23
2.6	Top tool holder with bakelite insulation shown in brown color (dimensions are in mm) . . . . .	24
2.7	Top Tool with four different tool radius (dimensions are in mm) . . . . .	24
2.8	Top Tool assembly with tool holder . . . . .	25
2.9	Parts to fix bend fixture on small ISMF CNC machine (dimensions are in mm) . . . . .	25
2.10	Bend fixture assembly . . . . .	26
2.11	Fabricated bend fixture parts . . . . .	27
3.1	Tool and die (Analytical rigid) . . . . .	29
3.2	Sheet specimen (Deformable shell) . . . . .	29
3.3	Tool, die, and sheet assembly at start of simulation (a) Front view, (b) Isometric view . . . . .	30
3.4	Mesh generated on sheet . . . . .	31
3.5	Bend angle (a) Before springback, (b) After springback for aluminum [16] . . . . .	32
3.6	Bend angle comparison (a) Before springback, (b) After springback for aluminum . . . . .	32
3.7	Bending force comparison (a) Published results [16] (b) Results obtained in Abaqus simulation for aluminum without friction . . . . .	33

3.8	Punch force comparison (a) Published results [16] (b) results obtained in Abaqus simulation for aluminum with coefficient of friction 0.1348	33
3.9	Effect of uniform sheet thickness on bend angles for shell model with coefficient of friction 0.1348 [16]	34
3.10	Effect of element size on bend angles with coefficient of friction 0.1348 [16]	34
3.11	Effect of element size on bending force for frictionless process (a) Published results [16] (b) Results obtained in simulation	35
3.12	Effect of plane strain model and shell model on bend angles (a) frictionless [16] (b) with coefficient of friction 0.1348 [16]	35
3.13	Effect of 2D and 3D models on bending force (a) published results [16] (b) results obtained in Abaqus, without friction (c) published results [16] (d) results obtained in Abaqus, with coefficient of friction 0.1348	36
3.14	Effect of punch stroke on bend angle ratios [17]	37
3.15	Tool, die, and sheet assembly at start of deformation (a) Front view, (b) Isometric view	38
3.16	Comparison between results obtained in Abaqus simulation and published result	39
3.17	Stress-strain curve for both materials, Weldox 1100 and Weldox 1300 [18]	40
3.18	Comparison of Finite Element Analysis and Experimental Results	41
3.19	Mesh convergence study in solid analysis	42
3.20	Deformable tool and support analysis for material selection of bend fixture	43
3.21	Maximum stresses generated in (a) Deformable tool and (b) Support	44
3.22	Punch and Die parts modeled in Abaqus software	46
3.23	Measurement of springback angle in bending process	47
3.24	Friction coefficient effect on springback for IFHS 350 steel for thickness 0.7 mm(a) Isotropic model and (b) Anisotropic model	48
3.25	Friction coefficient effect on springback for IFHS 350 steel for thickness 0.7 mm(a) Isotropic model and (b) Anisotropic model	49
3.26	Die fillet radius effect on springback for HSQ 440 steel (a) Isotropic model and (b) Anisotropic model	50
3.27	Modelled Punch and Die part in Abaqus software	50
3.28	Modelled sheet specimen in Abaqus software	51
3.29	Mesh generated on sheet	52
3.30	FE and experimental springback results comparison for different tool radius	54

4.1	Width effect on springback . . . . .	56
4.2	Initial curvature present in sheet specimens . . . . .	56
4.3	Deformation zone in bending region was selected to compare radius of curvature as springback . . . . .	57
4.4	Experimental setup . . . . .	58
4.5	Close-up view of electric circuit completion between both tools and sheet	59
4.6	Image was taken from recorded video (a) after deformation and (b) after springback . . . . .	61
4.7	Results of analysis of variance . . . . .	62
4.8	Model summary of Anova analysis . . . . .	62
4.9	Main effect plots of various process parameters on springback . . . . .	63
4.10	Interaction plots for current and other parameters . . . . .	64
4.11	Interaction plots for Frequency and other parameters . . . . .	64
4.12	Interaction plots for duty cycle and other parameters . . . . .	65
4.13	Interaction plots for remaining parameters . . . . .	66
4.14	Variation in bend profiles in Deformation zone with and without electric current and other parameters same (Freq. = 100 Hz, Duty cycle = 5%, Feed = 20 mm/min and Dwell = 0 s), (a) Tool radius 2 mm and (b) Tool radius 6 mm. . . . .	66
4.15	Effect of frequency on springback at (duty cycle 5%, Feed 20mm/min, and dwell 0 s) (a) Tool radius 2 and Current 135 A, (b) Tool radius 2 and Current 195 A, (c) Tool radius 6 and Current 135 A and (d) Tool radius 6 and Current 195 A . . . . .	67
4.16	Effect of duty cycle on springback at (Feed 20mm/min, and dwell 0 s) (a) Tool radius 2 and Current 135 A, (b) Tool radius 2 and Current 195 A, (c) Tool radius 6 and Current 135 A and (d) Tool radius 6 and Current 195 A. . . . .	68
4.17	Effect of feed on springback at (duty cycle 5%, and dwell 0 s) (a) Tool radius 2 and Current 135 A, (b) Tool radius 2 and Current 195 A, (c) Tool radius 6 and Current 135 A and (d) Tool radius 6 and Current 195 A. . . . .	69
4.18	Effect of dwell on springback at (duty cycle 5% and Feed 20mm/min) (a) Tool radius 2 and Current 135 A, (b) Tool radius 2 and Current 195 A, (c) Tool radius 6 and Current 135 A and (d) Tool radius 6 and Current 195 A. . . . .	70



A.1	Electroplasticity effect on commercially available stainless steel scale .	74
A.2	Normal plot . . . . .	75
A.3	Main effects of process parameters on springback . . . . .	76
A.4	Interaction effects on springback between parameters . . . . .	77
A.5	Effect of electric current on bending force for (a) EDD Steel and (b) IF Steel . . . . .	78
A.6	Effect of current on springback (a) EDD Steel and (b) IF Steel . . . . .	79
A.7	Effect of electric current on bending force for Ti-6Al-4V . . . . .	79
A.8	Effect of current on springback for Ti-6Al-4V . . . . .	79

# List of Tables

3.1	Abaqus simulation results for different sheet thickness. . . . .	34
3.2	Abaqus simulation results for different shell element size. . . . .	34
3.3	Abaqus simulation results for different model approach for frictionless condition. . . . .	36
3.4	Abaqus simulation results for different model approach for coefficient of friction 0.1348. . . . .	36
3.5	Abaqus simulation results for different model approaches for two different materials . . . . .	41
3.6	Mesh convergence results for solid model in Abaqus for coefficient of friction 0.1348. . . . .	42
3.7	Effect of width on springback keeping all other same conditions. . . .	53
3.8	Effect of tool radius on springback keeping all other same conditions.	54
4.1	Process parameters used for HSQ steel experiments . . . . .	60
A.1	Process parameters used for spring steel experiments . . . . .	74

# Chapter 1

## Introduction and Literature Review

### 1.1 Electricity Assisted Forming

Electricity assisted forming is a metal forming technique in which deformation takes place at expense of mechanical as well as electrical energy. Electricity passes through specimen while deformation process occurs. Main effects of electric current on deformation process are increase in formability and decrease in springback phenomenon.

Formability is defined as ability of material to deform plastically before failure, whereas springback is defined as the recovery of elastic strains after unloading. In metal forming processes formability is a desirable property, whereas springback is not desirable because springback induces geometrical inaccuracies in formed components.

Hence electricity assisted forming is a newly developed technology in which main focus is on to deform high strength materials by increasing their formability as well as reducing springback.

Three main benefits of electricity assisted forming includes:

- Reduction in flow stresses required for plastic deformation.
- Increase in deformation before failure.
- Reduction in springback after unloading.

Electric current is flow of charged particles through conductive material. These charged particles are often moving electrons, which if pass during metal deformation process, interact with already moving dislocations in metals. The interaction between

moving electrons and dislocations is known as 'Electroplastic Effect'. The electroplastic effect is sometimes results in reduction of flow stresses as well as springback and increase in deformation prior to failure. In this thesis work electroplastic effect on sheet metal bending process is studied.

## 1.2 Sheet Metal Bending

Sheet metal bending is a forming process in which sheet metal is subjected to bending stresses and hence is changed into a curved sheet from its flat straight shape. It can be classified as V-shape, U-shape or in channel shape bending. V shape bending is also known as air bending in which V shape punch is forced into V-die opening. Sheet comes in contact with only punch tip and with outside edges of V-shape die hence named as air bending Fig. 1.1.

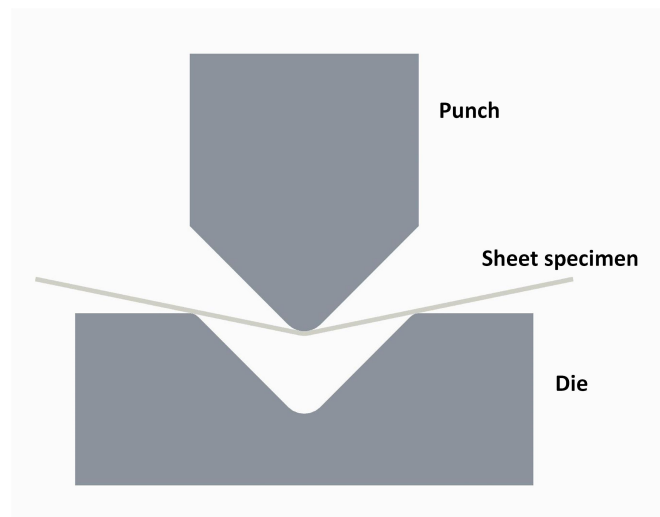


Figure 1.1: Sheet metal air bending

U-shape die is used for U-die bending, here contact between sheet and die takes place over complete surface of die cavity, at the end of punch stroke. In U-die bending process die radius plays an important role in shaping the final component as demonstrated in Fig. 1.2

## 1.3 Electricity Assisted Bending

Electric assisted bending is the process in which bending of sheet takes place in presence of electrical energy also. It assists in deformation of sheets, hence mechanical

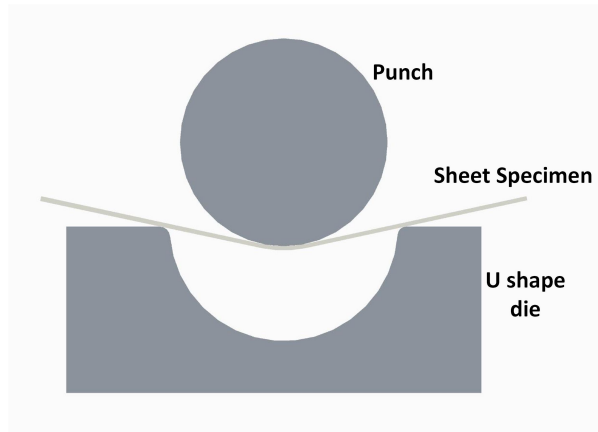


Figure 1.2: Sheet metal U-die bending

energy required for the bending reduces. Electric flow through metal helps in dislocation motion, which reduces bending forces and hence the mechanical power.

In sheet metal bending major drawback is springback phenomenon, which induces geometrical inaccuracies. Metals with higher strength (like titanium and tungsten alloys) show more springback compared with low strength metals and they require higher input of mechanical energy. Electricity assisted bending reduces the springback and also results in less mechanical energy input.

The schematic setup for electricity assisted bending is shown in Fig. 1.3

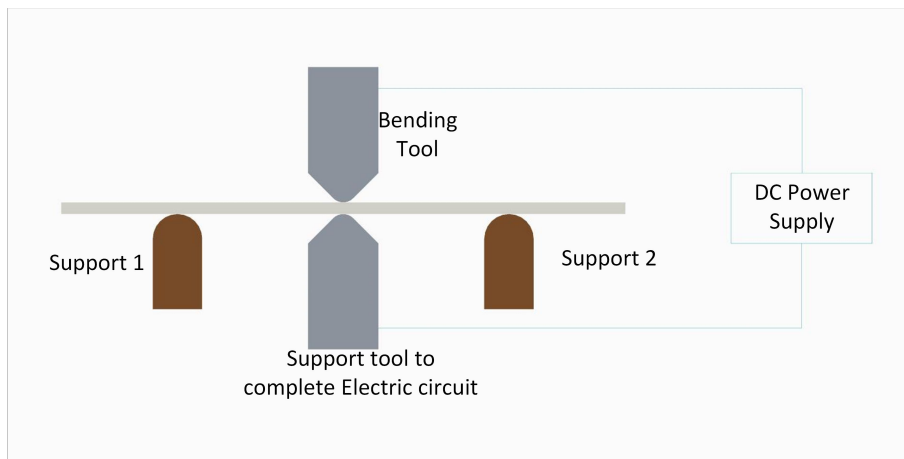


Figure 1.3: Schematic diagram of Electric Assisted Bending

### 1.3.1 Background and Motivation

Automobile and aerospace industries are two major industries which use sheet metal forming processes for making different components. Metals like tungsten, molybde-

num and titanium alloys have good strength to weight ratio compared to aluminium and steel alloys. Because of less formability, these metals are not easy to form using conventional forming processes. The use of these metals in industries can provide same strength with lesser weight of parts, which in turn increases overall efficiency. Hence researchers are continuously trying to develop new forming techniques. Electricity assisted forming can be an alternate option to form these high strength metals.

### 1.3.2 Literature Review

Effect of flow of electrons on the deformation process of metals was first investigated by Troitskii [1]. Troitskii investigated the effect of DC pulsed current on formability of various metals. To reduce resistive heating effect due to current flow liquid nitrogen was used. It was reported that current pulses have no effect on elastic part of deformation curves. Surface examination by microscope suggested that there was no significant change in slip-band. The author also investigated that reduction in flow stress was achieved because of electroplastic effect not due to resistive heating.

Troitskii [2] studied the effect of DC pulse current polarity as well as the effect of pulse frequency on stress relaxation and creep. Stress relaxation for different crystals (zinc and cadmium) was observed at different loads in presence of pulsed DC current. Also to reduce resistive heating effect, tests were conducted at a very low temperature(-196°) by using liquid nitrogen. It was observed that increase in pulse frequency and the decrease in current density, results in the increase of stress relaxation refer Fig. 1.4.

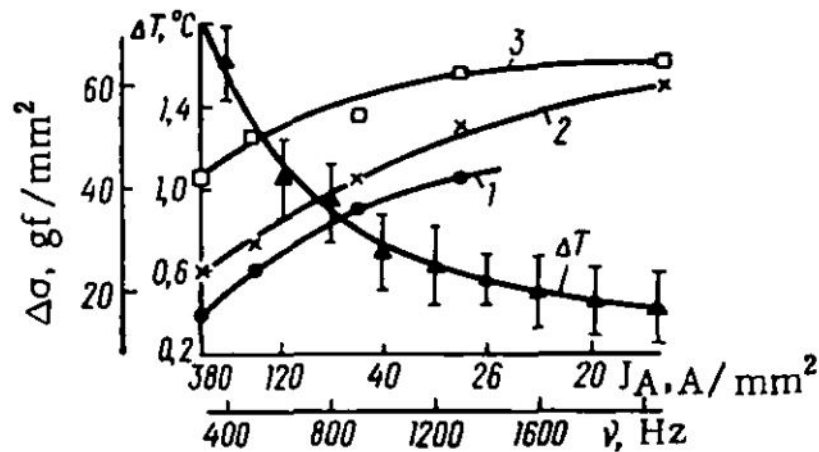


Figure 1.4: Effect of frequency on stress relaxation for (1) 200 gf, (3) 300 gf, and 400 gf [2].

The author concluded that current polarity creates difference in stress relaxation around 15-25%. It was concluded that at high-frequency results in the splashing of electron clouds in the lattice which results in the increase in the frequency of elastic vibrations and hence increase in electroplastic effect. Polarity effect was attributed to variation in interaction between free electrons and dislocations.

Okazaki et. al. [3] conducted tensile test experiments under the influence of high current pulses on materials having different crystal structures(BCC for Fe, FCC for Pb, HCP for Ti and tetragonal for Sn). It was observed that at the instant of current pulse application, stress values drop suddenly and on termination of the pulse, stress returns gradually to the original values Fig. 1.5

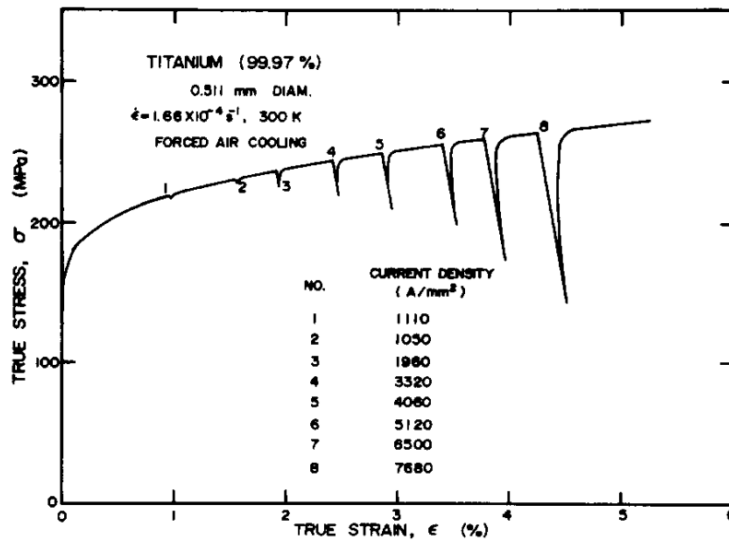


Figure 1.5: Effect of current pulses at different strain values [3].

It was concluded that there were no changes in dislocation structure with the application of current pulses as after switching off the pulses, stress reached to its original values. Hence only effect was the enhancement of mobility of dislocations. Also it was observed that different crystal structures behave differently with the application of current and was concluded that effect of pulsed current pulse on flow stress decreases in the order of BCC(Fe), HCP(Ti), FCC(Pb) and tetragonal(Sn) refer Fig. 1.6. Authors also estimated that with forced cooling( $\Delta T = 20K$ ) at  $8000 A/mm^2$ , decrease in flow stress due to resistive thermal heating account for only about 10%.

Stashenko et. al. [4] observed creep phenomenon with the application of pulsed current on zinc single crystals. They observed that electron dislocation interaction is a primary effect compared to other secondary effects as skin effect, pinch effect

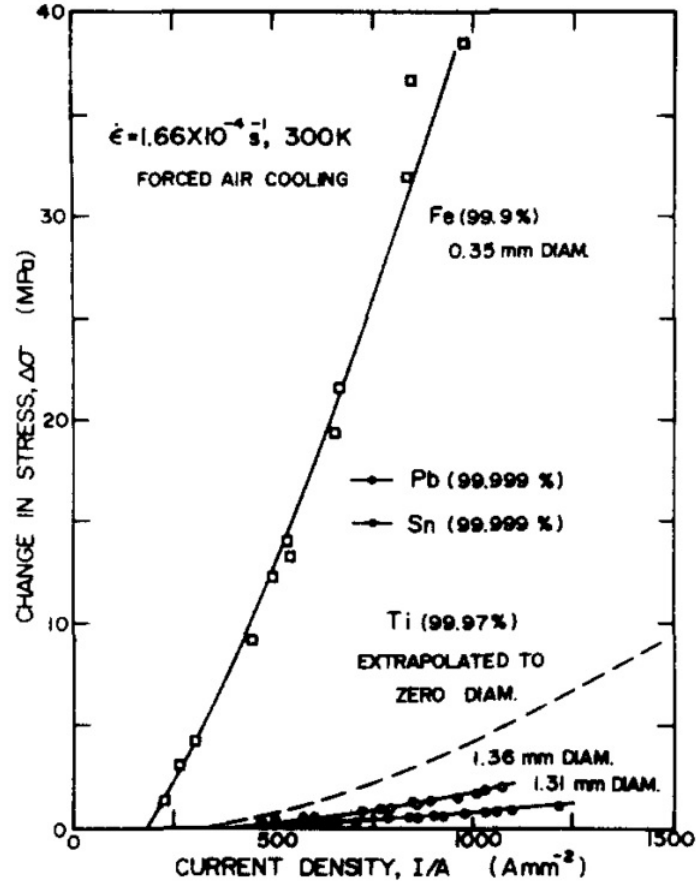


Figure 1.6: Effect of current pulses on different crystal structures [3].

and ampere force effect. Effect of current pulses at current density  $25 \times 10^7 \text{ A/mm}^2$ , frequency 100 Hz and duration of pulses varied from 3 to  $25 \times 10^{-5} \text{ s}$ , on strain behavior during creep phenomenon Fig. 1.7. Also, the effect of pulse frequency was observed by conducting same experiment at a different frequency (range 2 Hz - 600 Hz). It was found that strain increases with the decrease in frequency. The strain values are found the maximum in the frequency range of 2 Hz - 200 Hz.

Troitskii [5] concluded that the force which helps accelerating dislocations is proportional to the difference in drift speed of electrons (drift speed is defined as the speed of some flowing particles like electrons, in material due to applied electric field) and velocity of dislocations. They proposed that drift speed of electrons is directly proportional to current density, hence current density determines the influence of reduction of flow stress of metals.

Conrad [6] conducted experiments on zinc, titanium, aluminium and copper with high density DC electric current pulses of  $100 \mu\text{s}$  and proposed that after exceeding a



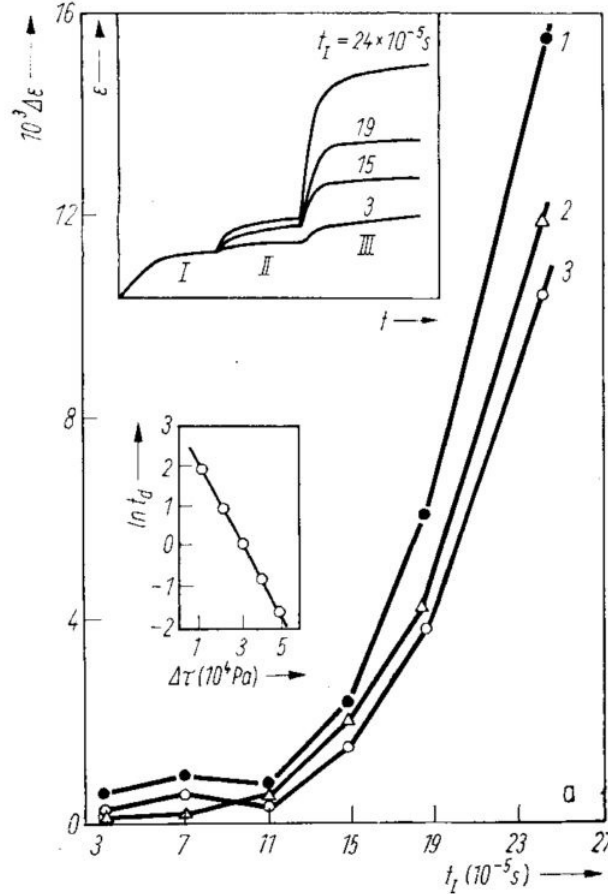


Figure 1.7: Deformation in creep at pulse duration of (1) 5 min, (2) 1 min and (3) 30 sec. Top inset figure showing (I) Creep without current, (II) Creep with equivalent heating and (III) Creep with pulse current with different duration. Bottom inset figure shows the logarithmic dependence of the delay time  $t_d$  of the appearance of  $\Delta\epsilon$  on loading  $\Delta\tau$  [4].

critical current density, there occurs a five order of magnitude increase in the strain rate at current densities approaching  $106 \text{ A/cm}^2$ . This effect of the current, decreased with strain for FCC metals but was relatively independent of strain for BCC metals and  $\alpha$ -Ti. The author also mentioned that high-density current, whether continuous or pulse can significantly enhance the plastic deformation rate in metals in addition to the side effect of Joule heating.

Tang et.al. [7] conducted electric pulse assisted wire drawing of steel and reduction in stress by about 50% as well as the reduction in minimum extruded wire diameter was observed refer Fig. 1.8. It was observed that surface quality of extruded wires also improved when extrusion was performed under the assistance of electric current pulses. It was concluded that drift velocity of electrons in the metals is more than

the dislocation velocity and hence electrons are assisting the dislocations to overcome the obstacles and hence drawing stress was reduced.

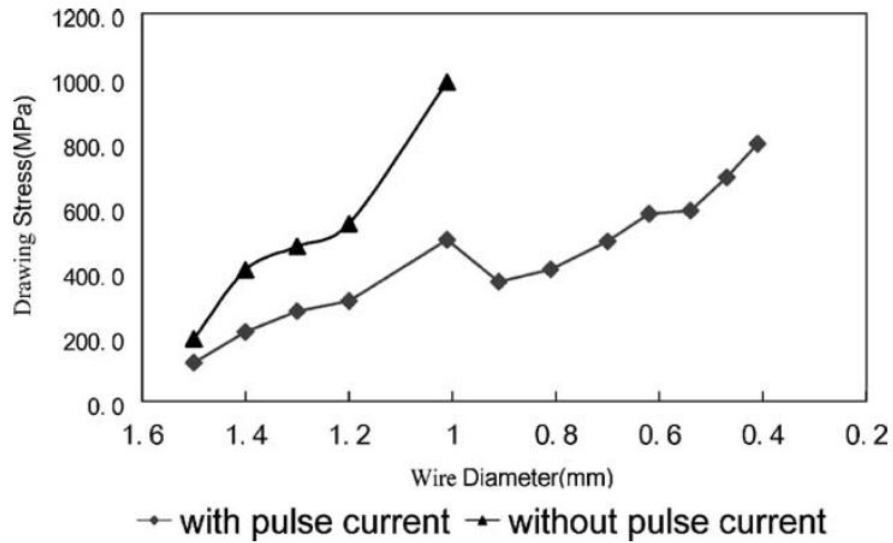


Figure 1.8: Drawing stress at different extruded wire diameters [7].

Zhou et.al. [8] conducted grain refinement studies on brass material without solid-phase transformation using electric pulse current as well as heat treatment at same temperature and compared grain structure. It was observed that grain size for the case of electric pulse current was  $3 \mu\text{m}$  whereas for annealing heat treatment size was 15 to  $20 \mu\text{m}$  Fig. 1.9.

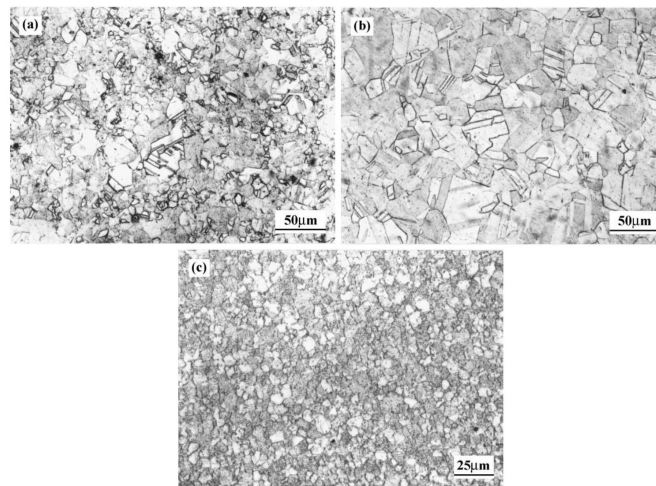


Figure 1.9: Grain refinement for cold worked brass by various methods (a) annealing at  $500^{\circ}\text{C}$ , (b) annealing at  $650^{\circ}\text{C}$  and (c) grain refinement by using high-density electric current [8].

Mechanical properties were also measured for the both experiments and it was observed that yield strength of the electro-pulsed sample was 89% higher than the annealed (at 650°C) sample. Hence it was concluded that mechanical properties of the electro-pulsed sample were better than annealed samples which were correlated with refinement in grain structure.

Reduced grain size in electro-pulsed experiments was correlated with the increase in nucleation rate which retarded the subsequent rate of grain growth. High nucleation rate was explained with respect to:

- High heating rate.
- Enhanced dislocation mobility.
- Enhanced migration of atoms.

Dislocation density was also studied and it was observed that the dislocation density in electropulsed workpiece was lower than the annealed workpiece at 650°C refer Fig. 1.10.

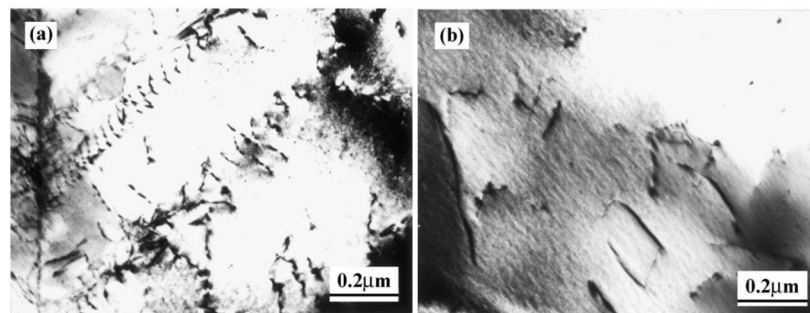


Figure 1.10: Dislocation density comparison for brass material when (a) annealed at 650°C and (b) treatment with high-density electric current [8].

Perkins et.al. [9] conducted electric current assisted open die forging for various metals (6061 T6511 Al, 7057 T6 Al, 2024 T4 Al, 2024 T351 Al, C11000 Cu, 360 yellow brass, 464 naval brass, 304 Stainless steel, A2 tool steel and Titanium). It was observed that all metals except 360 yellow brass show electroplastic effect. There is some threshold current density value for each metal, at which significant reduction in flow stress occurs refer Fig. 1.11.

Authors also conducted some experiments to see the effect of current density and current amplitude on the stress-strain relationship. They used different size specimens and at the same time different current amplitude to maintain constant current density. Current amplitude used in experiments were 2250 A and 560 A for 12.7 mm and 6.4

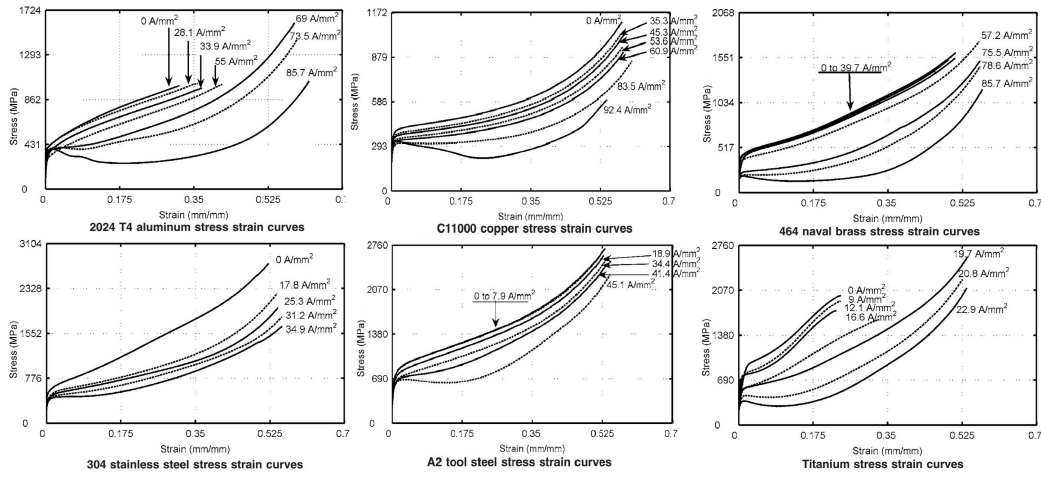


Figure 1.11: Electric assisted open die forging for various metals [9].

mm diameter specimens respectively to maintain current density ( $18 \text{ A/mm}^2$ ). It was found that, it is current density which plays role in electroplasticity rather than current amplitude as for both experiments stress strain curve came approximately same refer Fig. 1.12

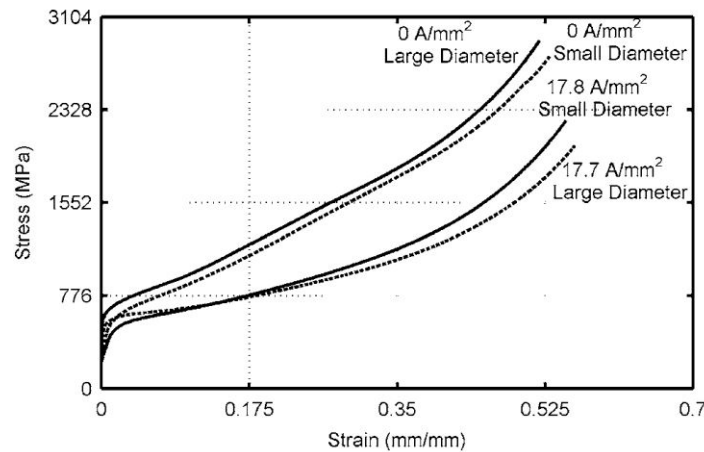


Figure 1.12: Effect of two different current amplitudes but same current density [9].

Fan et al. [10] performed electrically assisted incremental sheet metal forming for magnesium AZ31 and titanium alloys by considering only Joule heating effect. Increase in temperature due to Joule heating was correlated with the increase in ductility of the material at contact zone of tool and sheet. They also considered various parameters other than current density such as feed rate, tool diameter, and step size and concluded that these parameters also affect formability. Authors concluded that with the increase in electric pulsed current wall angle increases and it can reach up to  $64.3^\circ$  at current 500 A.

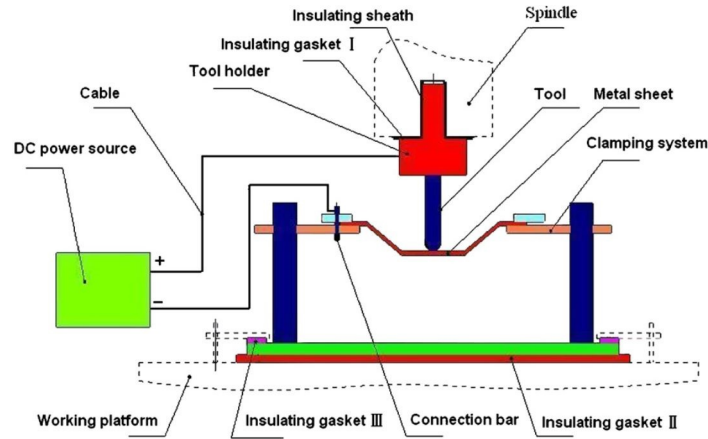


Figure 1.13: Incremental Sheet Metal Forming with the assistance of DC pulsed current [10].

Ross et al. [11] performed compression and tension tests on Ti-6Al-4V alloy in presence of direct current. Authors demonstrated that there is a significant difference between isothermal forming at  $260^{\circ}$  and electrically-assisted forming refer Fig. 1.14

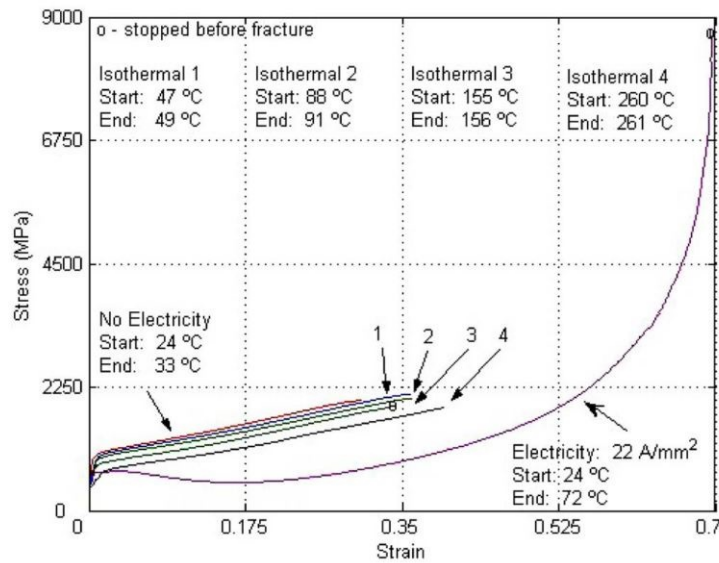


Figure 1.14: Effect of isothermal heating in compression test [11].

Stress weakening was observed in tensile tests, which increases with current density. Also, there was no necking initiation was observed at maximum stress but it got shifted to greater strain values refer Fig. 1.15

It was observed that to get electroplasticity effect in compression test required electric current was much higher than the tensile test. Reduction in yield strength and the increase in ductility was observed in compression tests refer Fig. 1.15

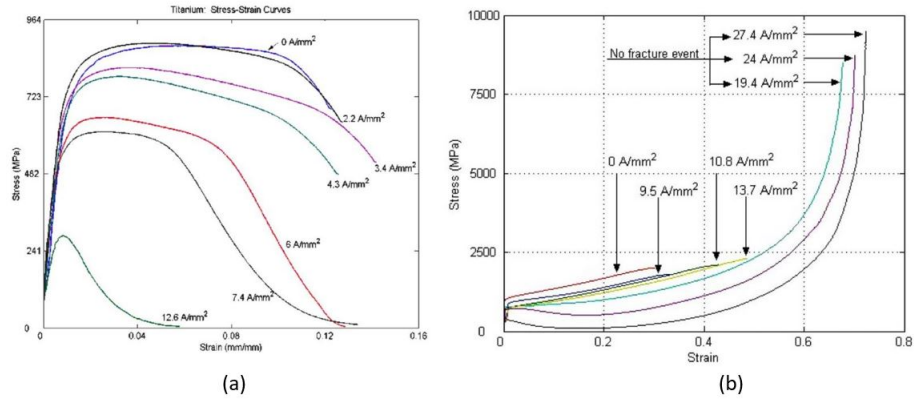


Figure 1.15: (a) Tensile test and (b) Compression tests results at different current densities [11].

They proposed that effect of resistive heating is very less compared to the effect of current on deformation, by conducting experiments using delayed current application. They explained that electrical flow immediately lowered flow stresses of titanium, a response which temperature would take a greater amount of time to achieve refer Fig. 1.16. It was observed that the temperature increased in isothermal heating was more compared with temperature increase in electric assisted current. But still, the effect of current was more compared with isothermal heating. Strain weakening effect was not observed in the case of isothermal heating experiments.

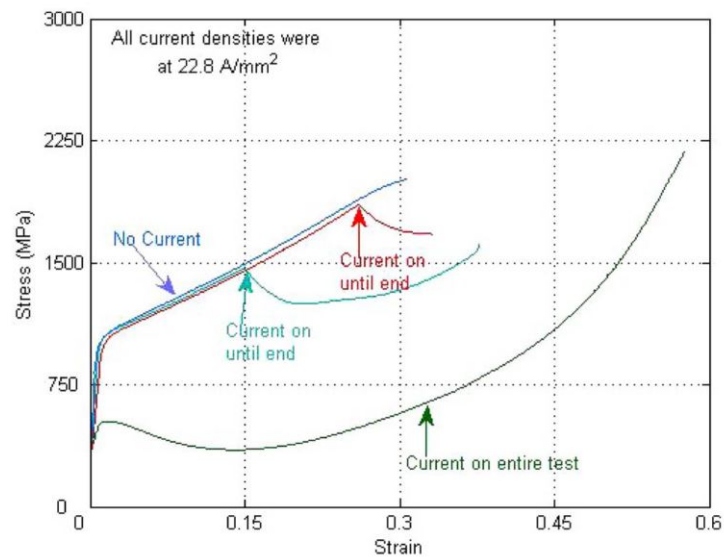


Figure 1.16: Instantaneous reduction of stress value when switching on current [11].

Effect of pulsed current was also observed by conducting the experiment with

pulsed current and current on and off at different strain values refer Fig. 1.17. The effect of pulsed current was so quick to observe hence concluded that effect is completely electroplastic rather than resistive heating. The current was kept on and off for every 2 s during experiments.

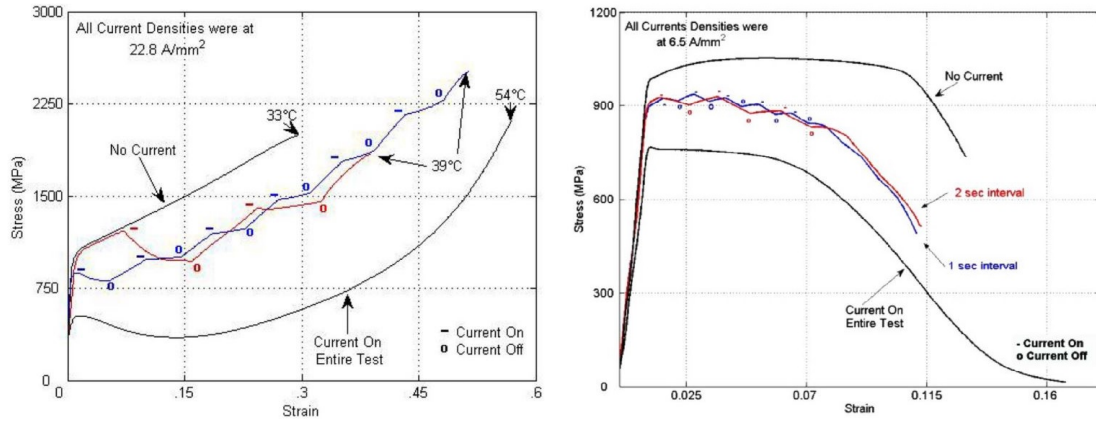


Figure 1.17: Effect of pulsed DC current in compression and tension tests [11].

Jones et.al. [12] conducted electricity assisted stretch forming on 304 stainless steel under different conditions. They used two different testing conditions, in which flow of electric current was changed refer Fig. 1.18. They observed that formability was decreased due to the use of electric current. It was concluded that accumulation of heat in stretched area was too much which caused failure at very early stage. They also observed that flow stress reduced when electricity was applied refer Fig. 1.19. They also presented electric current polarity effect on stretch forming process and concluded that there was no appreciable effect on formability and forming forces.

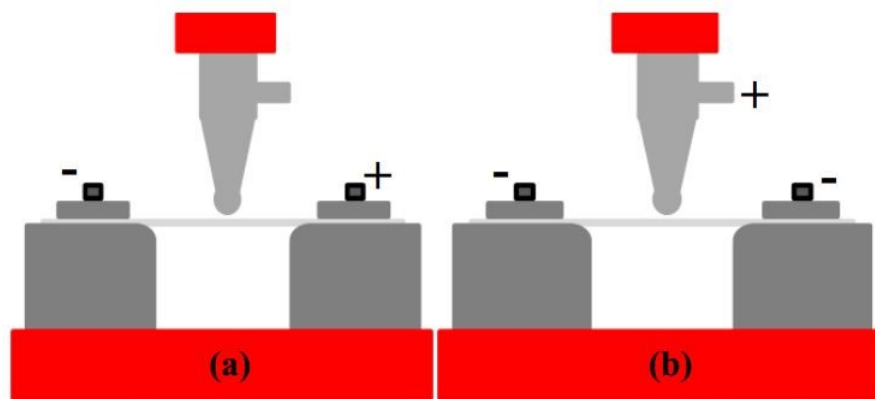


Figure 1.18: Flow of electric current (a) Across specimen (b) Through the tool to the common ground [12].

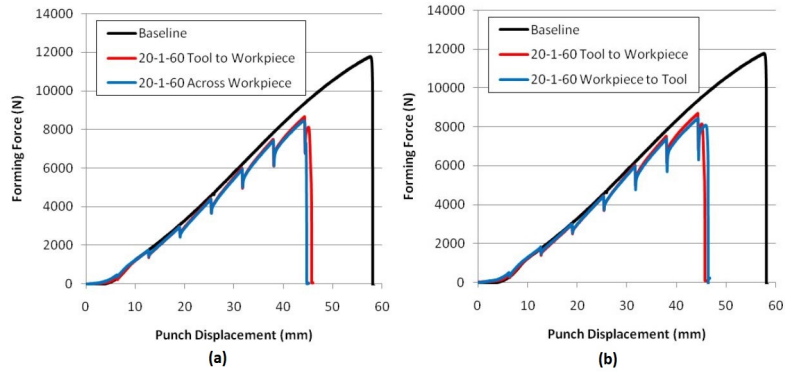


Figure 1.19: Effect of (a) Electric current and (b) Polarity of electric current on forces for stretch forming process at current density  $20 \text{ A/mm}^2$ , pulse duration 1 s and pulse period 60s, [12].

Salandro et.al. [13] conducted electric assisted bending tests on stainless steel. They also compared analytical and experimental results for without current. An analytical expression for bending forces refer Fig. 1.20 under plane strain assumption was derived.

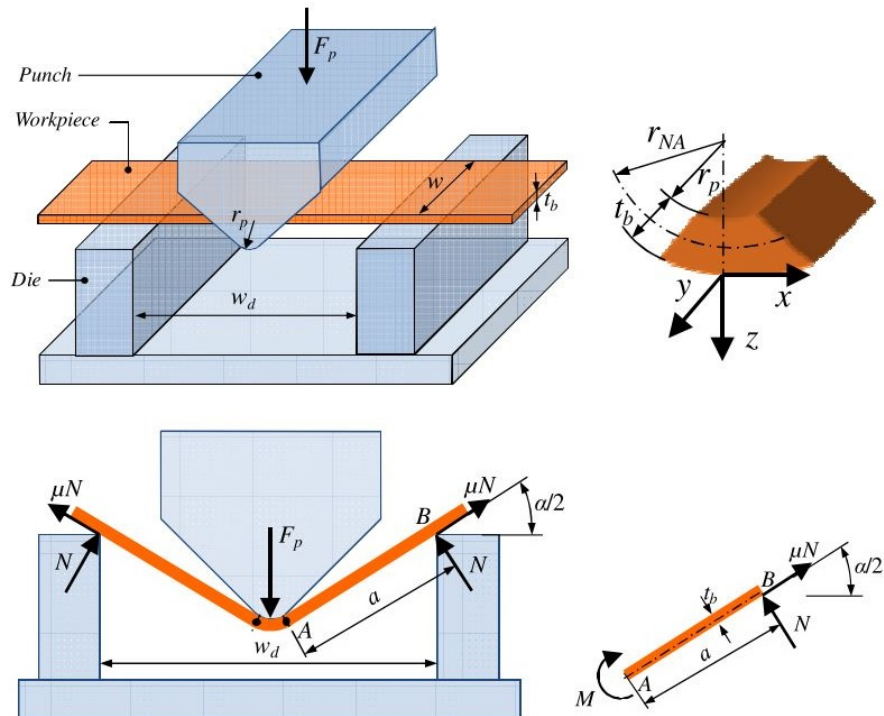


Figure 1.20: A simplified model for bending force analysis in air bending [13].



The bending force  $F_p$  was given as

$$F_p = K \cdot \frac{w \cdot t_b^2 \cdot \cos \frac{\alpha}{2} \cdot (\cos \frac{\alpha}{2} + \mu \cdot \sin \frac{\alpha}{2})}{\mu \cdot t_b \cdot \cos \frac{\alpha}{2} + w_d - 2(r_p + t_b) \cdot \sin \frac{\alpha}{2}} \cdot \left( \ln \sqrt{1 + \frac{t_b}{r_p}} \right)^n \quad (1.1)$$

where  $n$  and  $K$  are strain hardening exponent and strength coefficient respectively.

Authors also mentioned the effect of die corner radius on electricity assisted bending. They mentioned that sheet specimen weld itself to the fixture when the electrical pulse was applied, which increases bending force after each electric pulse, until small weld brakes. As a solution to this, they used very small corner radius for die and concluded that because of small die corner radius, the contact point between fixture and specimen did not change during process and welding is prevented refer Fig. 1.21

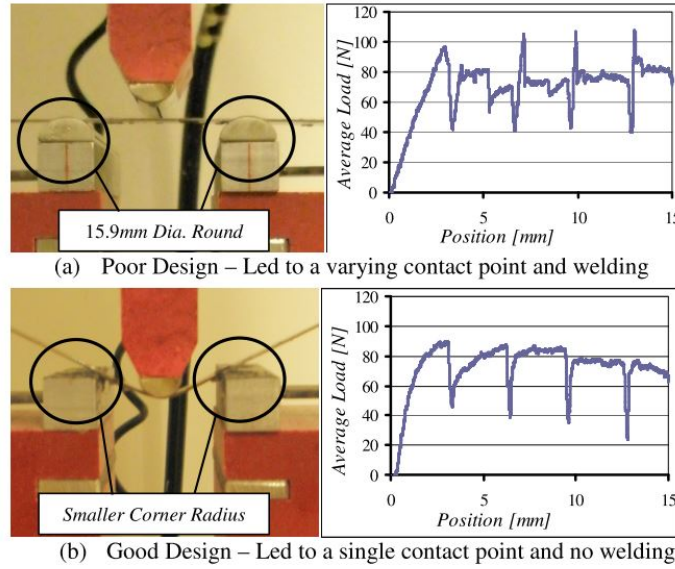


Figure 1.21: Effect of die corner radius on electrically assisted bending [13].

Jones and Mears [14] conducted compression tests for 304 stainless steel and Ti-6Al-4V materials under the assistance of electric current. Experiments were conducted under constant current density (CCD) condition as well as non-constant current density (NCCD) condition. For both materials reduction in flow stress was observed with increase in current density refer Fig. 1.22. It was observed that constant current density effect on flow-stress was more compared with non-constant current density. Empirical model was developed for constant current density condition and showed excellent mapping capability for both 304 Stainless Steel and Ti-6Al-4V materials.

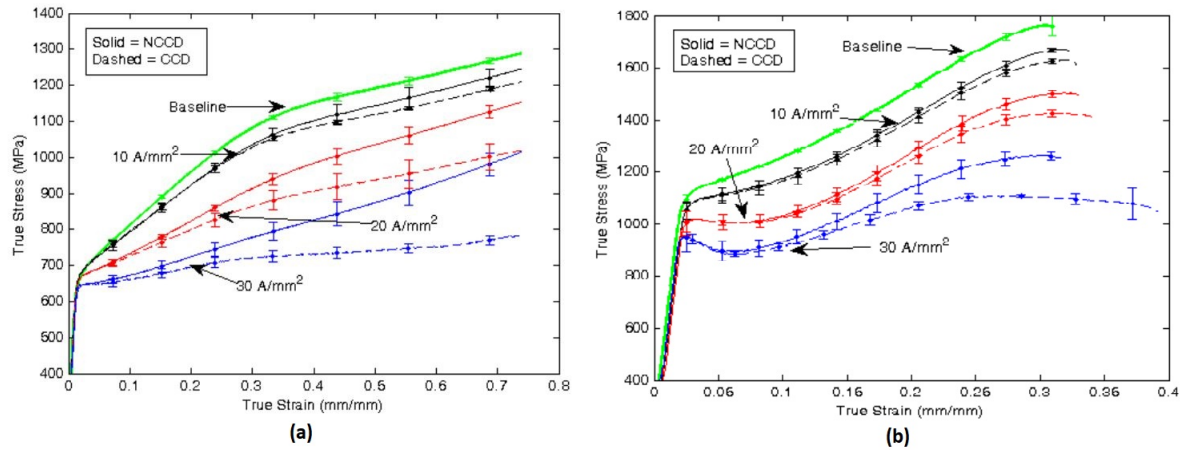


Figure 1.22: Effect of electric current density during compression test for (a) 304 Stainless steel and (b) Ti-6Al-4V [14].

Javed Asghar and N.V. Reddy [15] performed electrically assisted double sided incremental sheet metal forming on Ti alloy. It was realized that due to high spring back of Ti alloy, normal tool configuration of tool path that ensures the minimum distance between two tools, get disturbed refer Fig. 1.23. Disturbance in tool configuration results in the increase in current carrying length. It was concluded that increase in current carrying length results in higher resistive heating and decrease in current density, which results in less electroplastic effect and hence crack in the component was observed.

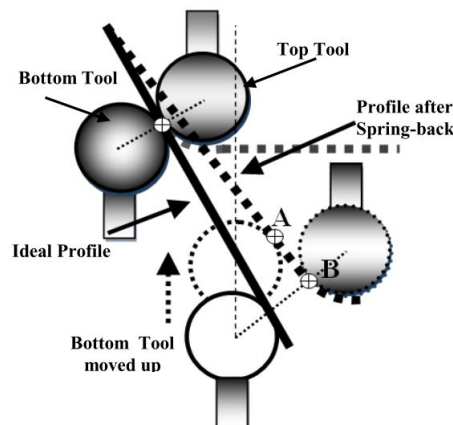


Figure 1.23: Effect of sheet springback on normal tool configuration [15].

## 1.4 Scope and Objective of Present Work

Continuous efforts are made to study the effect of electron and dislocation interaction for different materials. As it can be concluded from above presented literature review that electroplastic effect in metal forming process can provide tremendous opportunities. Which can help many industries to overcome the difficulties like:

- High mechanical energy input to perform particular forming operations, which increases with increase in material strength.
- High the strength of material higher the springback hence less accuracy.
- Handling the material in furnaces for heat treatment like grain recrystallization.

This study focuses on the electroplastic effect on springback in sheet metal bending process. Experiments has been carried out in such a way that resistive heating was minimized to reduce any thermal effect.

The main objective of this work is to see the effect of electric current on sheet metal bending process by keeping the electric current flow focused in deformation zone only. Hence, the objective is to minimize the resistive heating effect at the same time maximize the electroplastic effect.

## 1.5 Organization of Thesis

This thesis is presented in four chapters and content of each chapter is summarized below:

Chapter 1 presents the brief introduction of sheet metal bending and electroplasticity with literature survey.

Chapter 2 presents design and fabrication of bending setup.

Chapter 3 presents the results obtained from finite element analysis of the V-bending process.

Chapter 4 presents the experimental investigation of electroplasticity on various metals.

## Chapter 2

# Design and Fabrication of Bend Fixture

Bend fixture was designed to perform sheet metal bending operation with and without electricity. The design of bend fixture was prepared by considering following guidelines:

- To ensure minimum current carrying length a secondary tool was provided such a way that current will flow through only deformation zone.
- The design was made flexible enough to change tool and die of different dimensions according to requirement.
- As deformation process involves electric flow, die and tool were insulated from other bend fixture parts to provide safe electric flow.
- To measure bending forces, load cell was also accommodated in bend fixture design.

### 2.1 Material Selection

Material selection for die and tool is done by carrying finite element analysis refer section 4.1. Three-point bending process is modeled in Abaqus software considering both die and tool as deformable parts. Stresses and strains generated during bending process were extracted from simulation and then the material was selected of higher strength than the stress generated in FE analysis. Finite element analysis was done for steel sheet of 5 mm thickness and to consider various inaccuracies in analysis the factor of safety 3 was chosen while selecting die and tool material.

Stresses generated in FE analysis for both die and tool are of order 460 MPa and 100 MPa respectively. Hence material for die and tool was selected in such a way that its yield strength was three times higher than the maximum stress generated in FE analysis after considering the factor of safety '3'. The allowable stress is defined as;

$$\sigma_{allow.} = F o S . \sigma_{work.} \quad (2.1)$$

Hence allowable stresses for die and tool is considered as 1380 MPa and 300 MPa respectively.

Selection of material also depends on availability, machining cost, and surface finish required for the parts. For die and tool, EN8 steel (belong to standard BS 970-1955) was selected because of strength and availability.

For other parts of the bend fixture mild steel is selected as it is easily available and also strength is sufficient enough for assembly parts.

Die radius was selected by following ASTM E290 bending standard. Die radius is given by;

$$D = 2.r + 3.t \pm \frac{t}{2} \quad (2.2)$$

where D is the die diameter, r is the tool radius and t is the thickness of the sheet. Dimensions of other part are selected on the basis of available working space in CNC machine to accommodate each part after assembly.

## 2.2 Drawings of Bend Fixture Parts

After finalizing material and dimensions, drawing of each parts was created using Creo Parametric 3.0 software. Each part drawings with their dimensions are shown in following figures.

### 2.2.1 Base Plate

The base plate was designed to be placed on machine table to serve as a stiff surface to which other fixture parts are attached to be supported. Mild steel plate was selected for the base plate material and dimensions were made according to the available space on machine table refer Fig. 2.1.

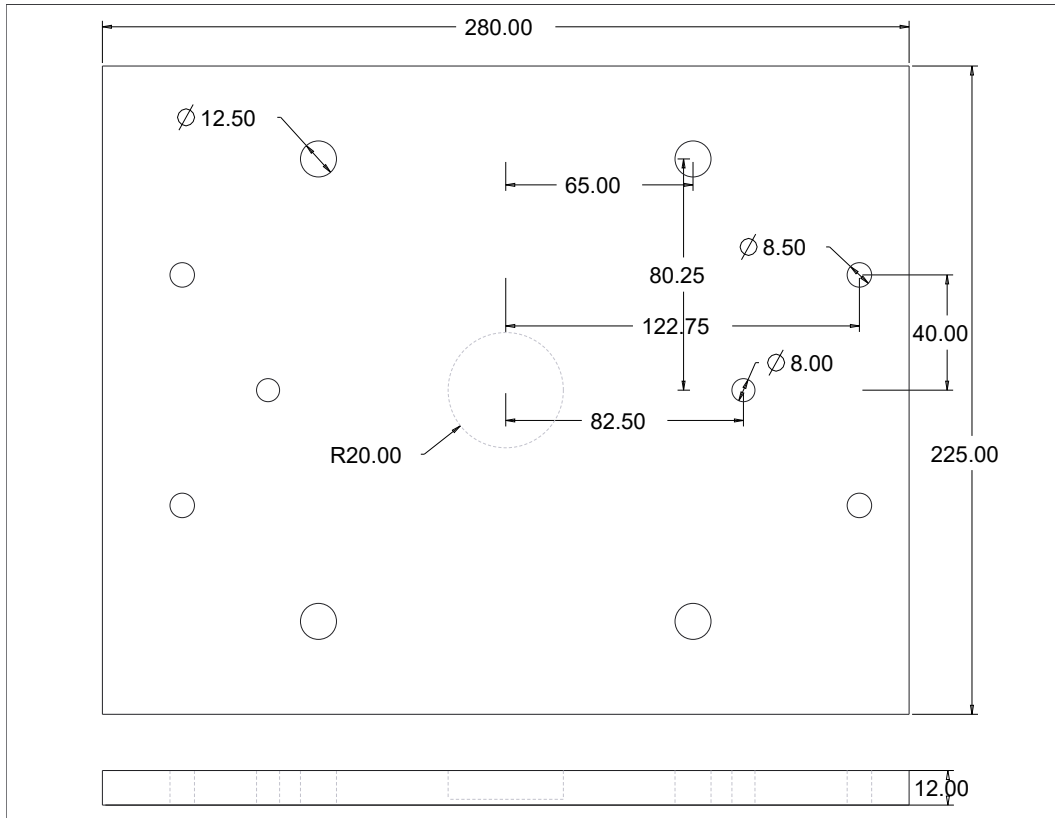


Figure 2.1: Base plate drawing (dimensions are in mm)

### 2.2.2 Die Holder

Die holder was designed in such a way that it provides flexibility to change different shapes of die without disturbing any other parts. This part made bend fixture flexible to adopt different sizes for the die. Mild steel was selected for this part and it was machined in CNC milling machine using end milling and drill tools for different cutting operations. For making square hole wire EDM was used. The die holder drawing is shown in Fig. 2.2

### 2.2.3 Die

Die dimensions were selected according to ASTM E290 bending standard refer Fig. 2.3. EN8 steel (BS 970-1955) was used for fabrication of the die. Curvature region and square hole was cut by using wire EDM and drilling were done by CNC milling machine. Die is one of the major parts in bend fixture design, hence dimensional tolerances and accuracies were extensively taken care while fabricating it.



## 2.2.4 Bottom Tool

To complete the electric circuit during electric assisted bending extra bottom tool was designed. It was supported on spring load, which during deformation process ensures close circuit. The bottom tool consists of two parts, one which supports on spring load and other which makes contact with sheet specimen. Insulation was provided between these two parts to ensure safe working condition refer Fig. 2.4.

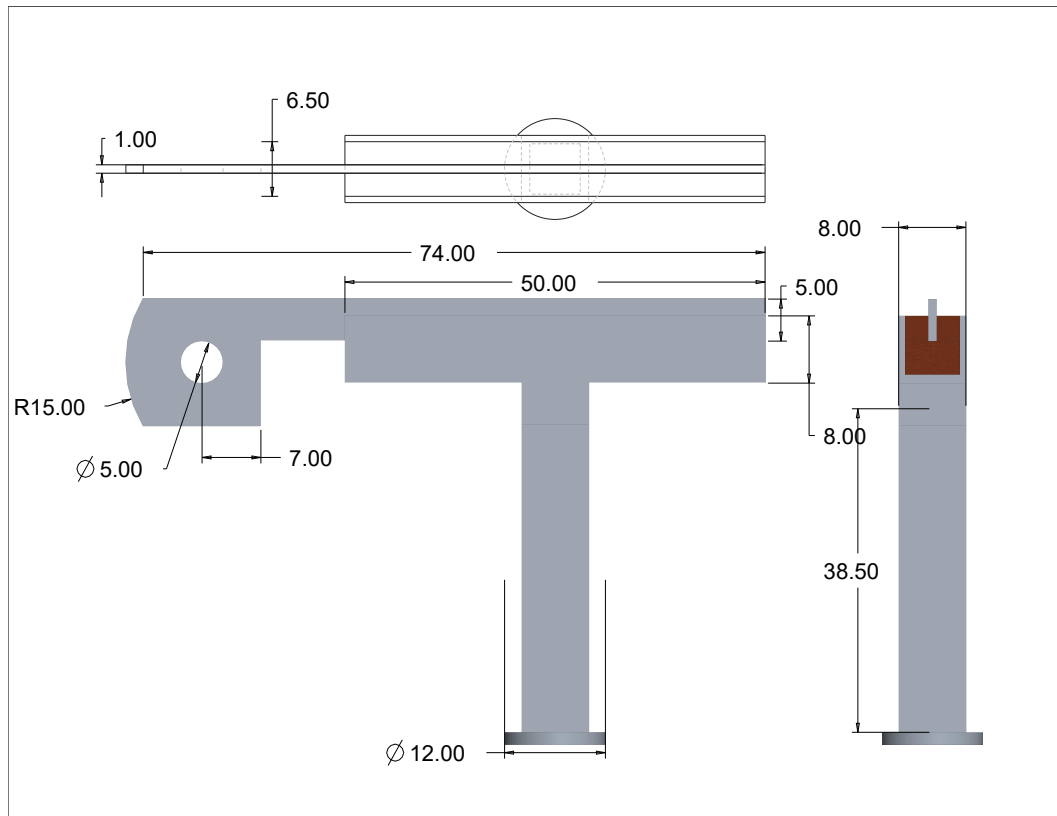


Figure 2.4: Bottom Tool with various parts(dimensions are in mm)

## 2.2.5 Top Fixing Plate

This plate was designed to use the bend fixture in AMINO Press machine. This plate mount with the top moving plunger of the machine and then tool mount on this plate. Dimensions were decided according to space available in the top plunger of the Press refer Fig 2.5.



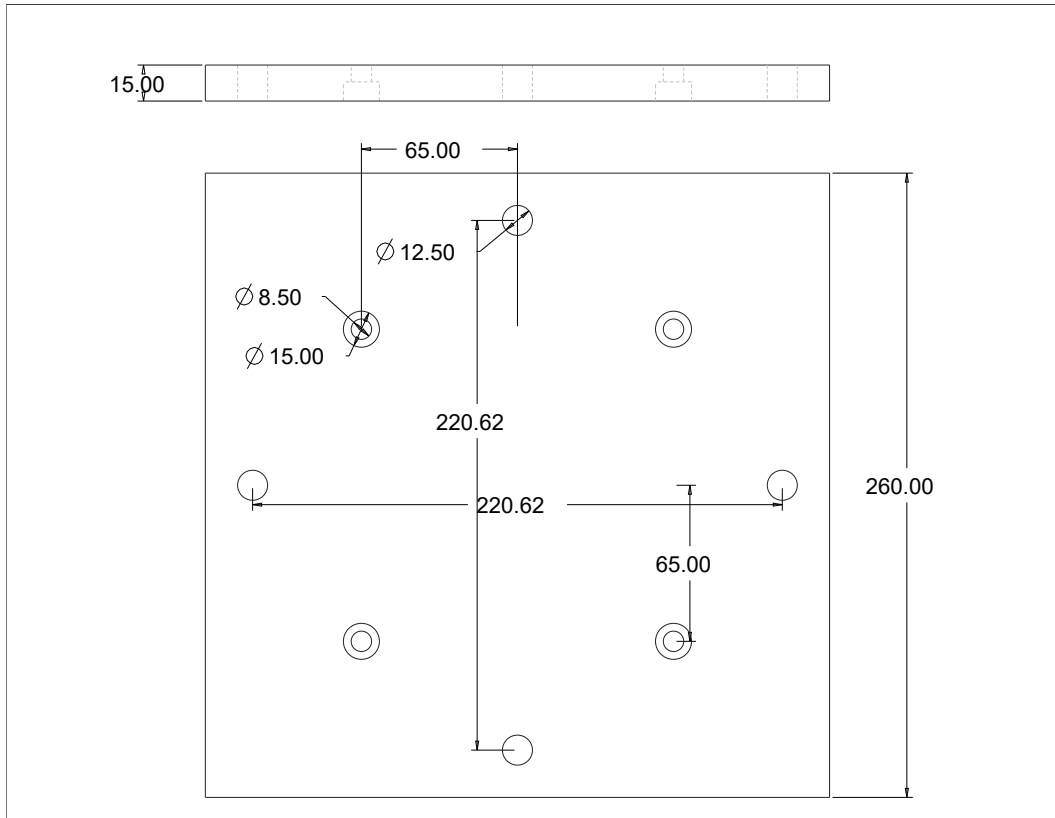


Figure 2.5: Top plate for fixing bend fixture in AMINO Press (dimensions are in mm)

## 2.2.6 Top Tool Holder

Top tool holder was designed in such a way that it provides flexibility to change the tool of a different dimension as well as proper insulation to stop electric current flow into the machine refer Fig. 2.6. Bakelite sheet and rods were used to provide insulation.

## 2.2.7 Top Tool

The top tool was designed in such a way that one tool itself was combination of four tools having different tool radius. Tool radius of 2, 4, 6 and 12 mm were considered for experiments refer Fig. 2.7.

To assemble top tool into tool holder another part was designed as shown in below Fig. 2.8

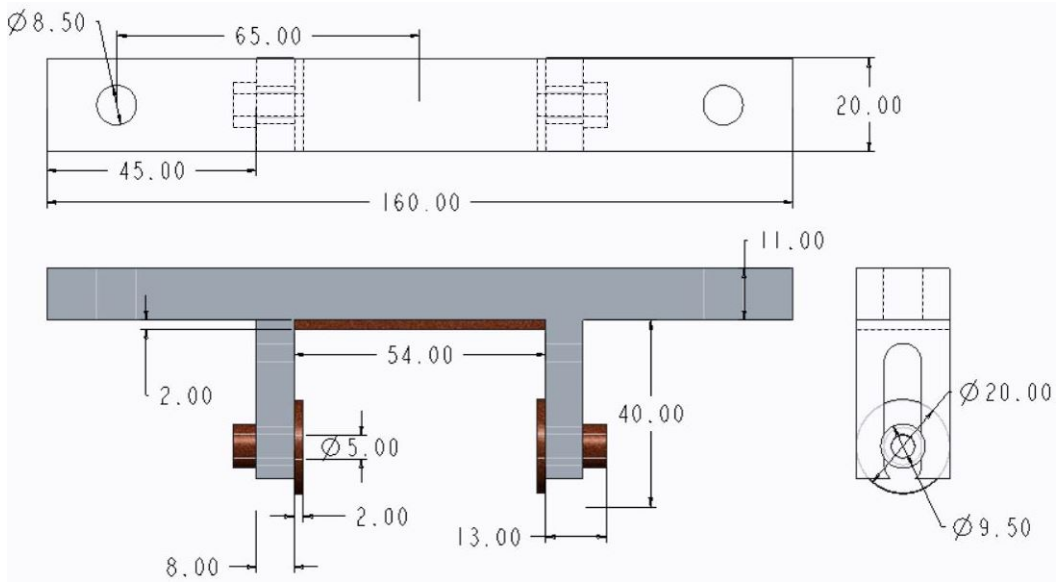


Figure 2.6: Top tool holder with bakelite insulation shown in brown color (dimensions are in mm)

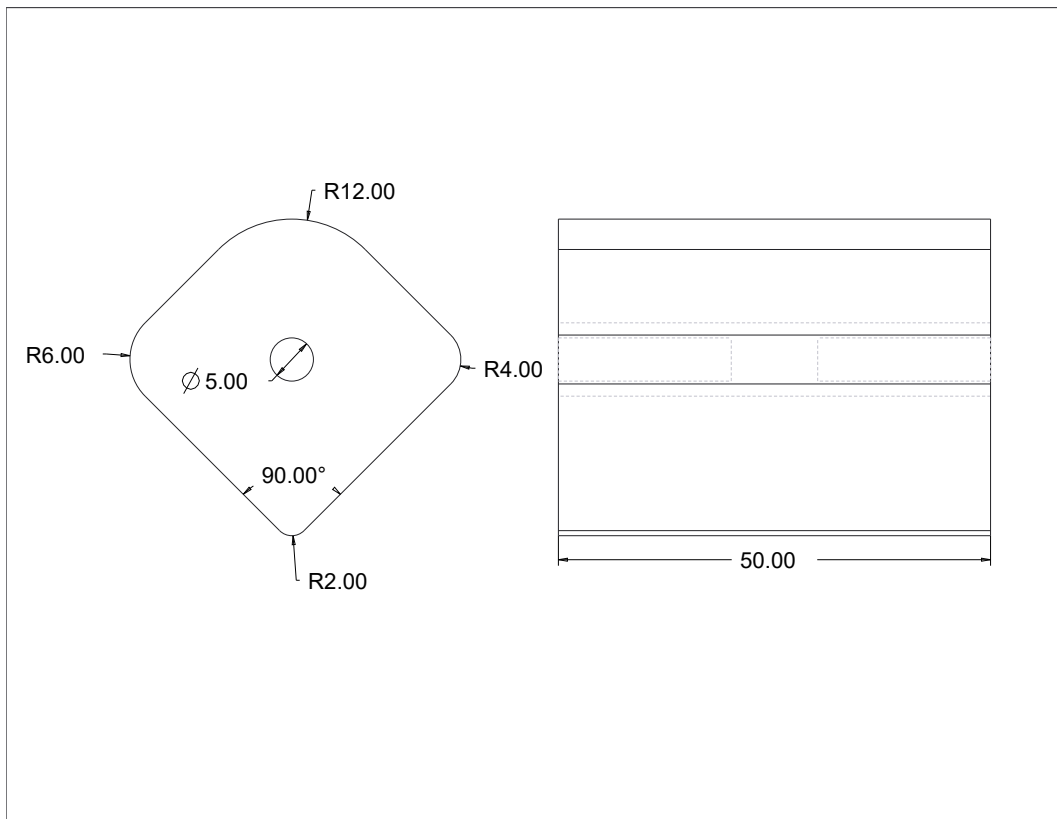


Figure 2.7: Top Tool with four different tool radius (dimensions are in mm)

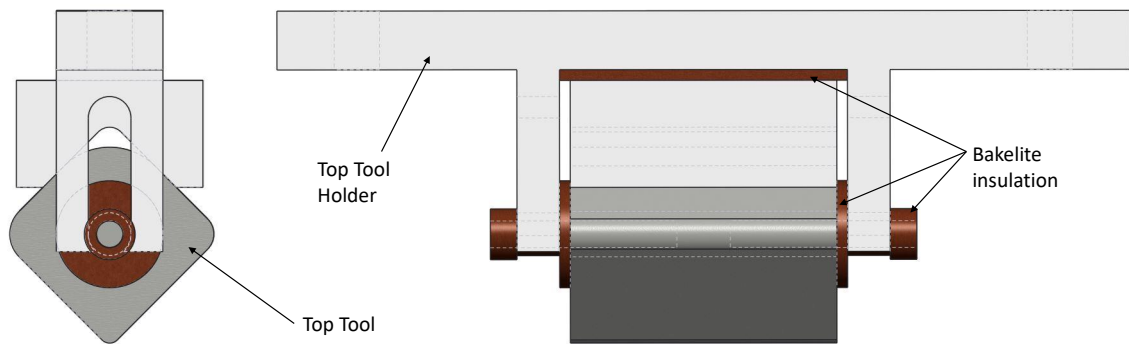


Figure 2.8: Top Tool assembly with tool holder

## 2.2.8 Other Parts to Fix Bend Fixture on CNC Machine

As bend fixture was designed such a way that it can be fixed on small CNC Incremental Sheet Metal Forming machine also. For this purpose, some other parts were designed refer Fig 2.9

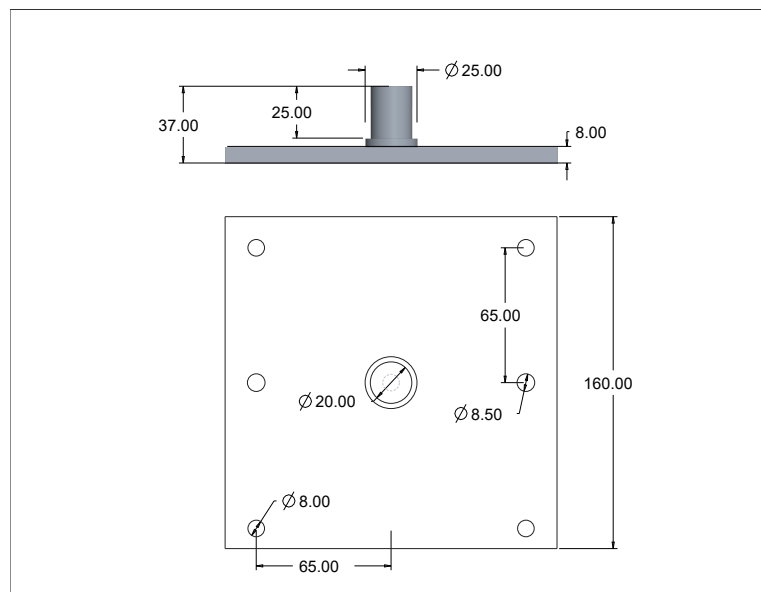


Figure 2.9: Parts to fix bend fixture on small ISMF CNC machine (dimensions are in mm)

## 2.3 Assembly of all Bend Fixture Parts

All above-designed parts are assembled in proper sequence. Bakelite sheets and rods are used as insulation material to prevent electric current flow into the machine. Bakelite has high melting temperature and good strength for compressive loads at the same time a good electrical insulator. For bottom tool, insulation was provided at two places one between die and die holder another one between bottom tool and the plunger. Similarly for top tool also, insulation was provided at two places refer Fig. 2.10.

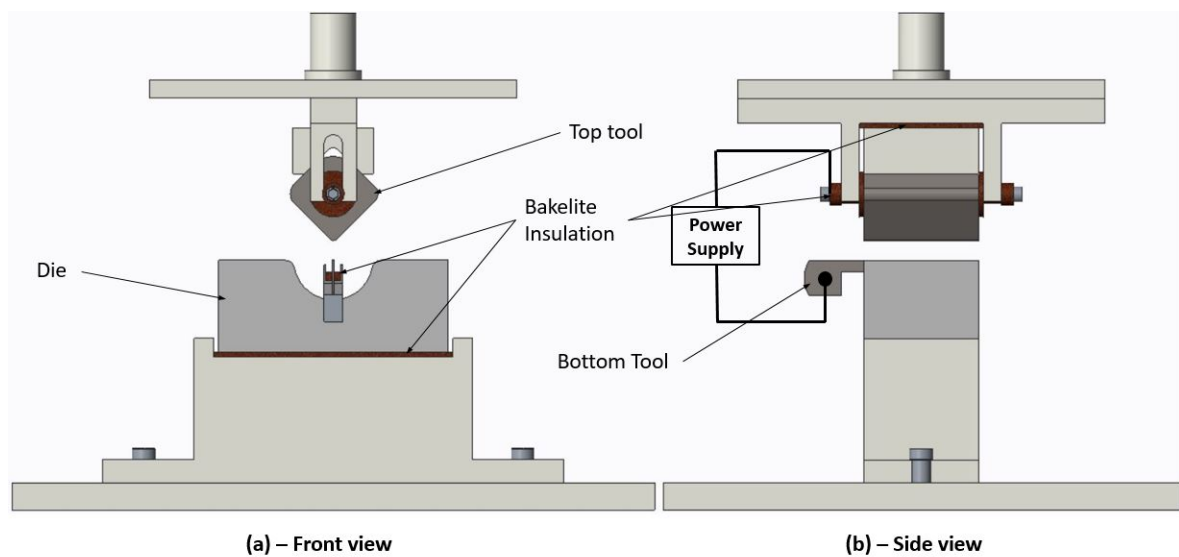


Figure 2.10: Bend fixture assembly

## 2.4 Fabrication of Fixture Parts

Fabrication of bend fixture was done in Central Workshop of IIT Hyderabad. Most operations were done on CNC vertical milling machine (BFW-Agni) and on wire EDM (Electronica) refer Fig 2.11. While performing various cutting operations biaxial tolerance of  $50 \mu\text{m}$  was maintained. As insulation is a very important aspect, it is taken into consideration in design as well as fabrication phase.

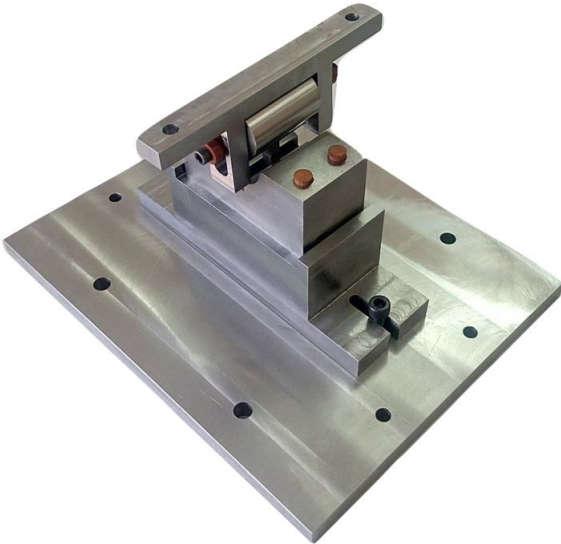


Figure 2.11: Fabricated bend fixture parts

# Chapter 3

## Finite Element Analysis of V-bending Experiments

### 3.1 Validation of Finite Element Analysis

Finite element analysis for sheet metal bending process is carried out and results are compared with experiments. Validation of finite element model is done by comparing FEA results with published results in literature. For validation, all process parameters and material properties are same as used in literature.

After validating FEA model with published literature, springback and bending force analysis was carried out for bending process and then results are compared with experiments.

#### 3.1.1 NUMISHEET Benchmark 2002 problem

For validating FEA model, NUMISHEET 2002 Benchmark problem [16] was modeled and results were compared with published results. U bending analysis was done in Benchmark problem to see effect of various parameters on springback and force values.

Tool and die were modeled as analytical rigid because deformation due to reaction forces can be neglected and study was focused on deformation sheet specimen refer Fig 3.1. The sheet was modeled as 3D deformable shell with thickness 1mm refer Fig. 3.2.

Aluminum was selected as material for bending simulation. Material properties are:

- Young's modulus - 70500 MPa

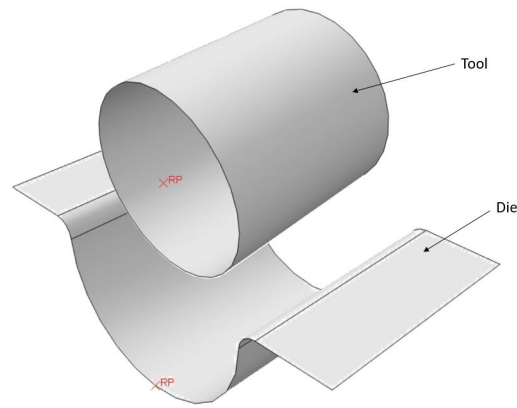


Figure 3.1: Tool and die (Analytical rigid)

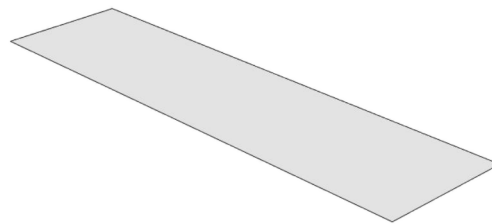


Figure 3.2: Sheet specimen (Deformable shell)

- Poisson's ratio - 0.346
- Initial yield stress - 197.01 MPa
- Hardening law -  $\sigma = (550.4) * (0.00812 + \epsilon_p)^{0.223}$

The tool was positioned in such a way that contact between sheet top surface and tool was maintained and at the same time bottom surface of sheet was in touch with the die surface. The entire process was modeled in two static general steps named as Deformation and Springback. In deformation step, the tool was specified to move by given punch stroke towards die and hence deformation was taking place. In next step, unloading of sheet specimen was modeled to see the springback effect.

Two steps were created to simulate complete sheet bending with springback:

- Deform - Tool moves in negative Y direction by specified punch stroke value.
- Springback - Tool retracts back (away) from deformed sheet and elastic recoveries take place in this step.

Boundary conditions to simulate Bending process:

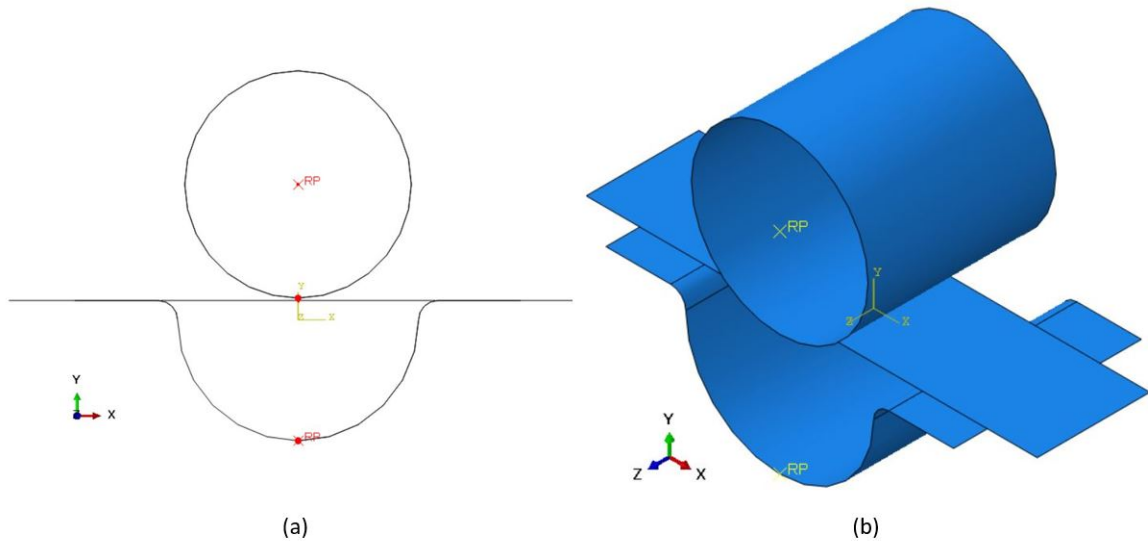


Figure 3.3: Tool, die, and sheet assembly at start of simulation (a) Front view, (b) Isometric view

- Die Constrain - At die reference point Encastre (Fix) was used to restrain its rigid body motion. This boundary condition remains active through both steps i.e. deform and springback.

$$U1 = U2 = U3 = UR1 = UR2 = UR3 = 0$$

- Tool Constrain - Translation degrees of freedom in directions other than punch stroke direction ( Y axis) are constrained also rotational degrees of freedom in all directions are constrained. This boundary condition was active in deform step only.

$$U1 = U3 = UR1 = UR2 = UR3 = 0$$

- Sheet Constrain - Sheet was constrained to move in X and Z direction to perform bending operation. These constraints are applied on the line created at middle of bottom surface of sheet. This boundary condition remains active only in deform steps.

$$U1 = U3 = UR1 = UR2 = UR3 = 0$$

- DeformY - In this boundary condition tool move in negative Y axis by given punch stroke value. This boundary condition was active only in deform step.

$$U2 = - (\text{Punch stroke})$$



- Retract - Tool was specified to move away from deformed sheet for springback after completion of deformation. This boundary condition was active only in springback step.

The interaction between tool and sheet and between sheet and die was defined as Surface-to-surface contact (Standard). Friction between these surfaces was defined as frictionless also with coefficient of friction 0.1348. For defining interaction, rigid bodies (tool and die) are considered as master and deformable sheet is defined as slave body. The interaction was active in deform step for both tool-sheet and die-sheet contacts whereas it was deactivated in springback step for die and sheet.

Mesh was generated for sheet using shell elements - S4R (4 noded reduced integration shell element). This element uses reduced integration rule hence only one integration point for the element to reduce computational time. S4R elements are suitable for thin sheets. Hourglass technique was selected to compensate for any induced error because of reduced integration rule. Mesh size was chosen as 1mm, hence total 3600 elements were generated. As analytical rigid bodies can not be meshed hence tool and die did not mesh.

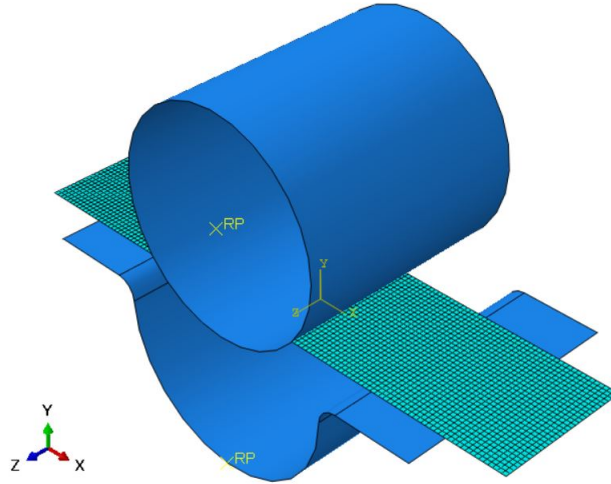


Figure 3.4: Mesh generated on sheet

### 3.1.2 Results and Comparison

#### Bend Angle

Bend angle before and after springback was calculated by using extracted data of nodal coordinates before and after springback from simulation results. These re-

sults were compared with published bend angle results in NUMISHEET benchmark problem 2002 [16].

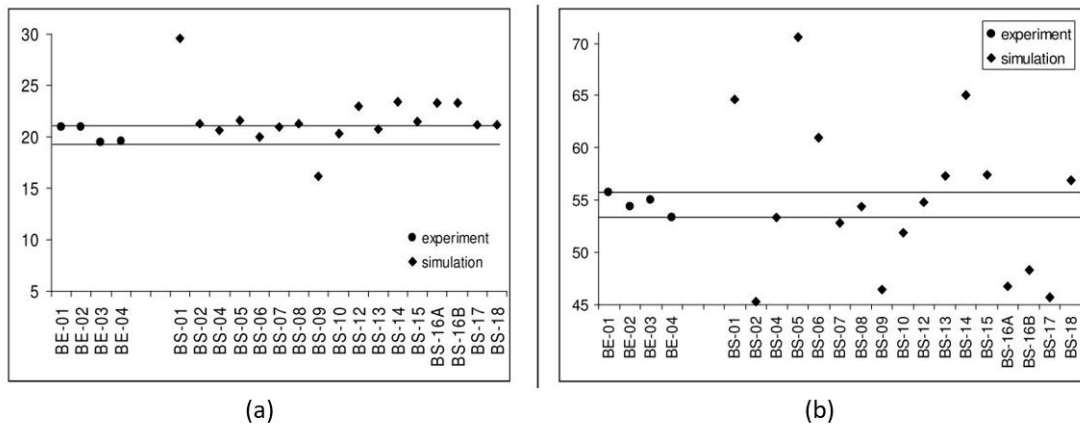


Figure 3.5: Bend angle (a) Before springback, (b) After springback for aluminum [16]

Comparison between published results and results obtained in Abaqus simulations shows very good agreement with error less than 2.5% refer Fig. 3.6.

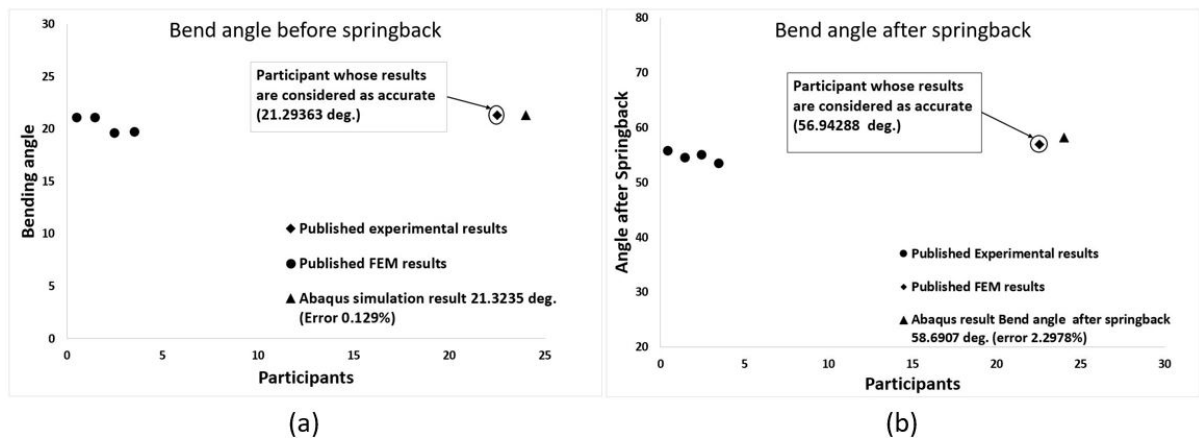


Figure 3.6: Bend angle comparison (a) Before springback, (b) After springback for aluminum

### Bending Force

Punch force was compared for both frictionless and with coefficient of friction 0.1348. Results from simulation and results from published data are plotted on the same graph to see the difference and it was observed that simulation results with frictionless process are matching approximately same refer Fig. 3.7. Also for results with

coefficient of friction 0.1348, the error of 7.5% was observed due to error in tracing published results refer Fig. 3.8.

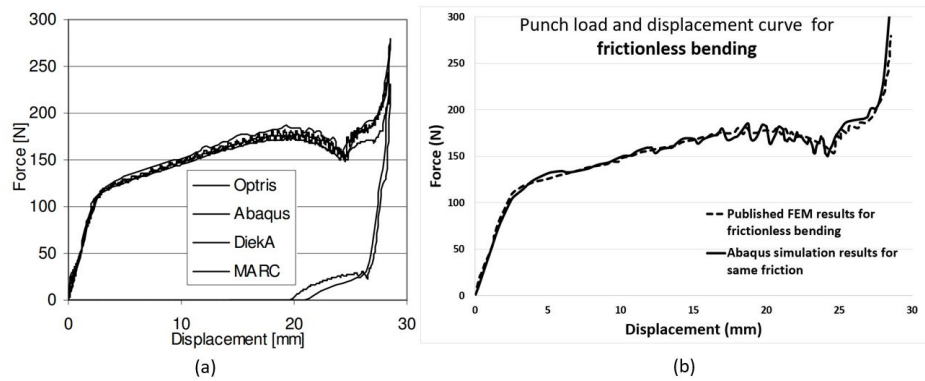


Figure 3.7: Bending force comparison (a) Published results [16] (b) Results obtained in Abaqus simulation for aluminum without friction

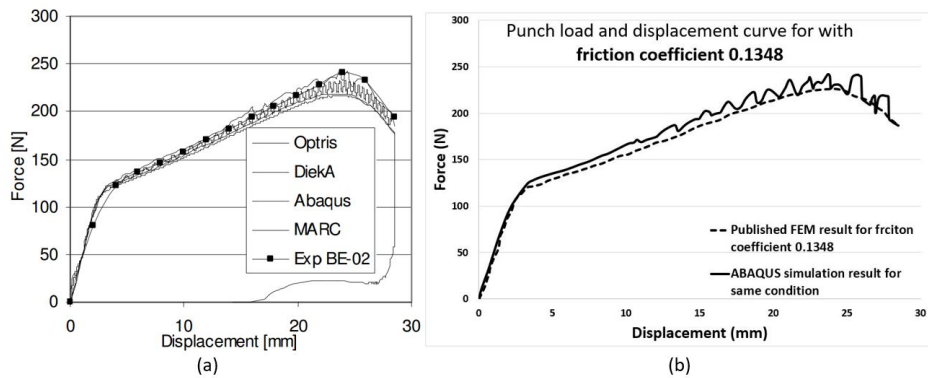


Figure 3.8: Punch force comparison (a) Published results [16] (b) results obtained in Abaqus simulation for aluminum with coefficient of friction 0.1348

### Effect of Sheet Thickness

Effect of sheet was simulated and compared with published results. It was observed simulation results are matching with published results with error of less than 5.5% refer Table 3.1.

### Mesh Convergence

Mesh convergence was performed for shell elements. Size for shell elements was varied from 0.25 mm to 2 mm and was observed that there is no significant effect of element size on bend angles before and after springback. Results were compared

Sheet thickness	Forming angle	springback angle
0.9	23.01	60.74
1.0	21.95	56.42
1.1	20.37	52.14

Figure 3.9: Effect of uniform sheet thickness on bend angles for shell model with coefficient of friction 0.1348 [16]

Table 3.1: Abaqus simulation results for different sheet thickness.

Sheet thickness (in mm)	Forming angle (in degree) (% error)	Springback angle (in degree) (% error)
0.9	22.56 (1.96%)	63.70 (4.65%)
1	21.32 (2.87%)	58.69 (3.87%)
1.1	20.08 (1.43%)	55.13 (5.42%)

with published benchmark problem and concluded that error between published and performed simulation results varies from 8-10% refer Table 3.2. Force data were also compared with published results. It was observed that with increase in element size fluctuation in force increases. Results show less fluctuation in case of very fine mesh i.e at mesh size 0.25 mm refer Fig. 3.11

Element size (mm)	forming angle	springback angle
0.25	21.83	53.89
0.5	21.84	53.90
1.0	21.77	53.46
2.0	22.75	no conv.
2.0 irregular	21.79	no conv.

Figure 3.10: Effect of element size on bend angles with coefficient of friction 0.1348 [16]

Table 3.2: Abaqus simulation results for different shell element size.

Element Size (in mm)	Forming angle (in degree) (% error)	Springback angle (in degree) (% error)
0.25	20.99 (3.83%)	58.48 (8.52%)
0.5	21.22 (2.84%)	58.76 (9.01%)
1	21.28 (2.25%)	59.08 (10.51%)
2	22.59 (0.70%)	not conv.

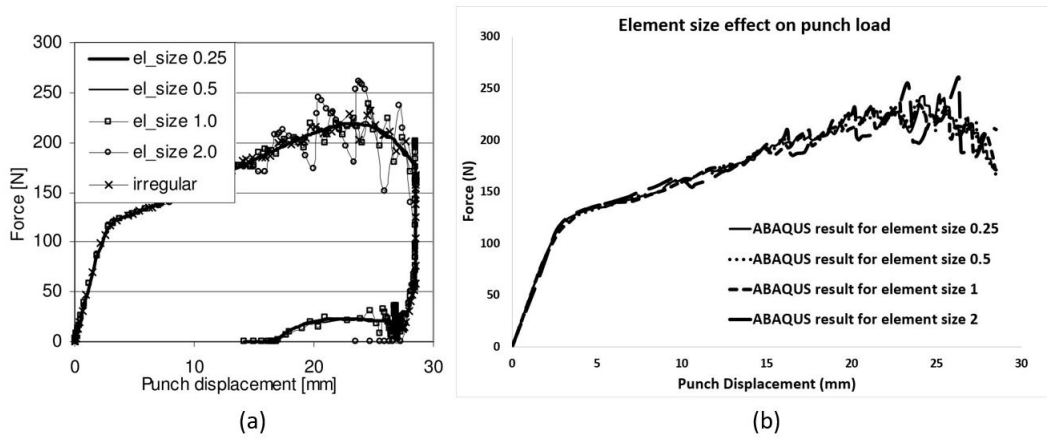


Figure 3.11: Effect of element size on bending force for frictionless process (a) Published results [16] (b) Results obtained in simulation

### 2D vs. 3D Modeling

Comparison between 2D model and 3D model was carried out to see the effects. As for 2D modeling, the plane-strain condition is assumed, which neglects any lateral bending effects. Whereas in 3D modeling lateral bending can be captured and hence the effect on results can be seen. It was observed that simulation results are matching with published results. Results are compared for both frictionless and with coefficient of friction 0.1348. Springback angles were also compared for, both models and it was concluded that for frictionless bending process these models give 5% Table 3.3 variation between 2D and 3D models. Whereas, models with coefficient of friction 0.1348 variation reduces to 3.5% refer Table 3.4.

	forming angle	springback angle
Plane strain	20.94	47.69
Shell	20.89	43.30

(a)

	forming angle	springback angle
Plane strain	20.90	53.55
Shell	20.92	53.27

(b)

Figure 3.12: Effect of plane strain model and shell model on bend angles (a) frictionless [16] (b) with coefficient of friction 0.1348 [16]

Figure 3.13 shows effect of shell and plane strain models on force for frictionless as well as with coefficient coefficient of 0.1348.

Table 3.3: Abaqus simulation results for different model approach for frictionless condition.

Abaqus model	Forming angle (in degree) (% error)	Springback angle (in degree) (% error)
Plane Strain	21.02 (0.4%)	51.28 (7.52%)
Shell	21.27 (1.84%)	48.22 (11.36%)

Table 3.4: Abaqus simulation results for different model approach for coefficient of friction 0.1348.

Abaqus model	Forming angle (in degree) (% error)	Springback angle (in degree) (% error)
Plane Strain	21.16 (1.26%)	61.42 (14.69%)
Shell	21.27 (1.68%)	59.13 (10.99%)

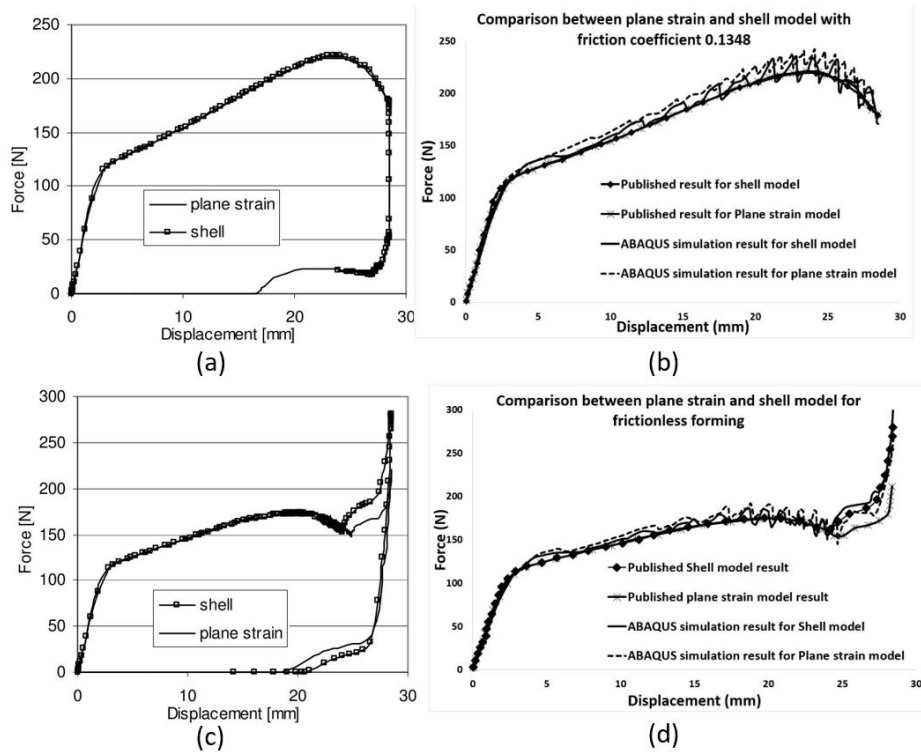


Figure 3.13: Effect of 2D and 3D models on bending force (a) published results [16] (b) results obtained in Abaqus, without friction (c) published results [16] (d) results obtained in Abaqus, with coefficient of friction 0.1348

### 3.1.3 Shell model analysis

Different journals were followed to validate the FEA model. For each model, boundary conditions (constraints) were kept same and other materials and geometrical parameters were changed according to published journal.

Micari et.al. [17] published shell model analysis of V-bending process for aluminum alloy material. They published effect of punch stroke on springback for which graphs between K (bend angle ratio after and before unloading) and punch stroke refer Fig. 3.14.

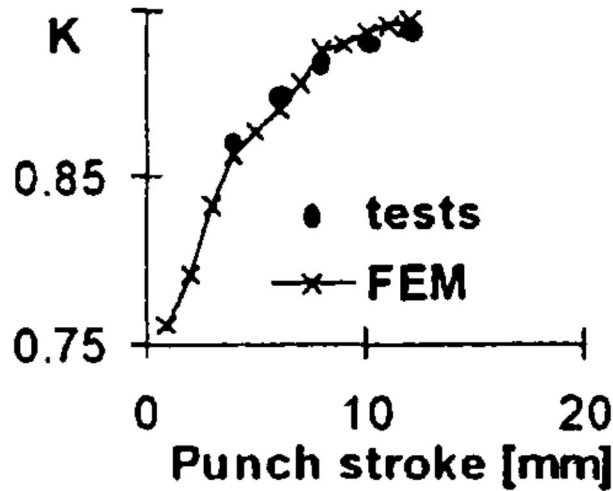


Figure 3.14: Effect of punch stroke on bend angle ratios [17]

Shell model was created in Abaqus software by keeping each parameter same as published [17] and by applying boundary conditions similar to the FEA analysis performed in section (3.0.1). Material for bending simulation was selected same as given in journal [17]. Material selected and its properties are as follows:

- Material - Aluminum
- Sheet thickness - 6 mm
- Young's modulus - 71700 MPa
- Poisson's ratio - 0.33
- Initial yield stress - 157 MPa
- Hardening law -  $\sigma = 563\epsilon_p^{0.257}$

Full model was symmetric about YZ-plane, hence only half model was considered for simulating bending process. The tool was positioned in such a way that contact between sheet top surface and tool was maintained at the starting of deformation process and at the same time bottom surface of sheet was in touch with the die surface. Two static general steps deformation and springback were created to see complete physical phenomenon.

- Deform - Tool moves in negative Y direction by specified punch stroke value.
- Springback - Tool retracts back (away) from deformed sheet and elastic recovery takes place in this step.

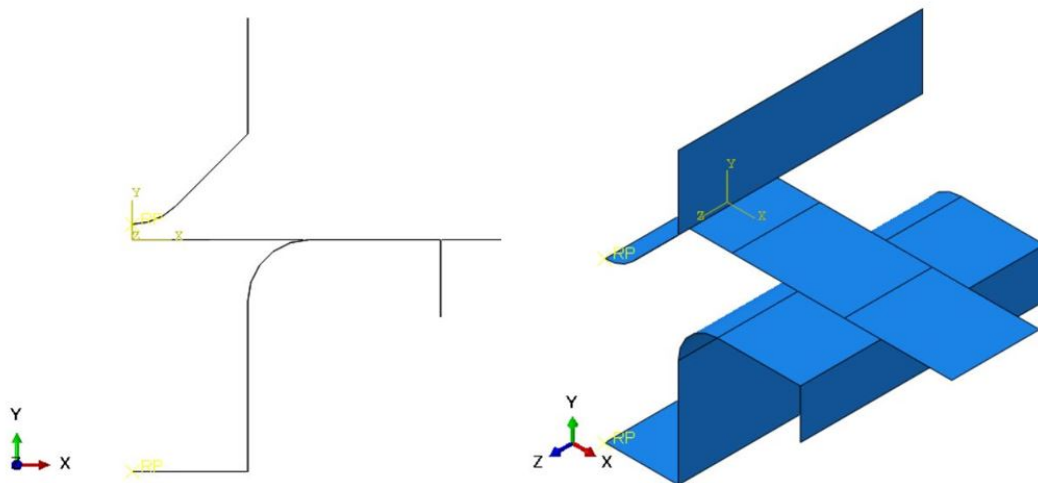


Figure 3.15: Tool, die, and sheet assembly at start of deformation (a) Front view, (b) Isometric view

All boundary conditions were kept same except punch stroke values, which kept changing according to published result [17].

The interaction between tool - sheet and die - sheet was defined as the surface-to-surface contact (Standard). Friction between these surfaces was defined by friction coefficient 0.05. All other things were kept same as for NUMISHEET model.

Mesh was generated for sheet using shell elements - S4R (4 noded reduced integration shell element). Mesh size was chosen as 1mm, hence total 910 elements were generated.



## Results Comparison

Results were compared between simulated model and published in paper. It was concluded that results are matching within 2% error. Fig. 3.16 shows variation between bend angle ratio with different punch stroke. It was observed that as punch stroke increases springback increases.

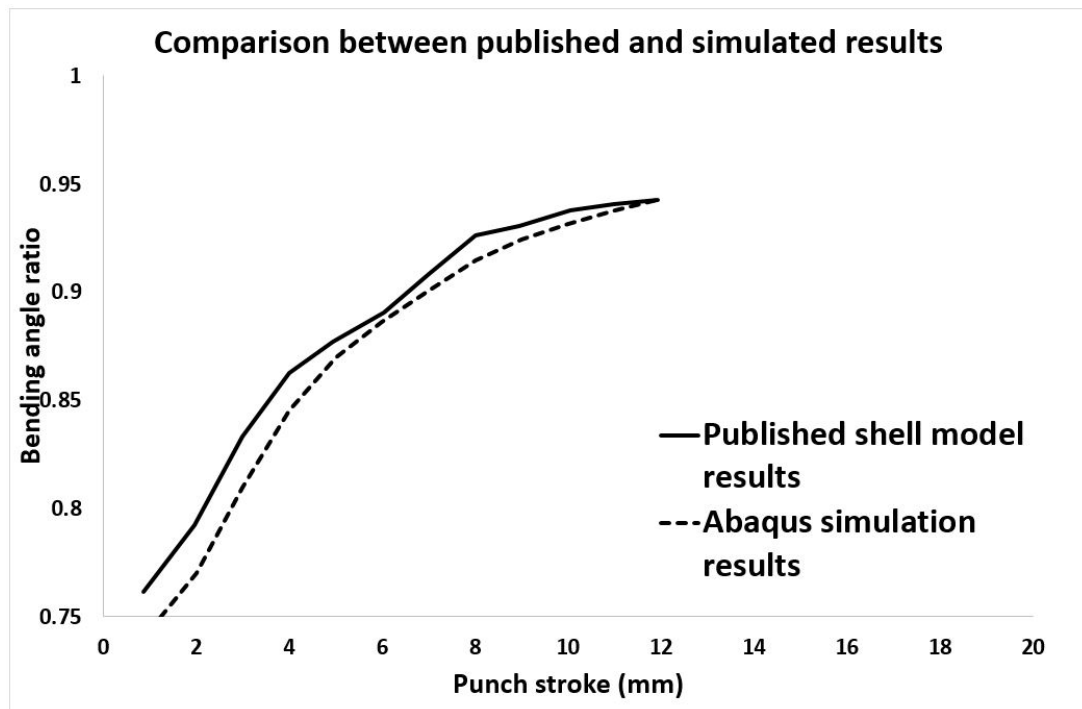


Figure 3.16: Comparison between results obtained in Abaqus simulation and published result

### 3.1.4 Solid Model Analysis

Vorkov et.al. [18] published simulation results for springback prediction of high-strength steels in air bending. Authors compared springback for two different materials also they obtained springback experimentally and compared it with FEA results. They observed that there is 4.7% and 1.5% error is for shell model analysis for Weldox 1100 and Weldox 1300 steels respectively. Whereas for solid analysis error for both materials got reduced to 2.1% and 1.1% respectively. Hence it was concluded that solid element analysis is more accurate as compared to shell element analysis refer Fig. 3.18.

The same model was created in Abaqus software to compare the results with published results.

Material properties and geometrical parameters were kept same as provided in paper [18]. Solid model with mesh size 1 mm in length direction and 5 number of elements in thickness direction was created, hence the total number of elements 3920 were generated. Elements of type C3D8R (8-noded linear brick, reduced integration, hourglass control solid element) were chosen for this analysis. All boundary conditions were kept same as discussed in section 3.0.1. Material for bending simulation was high strength steel Weldox 1100 and Weldox 1300. Material properties are:

- Sheet thickness - 4.15mm for Weldox 1100 and 4.10mm for Weldox 1300
- Young's modulus - 175 GPa
- Poisson's ratio - 0.33
- Initial yield stress - 1078.7 MPa for Weldox 1100 and 1046.3 MPa for Weldox 1300
- For plastic stress and strain values, tensile stress strain curve was given in Fig. 3.17

Two steps, Deform and Springback were created to see complete bending process and results were compared with published results.

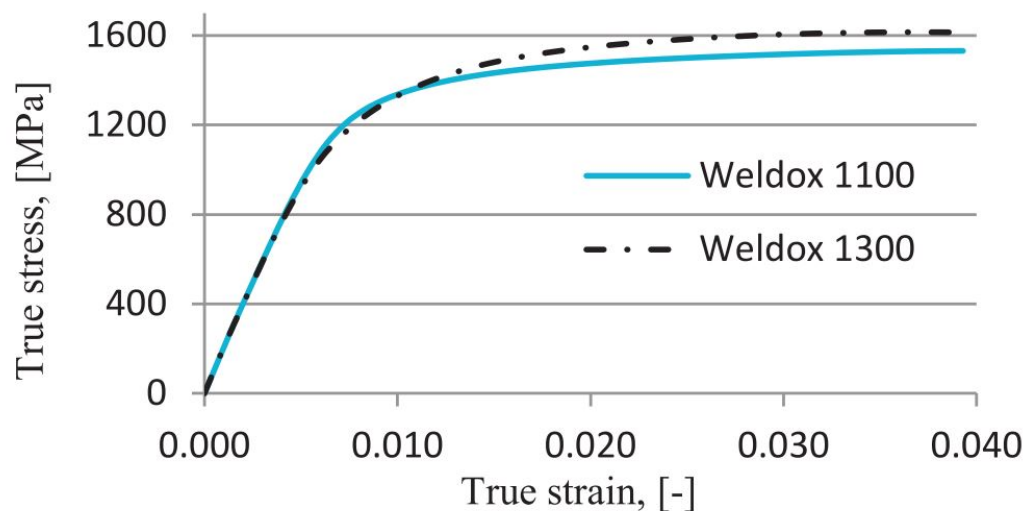


Figure 3.17: Stress-strain curve for both materials, Weldox 1100 and Weldox 1300 [18]

Material	Model	Springback, °	Calculation time, min	Error, %
Weldox1100	Experiment	23.5	-	-
	Shell	24.6	2.5	4.7
	Solid	24.0	60.0	2.1
Weldox1300	Experiment	26.2	-	-
	Shell	25.8	2.5	1.5
	Solid	25.9	60.0	1.1

Figure 3.18: Comparison of Finite Element Analysis and Experimental Results

Table 3.5: Abaqus simulation results for different model approaches for two different materials

Material	Model	Springback angle (in degree) (% error )
Weldox 1100	Shell	25.24 (7.38%)
	Solid	24.98 (6.29%)
Weldox 1300	Shell	27.54 (5.10%)
	Solid	26.72 (1.97%)

## 3.2 Shell and Solid Analysis Comparison for FEA Models

After validating FEA model with published results, solid vs. shell analysis was conducted to compare accuracy between these two models. For results comparison, NUMISHEET [16] results for shell analysis were used. To compare final results first mesh convergence for elements in thickness direction was performed. It was observed that results converge when the number of elements through the thickness is greater than 5.

Mesh convergence was done for the number of elements in the thickness direction, only to see the effect on springback. The number of elements were varied from 2 elements to 8 elements in thickness and was observed that after 6 results get stabilize at one value refer Table 3.6. Error with reference to shell model results was also presented in table.

Fig. 3.19 shows that when the number of elements increases above 5 results become constant, which suggests that springback prediction is accurate enough only when the number of elements through the thickness is equal to or more than 5 elements.

Table 3.6: Mesh convergence results for solid model in Abaqus for coefficient of friction 0.1348.

Number of elements through thickness	Forming angle (in degree) (% error)	Springback angle (in degree) (% error)
2	20.99 (3.89%)	67.68 (19.54%)
4	21.11 (3.33%)	59.72 (8.82%)
6	21.159 (3.12%)	58.77 (7.35%)
8	21.157 (3.11%)	58.398 (6.76%)

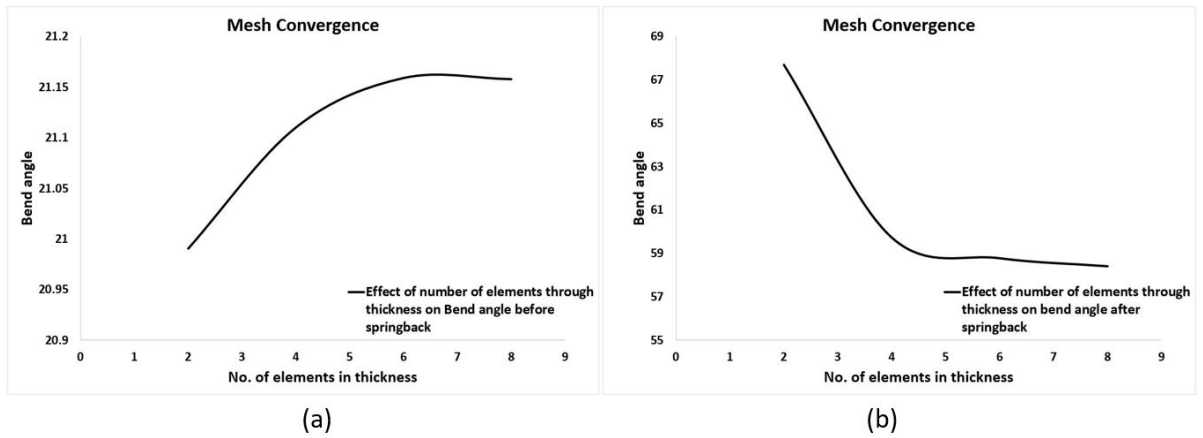


Figure 3.19: Mesh convergence study in solid analysis

### 3.3 FEA Analysis for Material Selection of Bend Fixture

Finite element analysis for steel material (thickness 5 mm) was carried out for deformable tool and support considering only elastic deformation for both parts. Stress results were extracted and used for setting up the material selection criterion for bend fixture. Elastic properties were given for tool and support whereas for sheet both elastic and plastic properties were given.

Material properties and dimensions were taken from S.Jiang [19].

Half model for stress analysis was developed refer Fig. 3.20 and tool, sheet, and supports are considered as solid deformable bodies. Generated stresses in tool and support provided criteria to select material for these parts. The material was selected such that the yield strength for that material must be higher than stress generated, to avoid any plastic deformation in tool and die. Two static, general steps were created

as deform and springback. Deform step was to simulate deformation process whereas in springback elastic recoveries were simulated.

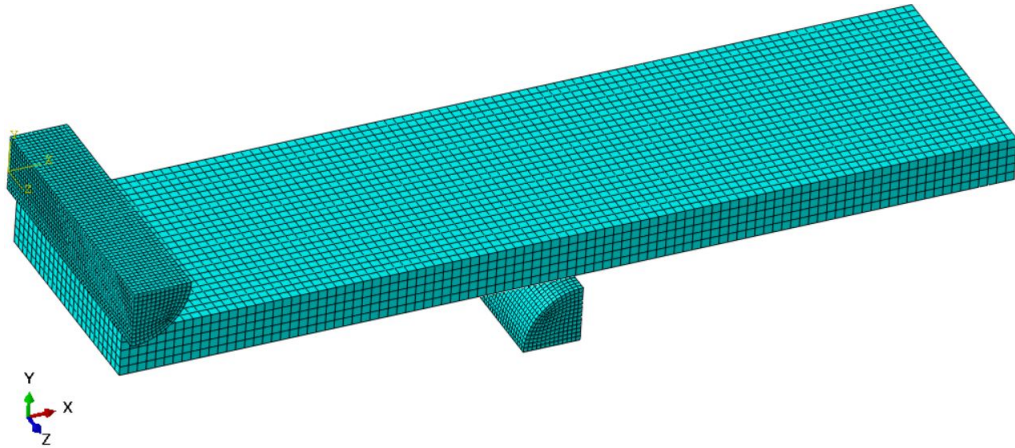


Figure 3.20: Deformable tool and support analysis for material selection of bend fixture

Boundary conditions for the bending process:

- Support Constrain - As support is a deformable part hence to constraint all rigid body motion XZ plane (at bottom) in support was selected refer Fig. 3.20. This boundary condition was active in both deform and springback step.

$$U1 = U2 = U3 = UR1 = UR2 = UR3 = 0$$

- Tool Constrain - Translation motion in all direction except Y axis and rotation in along all axis was constraint at the selected XZ plane (at top) in tool refer Fig. 3.20. This boundary condition was active in all steps.

$$U1 = U3 = UR1 = UR2 = UR3 = 0$$

- Sheet Constrain - At left face of sheet YZ plane was selected to constrain translation in X axis and rotation in X and Z axis. This boundary condition was active in only deform step.

$$U1 = U3 = UR1 = UR2 = UR3 = 0$$

- DeformY - At tool plane XZ was selected (at top) to give specified punch stroke in negative Y direction refer Fig. 3.20. This boundary condition was active only in deform step.

$$U2 = -(\text{punch stroke} = 12.7)$$

- Retract - At the same XZ plane on tool translation motion in positive Y direction was given retraction of tool. This boundary condition was active only in springback step.

$$U2 = 5$$

For meshing tool and support solid elements - C3D8R( 8-node linear brick, reduced integration solid elements) were used. Mesh size of 0.5 mm for both tool and support is used, hence total 9000 elements for each part were generated.

### 3.3.1 Stresses Generated During Bending Process

At both tool and support generated stress values were extracted. Results show that at tool stress of magnitude 460 MPa and on support 100 MPa refer Fig. 3.21.

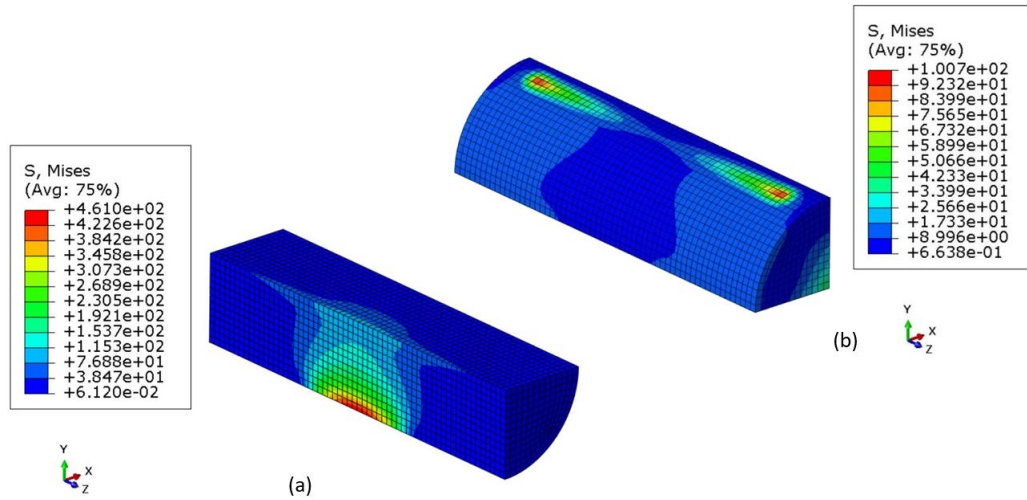


Figure 3.21: Maximum stresses generated in (a) Deformable tool and (b) Support

## 3.4 Finite Element Analysis for IFHS 350 and HSQ 440 Steel U-die Bending Process

The U-die bending process was modeled in Abaqus software to see springback and force variation by varying fixture dimensions and friction conditions. Material selected for this analysis was IFHS 350 and HSQ 440 steel. The material properties were provided by TATA Steel.

Punch and die of U-shape was modeled as analytical rigid refer Fig. 3.22, because deformation in these parts was neglected during experiment. Sheet specimen was

modeled as shell part to see the springback and forces variation with parameters. As the material properties were provided for three different thickness hence simulation for all provided thickness were performed. The material properties in rolling direction are:

- Sheet thickness - IFHS 350 steel 0.7 and 0.8 mm, and HSQ 440 steel 1.43 mm
- Young's modulus - 220000 MPa
- Poisson's ration - 0.33
- Yield strength - 205.5 Mpa and 185.15 Mpa for IFHS 350 steel of thickness 0.7 mm and 0.8 mm respectively. 333.4 MPa for HSQ 440 steel
- Hardening law -

$$\sigma = 600 * \epsilon_p^{0.227} \quad (3.1)$$

$$\sigma = 600 * \epsilon_p^{0.23} \quad (3.2)$$

$$\sigma = 750 * \epsilon_p^{0.198} \quad (3.3)$$

for IFHS 350 0.7 mm thickness, 0.8 mm thickness and C Mn 440 steel respectively

- Anisotropic r-values -  $r_o = 1.213$ ,  $r_{45} = 1.875$  and  $r_{90} = 1.367$

for IFHS 350 0.7 mm thickness

$$r_o = 1.389, r_{45} = 1.473 \text{ and } r_{90} = 1.77$$

for IFHS 350 0.8 mm thickness

$$r_o = 0.769, r_{45} = 1.03 \text{ and } r_{90} = 0.956$$

for HSQ 440 1.43 mm thickness

For defining planar anisotropy in Abaqus  $R_{11}$   $R_{22}$   $R_{33}$   $R_{12}$   $R_{13}$   $R_{23}$ , need to be evaluated. R values are defined as stress ratio between stress generated at that particular plane and some reference stress constant value refer Abaqus 6.13 user manual section 23.26. Let yield stress  $\sigma_y$  is to be defined as equal to  $\sigma_{11}$  in metal

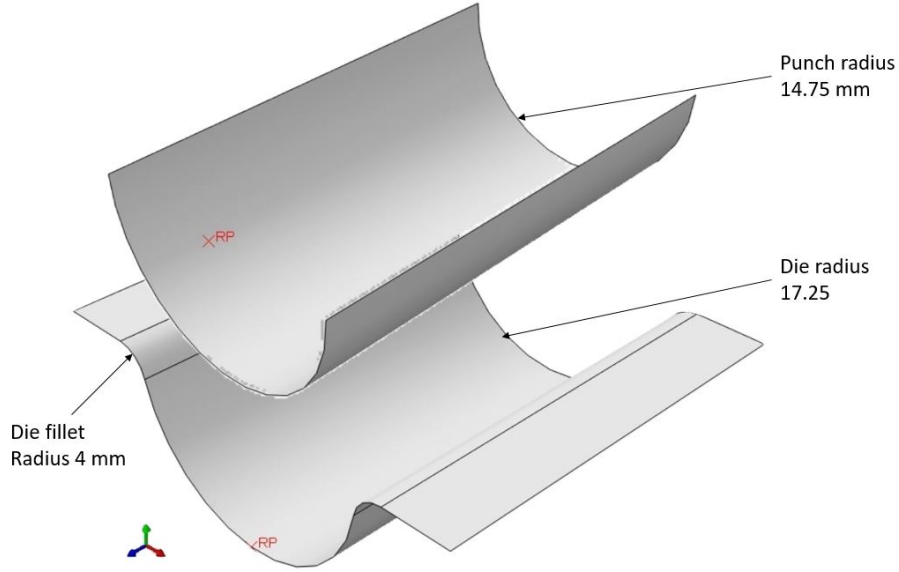


Figure 3.22: Punch and Die parts modeled in Abaqus software

plasticity model, then these R-values are formulated as:

$$R_{11} = 1 \quad (3.4)$$

$$R_{22} = \sqrt{\frac{r_{90}(r_o + 1)}{r_o(r_{90} + 1)}} \quad (3.5)$$

$$R_{33} = \sqrt{\frac{r_{90}(r_o + 1)}{r_o + r_{90}}} \quad (3.6)$$

$$R_{12} = \sqrt{\frac{3(r_o + 1)r_{90}}{(2r_{45} + 1)(r_o + r_{90})}} \quad (3.7)$$

$$R_{23} = 1 \quad (3.8)$$

$$R_{31} = 1 \quad (3.9)$$

Steps and boundary conditions and interaction properties were kept same as discussed in section 3.1.

Mesh was generated for sheet using shell elements - S4R ( 4-node doubly curved thin or thick shell, reduced integration, hourglass control shell element). Reduced integration with hourglass method was used to save computational time and at the same time without any lose in accuracy.



### 3.4.1 Results and Discussion

#### Springback Calculation

In sheet metal bending, springback is defined as the deviation in bend angle from actual value after the unloading process. Hence springback is the difference between the angle of flat portion of bend sheet at end of loading and angle of flat region of bend sheet after the complete removal of loading. So in FE analysis springback is the reduction in bend angle between deform and Springback step. If the bend angle after deformation is  $\alpha_i$  and bend angle after retract step is  $\alpha_f$ , then springback is defined as  $(\alpha_i - \alpha_f)$  refer Fig.3.23.

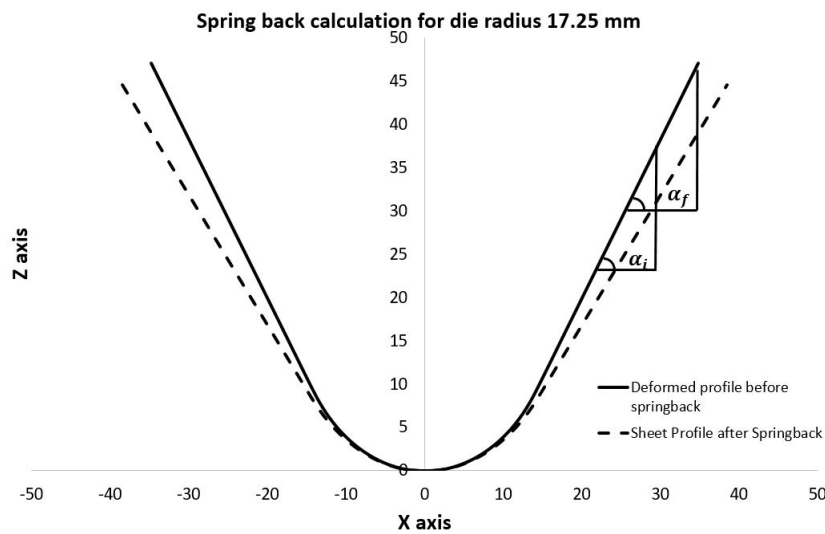


Figure 3.23: Measurement of springback angle in bending process

#### Friction Effect on Springback

Effect of friction between contacting surfaces was observed by simulating complete bend process by changing coefficient of friction from 0, 0.1, 0.15, and 0.2 in design for all three materials. The effects were compared for three different fillet radius of 2, 4, 6 mm.

For IFHS steel with thickness 0.7 mm, it was observed that with increase in friction coefficient springback increases. There was slight increase in springback with decrease in fillet radius also. Magnitude of springback angle got reduced for same friction coefficient when die fillet radius got increased refer Fig. 3.24.

Results shows that there was approximately 1.5 deg. increase in springback angle with increase in friction. Slope of these plots indicates that with fillet radius effect

remains same but only magnitude got decreased.

Exactly same effect was observed for IFHS 350 steel of thickness 0.8 mm. With increase in friction springback got increase by magnitude of approximately 1.5 deg. for all cases of fillet radius except 6 mm. It was observed that for 6 mm fillet radius effect got decreased slightly and for this fillet radius there was only 0.5 degrees change in springback with increase in friction coefficient refer Fig. 3.25.

For HSQ 440 steel results show that there is no significant effect of die fillet radius on springback for both isotropic and anisotropic models refer Fig. 3.26.

Figure 3.26 shows slight variation in springback angle when coefficient of friction changes from 0 to 0.1, but as friction increases springback becomes almost constant.

### 3.5 Finite Element Analysis for HSQ steel V-bending Process

The V-bending process was modeled in Abaqus software to see springback and force during deformation. Simulations were carried out for HSQ steel material and material properties were provided by TATA Steel.

All experimental parameters were kept same as designed for bend fixture. Punch and die were created as analytical rigid parts refer Fig. 3.27 whereas sheet is selected as deformable 3D part refer Fig. 3.28. The sheet was partitioned in such a way that fine mesh was generated in deformation zone and at other places, coarse mesh was generated.

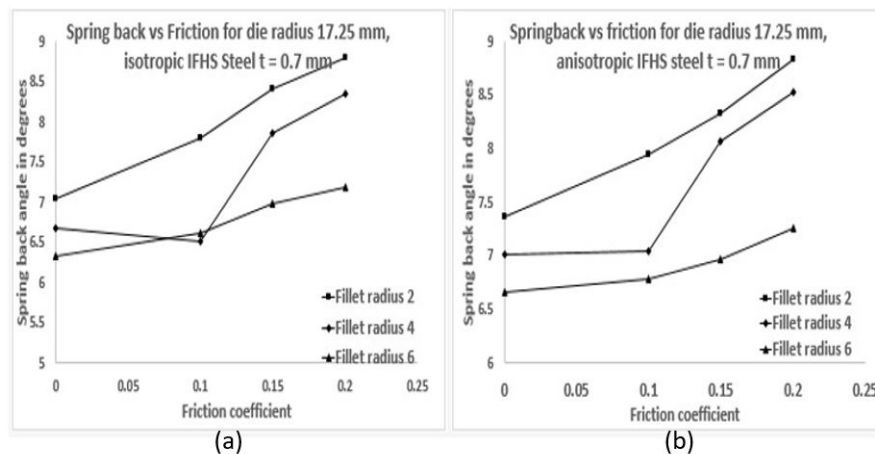


Figure 3.24: Friction coefficient effect on springback for IFHS 350 steel for thickness 0.7 mm (a) Isotropic model and (b) Anisotropic model

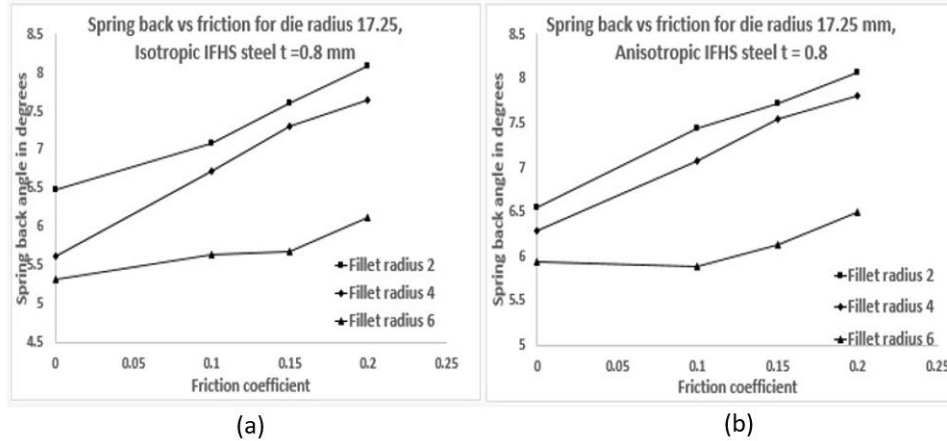


Figure 3.25: Friction coefficient effect on springback for IFHS 350 steel for thickness 0.7 mm (a) Isotropic model and (b) Anisotropic model

As sheet metal bending was carried out along the rolling direction, hence material properties in rolling direction were considered for FE analysis. Planar anisotropic constants were used to input anisotropic behavior in the analysis. Material properties were given for both elastic as well as plastic deformation. Young's modulus and Poisson's ratio are given for elastic behavior and for plastic behavior stress strain curve data is provided to Abaqus. Material properties in rolling direction are:

- Young's modulus - 200000 MPa
- Poisson's ratio - 0.33
- Initial yield stress - 326 MPa
- Hardening law -  $\sigma = 746.349(0.005189 + \epsilon_p)^{0.19071}$
- Anisotropic r-values -  $r_o = 0.8751$ ,  $r_{45} = 1.1986$  and  $r_{90} = 1.1326$

Anisotropic properties are given by providing potential options in Abaqus same as mentioned in section 4.2.

To see complete effect of sheet metal bending two static general steps were created:

- Deform - To simulate only deformation process. In this step punch moves in the negative Y direction by specified punch stroke.
- Springback - To simulate elastic recovery which occurs during unloading. In this step, punch retracts back (away) from the sheet and hence elastic recovery takes place.

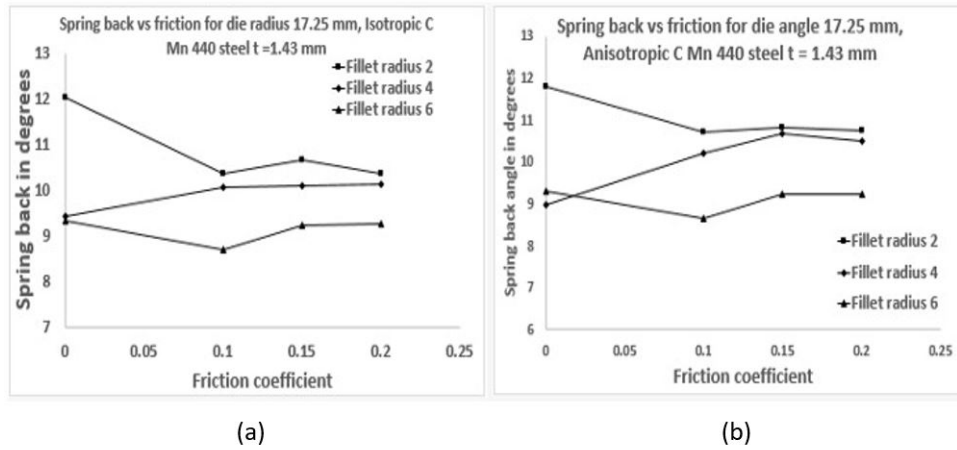


Figure 3.26: Die fillet radius effect on springback for HSQ 440 steel (a) Isotropic model and (b) Anisotropic model

Boundary conditions for V-bending process:

- Die Constrain - At die reference point Encastre(Fix) was used to restrain all degrees of freedom hence for die, rigid body motion was not allowed. This boundary condition remained active through both steps i.e. deform and spring-

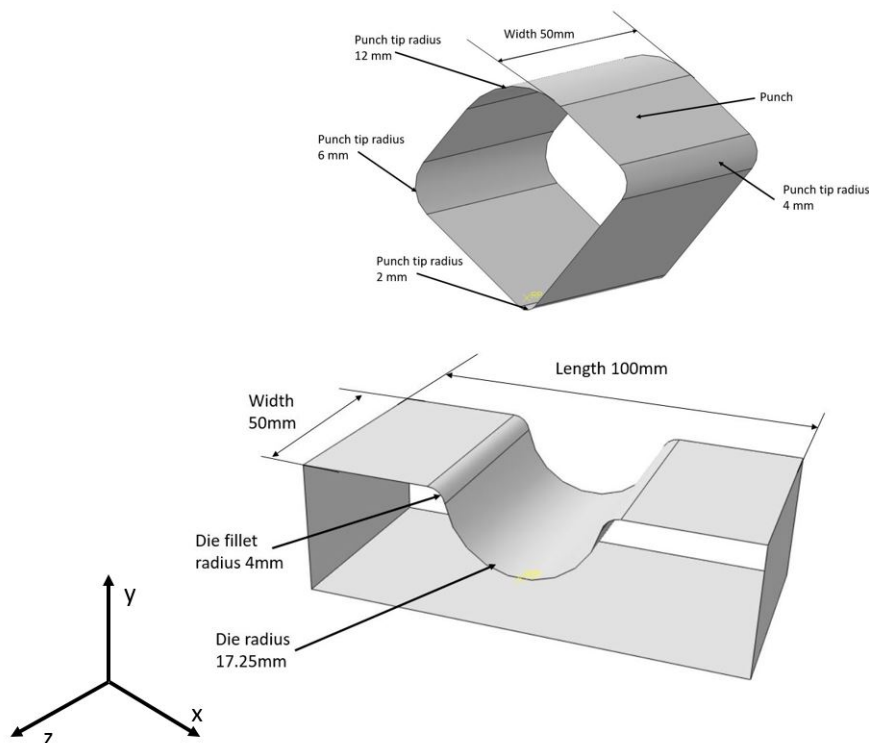


Figure 3.27: Modelled Punch and Die part in Abaqus software

back.

$$U1 = U2 = U3 = UR1 = UR2 = UR3 = 0$$

- Punch Constrain - Translation degrees of freedom (other than punch stroke direction Y axis) and all rotational degrees of freedom were constrained. Punch was allowed to move only in punch stroke direction. This boundary condition remained active in all steps.

$$U1 = U3 = UR1 = UR2 = UR3 = 0$$

- Sheet Constrain - Sheet was constrained to move in X and Z directions to perform bending operation. These constraints are applied on the line created in the middle of the bottom surface of the sheet. This boundary condition remained active only in deform step.

$$U1 = U3 = UR1 = UR2 = UR3 = 0$$

- DeformY - In this boundary condition Punch was allowed to move by given punch stroke value. This boundary condition remained active only in deform step.

$$U2 = -(\text{specified Punch Stroke})$$

- Retract - Punch was specified to move away from the sheet for springback after completion of deformation. This boundary condition remained active only in springback step

$$U2 = 5$$

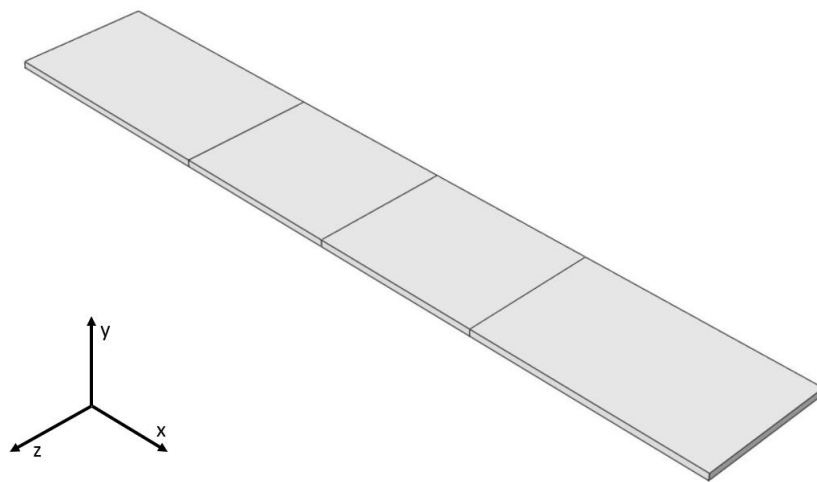


Figure 3.28: Modelled sheet specimen in Abaqus software

The interaction between die-sheet and punch-sheet was defined by using Surface-to-surface (standard) contact methodology. Simulation with coefficient of friction 0.01 and without friction was carried out to see the effect on springback and punch reaction force. Rigid body surfaces are considered as master surfaces and sheet is considered as slave surface. The interaction between punch and sheet was kept active for both steps. To simulate springback process also at the same time for avoiding rigid body motion of sheet in springback step interaction between die and sheet was deactivated in springback step.

Mesh was generated for sheet using solid elements - C3D8R( 8-node linear brick, reduced integration solid elements). Reduced integration methodology was used to reduce the computational time. To eliminate the errors induced due to reduced integration hourglass control method was selected. Mesh size of 0.25 mm in deformation zone whereas 2 mm in the place where no deformation takes was chosen. In thickness direction 6 elements were considered, hence total 30240 elements were generated refer Fig. 3.29. As analytical rigid bodies can not be meshed hence tool and die were not meshed.

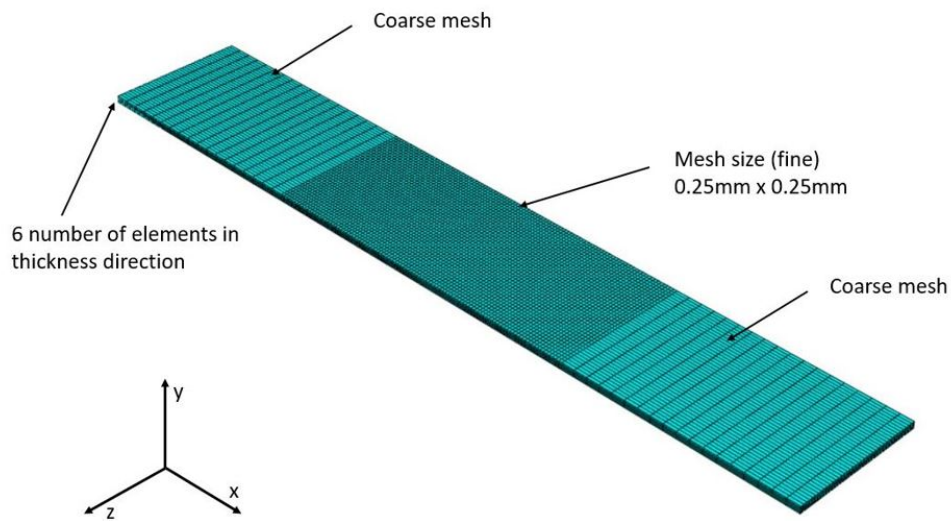


Figure 3.29: Mesh generated on sheet

### 3.5.1 Results and Discussion

#### Effect of Width on Springback

As it is well known fact that current density is the main factor for electroplastic effect, which suggest that with change in cross-sectional area of specimen effect also changes.

For the case of sheet metal bending cross-sectional area depends of sheet width and tool radius. With decrease in sheet width current density can be increased which in turns increases electroplastic effect.

Before selecting proper width to ensure maximum electroplastic effect, FEM simulation for width effect on bending, without current carried out and the results were compared with experiments. This analysis was to prove that with change in width, springback is changing solely due to current density and there is no mechanical factor involved in springback change.

Four different width samples were selected for this analysis (10 mm, 20 mm, and 40 mm) and punch stroke of 10 mm was kept same for all experiments. For FEM springback angles were measured and compared for different width simulations. Springback results are shown in following Table 3.7.

Table 3.7: Effect of width on springback keeping all other same conditions.

Sheet width (in mm)	Bend angle before unloading (in degree)	Bend angle after unloading (in degree)	Springback
10	61.99	53.79	8.19
20	61.97	53.76	8.21
40	61.77	53.57	8.21

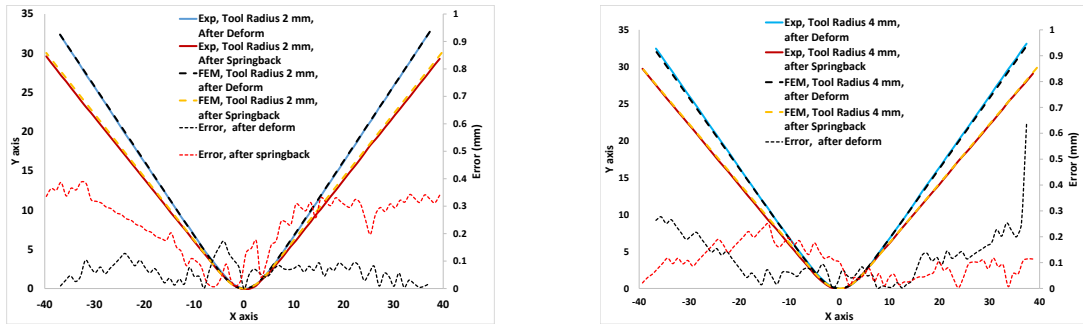
Results shows that there is no effect of width on springback for without electric assisted bending process.

### **Tool Radius Effect on Springback**

As tool radius also one of the deciding parameter in current density, hence before conducting electric assisted bending experiments, tool radius effect was simulated and compared with experiment results.

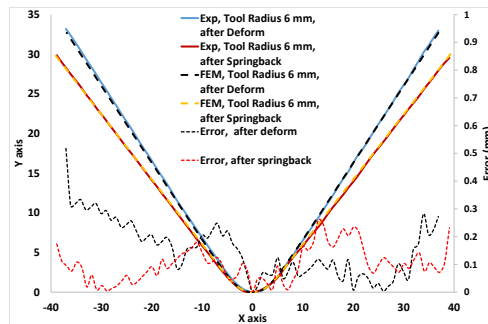
Bending simulations for tool radius 2 mm, 4 mm and 6 mm were performed. Punch stroke of 15 mm was kept same for all simulations and results were compared with experiments. For comparison bend sheet profiles were on same plots refer Fig. 3.30 to see any variation also bend results were also calculated refer Table 3.8.

Results shows due to difference in tool radius there is slight change in springback angles for bending processes. During electroplastic bending experiments interaction effect between tool radius and current density can be a good factor to create difference in springback.



(a)

(b)



(c)

Figure 3.30: FE and experimental springback results comparison for different tool radius

Table 3.8: Effect of tool radius on springback keeping all other same conditions.

Tool Radius (in mm)	Bend angle before unloading (in degree)	Bend angle after unloading (in degree)	Springback
2	87.14	77.52	9.62
4	87.22	77.58	9.64
6	88.30	78.52	9.78



# Chapter 4

## Experimental Investigation of Electroplasticity on HSQ steel

### 4.1 Experimental Planning

Experiments without the assistance of electric current were performed to see the effect of specimen width and tool radius effect on springback. As with change in sheet width and tool radius in electric assisted bending will cause change in current density which can results in springback. Hence effect of width and tool radius without electric current in necessary to examine, to differentiate between mechanical and electrical effect.

#### 4.1.1 Width effect

Bend angle springback was compared for different width specimen was compared and it was observed and it was found that springback is varrying randomaly with specimen width refer Fig. 4.1. To check repeatability each experiments were carried out three times.

Results were compared with FE analysis and was concluded that changes in springback in not due to some mechanical effect as FE results had shown no effect of width on springback.

To measure bend angle after springback, graph sheet of grid size 1 mm was used. It was observed that sheet specimens are having some initial curvature present. Because of initial curvature present in specimens, bend angle measurement was not accurate. Hence discrepancies in results of FEA and experiments were observed. On measurement of initial curvature present in each specimen was not uniform and was

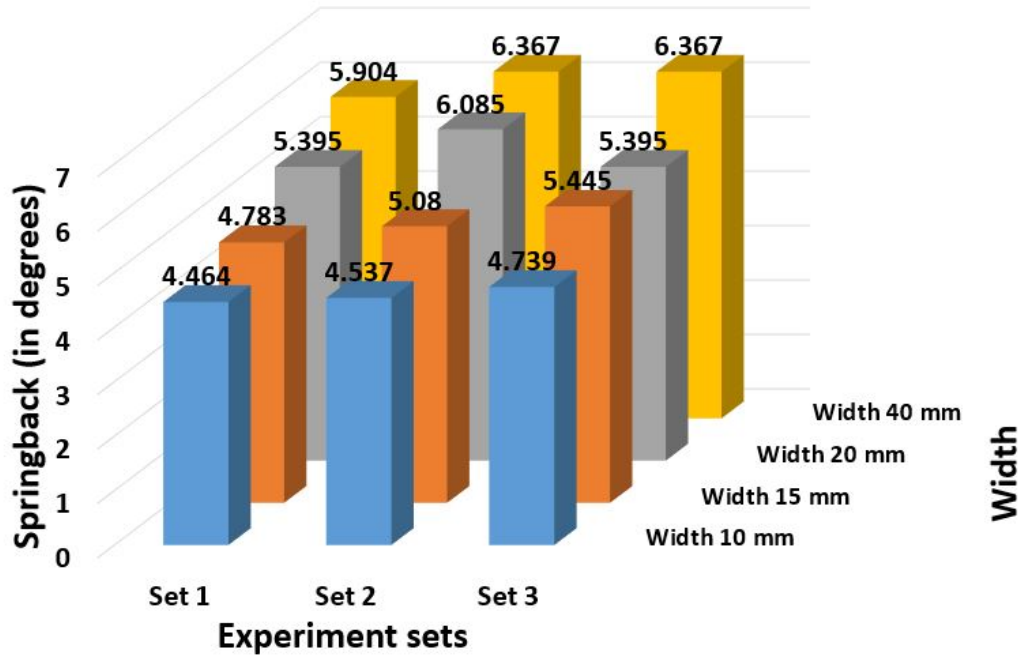


Figure 4.1: Width effect on springback

varying from 0 to 500  $\mu\text{m}$  Fig. 4.2.

**Present curvature in sheet**

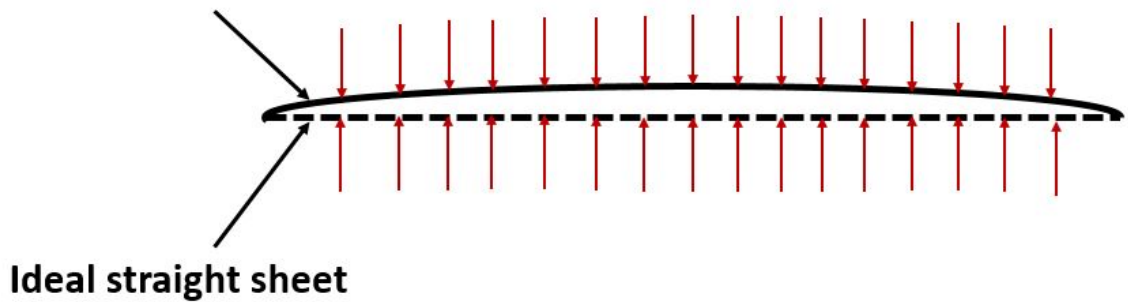


Figure 4.2: Initial curvature present in sheet specimens

Hence in presence of initial curvature in sheet specimens, bend angle measurement was not accurate for springback comparison, for comparison of springback radius of curvature was measured in deformation zone only Fig. 4.3. Difference between radius of curvature before and after springback was measured and reported as springback in sheet metal bending process.

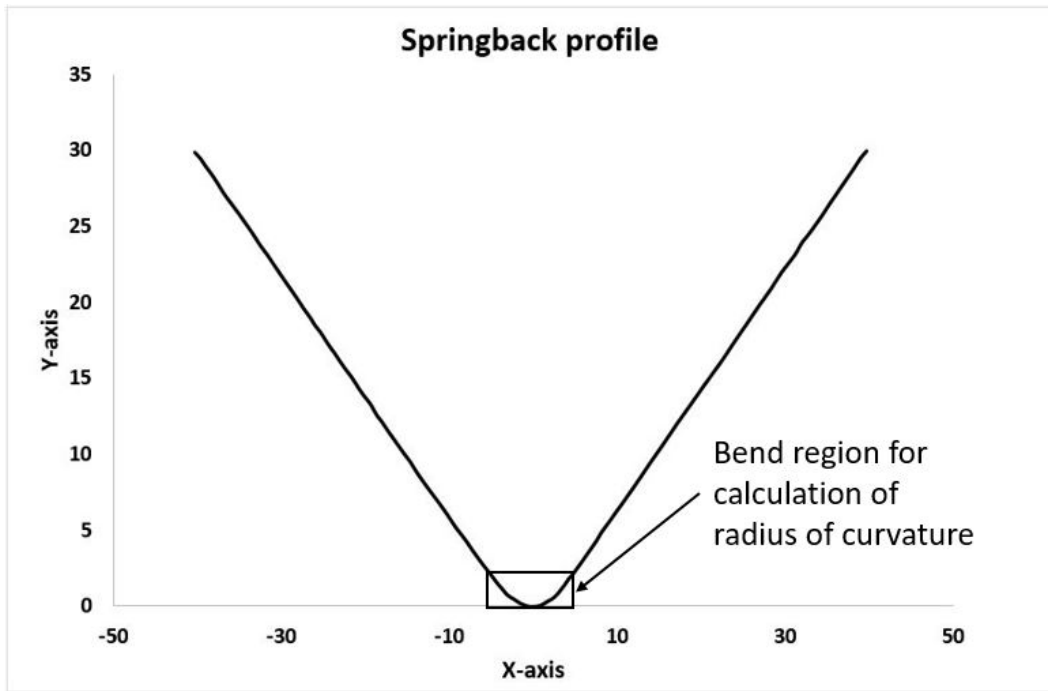


Figure 4.3: Deformation zone in bending region was selected to compare radius of curvature as springback

For measurement of radius of curvature before and after unloading, complete process was recorded by using Digital camera and images were taken out from that video at exactly after finishing of deformation process and after unloading process to trace bend profile before and after unloading. These traced points were used to fit a  $2^{nd}$  order polynomial and minimum radius of curvature was calculated from these fitted plots. The image tracing was done by using Matlab script for better accuracy.

## 4.2 Electric Assisted Bending Experiments for HSQ Steel

Bending experiments were carried out for HSQ steel under the effect of DC pulsed current. Springback was measured for this materials and then the effect of pulsed current was studied. Main focus of the study was to see, with the application of pulsed electric current whether any reduction in springback is happening or not. To see the effect of current on springback, final bend profile (i.e. sheet shape after springback) was compared for with and without current.

### 4.2.1 Experimental Setup and Procedure

Assembly of each bend fixture on CNC machine is a very crucial step, as fixture contains a large number of parts hence while assembling every aspect like insulation, proper alignment needs to be verified before starting the experiments.

Load Cell is being used to record force data by using NI (National Instruments) DAQ (Data Acquisition) system with LabView.

Electric connections are also very important factor for experiments. For electric connections, high-temperature insulation wire was used to prevent burning of wire. After connecting wires to punch and support tool electric parameters like current, frequency and duty cycle were need to be set. For setting these parameters circuit was closed by touching both top and bottom tool to each other. This process has to be repeated every time when there is any change in electric parameter settings.

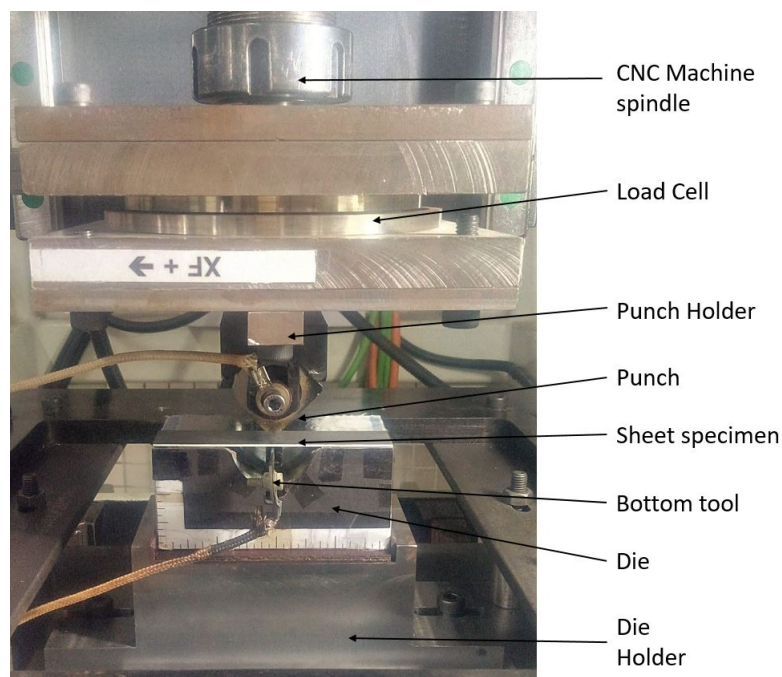


Figure 4.4: Experimental setup

### 4.3 Process Parameters

- Current - Electric Current is major process parameter according to literature as the flow of electrons assist in dislocation motion during deformation. Electricity was passed between two tools provided at top and bottom surface of the sheet refer Fig. 4.5. Bottom tool was designed in such a way that it touches sheet

bottom surface when sheet is placed on die, hence whenever deformation starts punch travels towards sheets and makes contact with sheet. At that instant electric circuit completes and flow of electricity starts. The bottom tool was mounted on spring force to ensure contact for each instant of time.

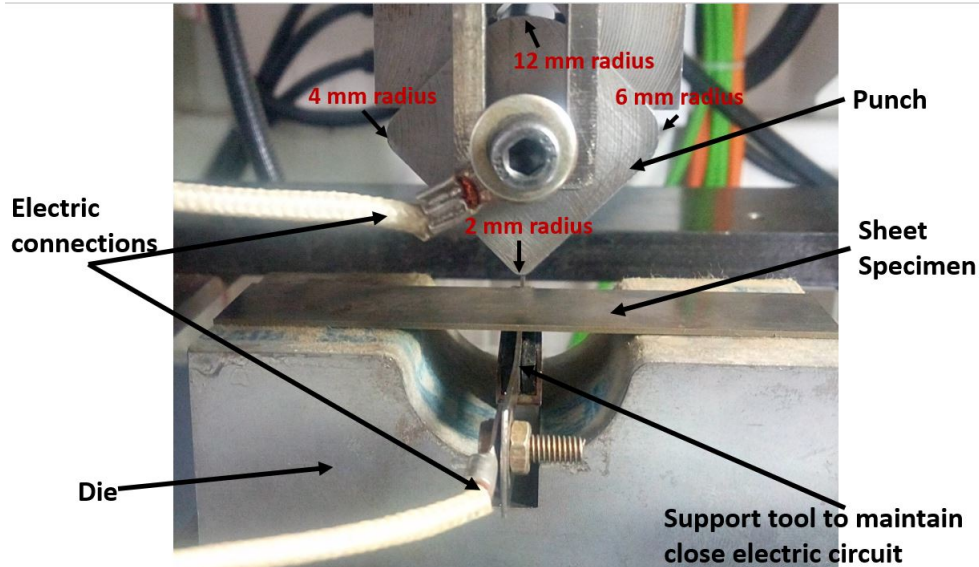


Figure 4.5: Close-up view of electric circuit completion between both tools and sheet

- Frequency - Pulsed current frequency is considered as an important factor in electroplastic effect. As frequency effect was observed in literature [2] that with increase in current frequency reduction in flow stresses increases as well as thermal effect due to resistive heating decreases.
- Duty Cycle - Duty cycle is defined as the percentage on-time of one pulse in one complete cycle, in other words, it shows that how much percentage of time electric pulse was on. Its effect can be related to resistive heating as with increase in duty cycle thermal heating increases.
- Tool radius - Tool radius is also an important factor as it makes difference in contact area, which in turn changes current density values. As tool radius decrease contact area in bend region decreases hence current density, for this particular process is defined as the ratio of current to contact area, increases. Hence electroplasticity effect increases and vice-versa.
- Feed rate - Feed rate given to punch decides time of deformation process, hence as feed rate increases deformation time decreases which results in less interaction between flowing electrons and moving dislocations. Hence slower the feed rate

more the electroplastic effect, but at the same time, it increases resistive heating effect also.

- Dwell time - After completing the deformation process punch was held stationary at that point for some period of time. As no deformation happens during this period of time and unloading starts after some delay, which creates internal stress relaxations which result in springback reduction.

For electroplastic bending experiments, all process parameters (current, frequency, duty cycle, tool radius, feed and dwell time) are considered to see their effect on springback. All factors with two levels are selected and experiments are conducted. For springback calculation change in radius of curvature in deformation zone was considered as a response parameter.

Sheet specimen of size 100 mm in length 20 mm in width and 1.02 mm thickness were selected to perform the experiments. Temperature measurement was done using Pyrometer and the maximum temperature reached during experiments was noted down. It was observed that maximum temperature reached approximately  $2800^{\circ}$ , hence thermal effect was neglected. The current density of 6.75 and 9.75 A/mm<sup>2</sup> are calculated for selected current values.

Table 4.1: Process parameters used for HSQ steel experiments

Factors	Levels	
Current (A)	135	195
Frequency (Hz)	100	170
Duty Cycle (%)	5	10
Tool radius (mm)	2	6
Feed (mm/min)	20	60
Dwell time (s)	0	60

By using a full factorial design of experiments total 64 number of experiments are conducted. To see the effect of these parameters on the radius of curvature, each experiment are recorded using high definition camera. Also at the same time, edge of the sheet specimens were colored by white and all other parts in experiment setup were marked as black see refer Fig. 4.6. From each recorded video snapshots at end of deformation and after springback are captured. To calculate the radius of curvature data for each experiment Matlab script was used.

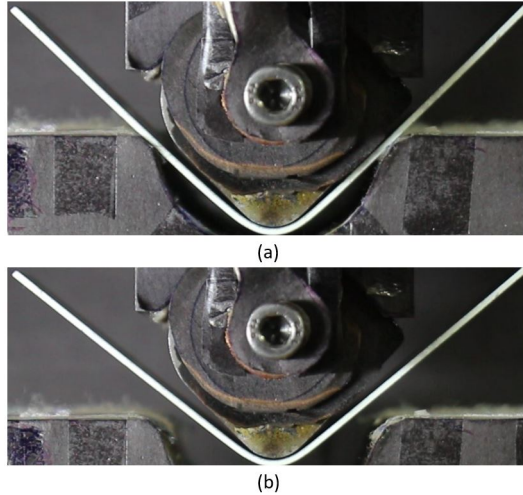


Figure 4.6: Image was taken from recorded video (a) after deformation and (b) after springback

## 4.4 Results and Discussion

### 4.4.1 Process parameters effect on springback

Effect of current density is clearly visible from main effect plots. As electric current is increasing difference in radius of curvature is also decreasing, which shows that springback is decreasing. Similar effect was observed with frequency also which shows decrease in radius of curvature difference hence springback. Duty cycle effect is not visible in present study of springback, which is expected as the temperature increase due to duty cycle was not significant (maximum temperature reached  $280^{\circ}\text{C}$  only). Also it was observed that with increase in frequency temperature rise decreases.

As discussed in section 3.5.1 there was very less effect of tool radius on springback, but for electroplastic bending this effect got increased because of change in current density due to change in contact area. It was observed that with increase in tool radius springback increases (contact area increases hence current density decreases).

It was observed that with increase in feed springback increases slightly. The slight increase in springback due to increase in feed suggests that with increase in feed rate the time during which current is on reduced hence increase in springback. As with feed rate  $20\text{ mm/min}$  time for deformation is  $45\text{ s}$ , whereas with feed rate  $60\text{ mm/min}$  it takes  $15\text{ s}$  to complete deformation.

Dwell time shows no effect on springback. As dwell time increases springback remains same, hence it can be concluded that during dwell time stress relaxation is not significant enough to create any changes in springback. As during dwell time current

flow is off, hence this parameter is showing no influence of current on springback.

Analysis of variance was performed and results are given in following Fig. 4.7 and Fig. 4.8.

### Analysis of Variance

Source	DF	Adj SS	Adj MS	F-Value	P-Value
Model	21	0.076941	0.003664	1.58	0.103
Linear	6	0.030696	0.005116	2.2	0.062
Current (A)	1	0.009072	0.009072	3.91	0.055
Frequency (Hz)	1	0.012366	0.012366	5.32	0.026
Duty Cycle (%)	1	0.000988	0.000988	0.43	0.518
Tool Radius (mm)	1	0.007369	0.007369	3.17	0.082
Feed (mm/min)	1	0.000611	0.000611	0.26	0.611
Dwell (s)	1	0.000289	0.000289	0.12	0.726
2-Way Interactions	15	0.046246	0.003083	1.33	0.229
Current*Frequency	1	0.002095	0.002095	0.9	0.348
Current*Duty Cycle	1	0.000049	0.000049	0.02	0.885
Current*Tool Radius	1	0.00923	0.00923	3.97	0.053
Current*Feed	1	0.006453	0.006453	2.78	0.103
Current*Dwell	1	0.002018	0.002018	0.87	0.357
Frequency*Duty Cycle	1	0.001699	0.001699	0.73	0.397
Frequency*Tool Radius	1	0.000127	0.000127	0.05	0.816
Frequency*Feed	1	0.000335	0.000335	0.14	0.706
Frequency*Dwell	1	0.000489	0.000489	0.21	0.649
Duty Cycle*Tool Radius	1	0.000017	0.000017	0.01	0.932
Duty Cycle*Feed	1	0.00054	0.00054	0.23	0.632
Duty Cycle*Dwell	1	0.000689	0.000689	0.3	0.589
Tool Radius*Feed	1	0.000343	0.000343	0.15	0.703
Tool Radius*Dwell	1	0.020751	0.020751	8.94	0.005
Feed*Dwell	1	0.00141	0.00141	0.61	0.44
Error	42	0.097538	0.002322		
Total	63	0.174479			

Figure 4.7: Results of analysis of variance

### Model Summary

S	R-sq	R-sq(adj)	R-sq(pred)
0.0481906	0.441	0.1615	0

Figure 4.8: Model summary of Anova analysis

Interaction effects also provide useful information related to each parameter refer below figures.



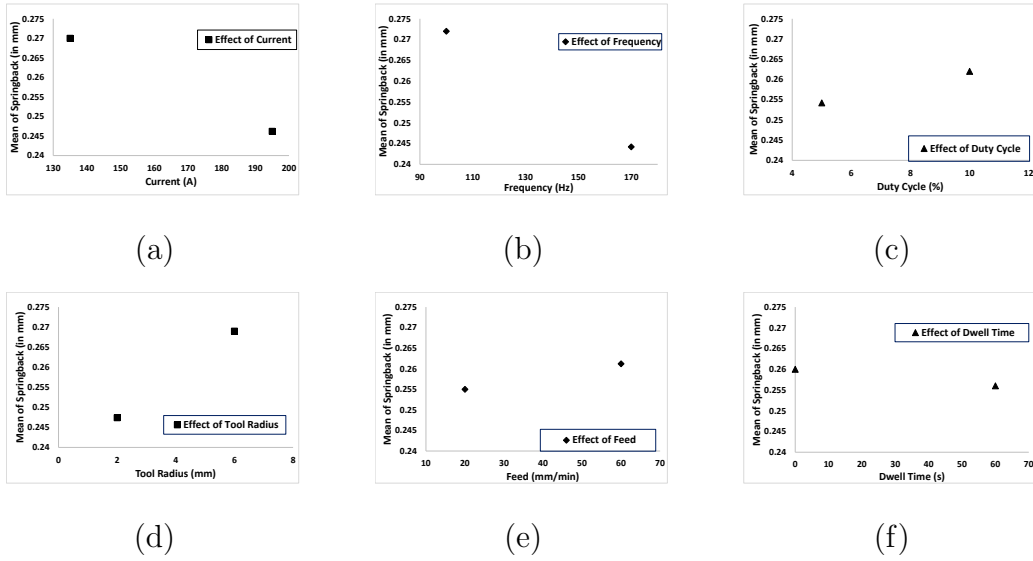


Figure 4.9: Main effect plots of various process parameters on springback

Interaction between current and other parameters show that the effect of electric current always increases with increase in current. It is observed that current and parameters like duty cycle and dwell time are not having any interaction effect. Whereas for interaction between current, tool radius it is observed that with increase in current effect got increased and springback was less at minimum tool radius and maximum current. Also interaction between current and feed it is observed that the effect is maximum when current is maximum and feed is minimum refer Fig. 4.10.

Interaction effects between frequency and other parameters are also observed and it was concluded that frequency not showing any interaction effect with other parameters except current. It was observed that at maximum frequency and maximum current springback was lower refer Fig. 4.11.

Interaction between duty cycle and tool radius and feed and dwell time is plotted and it was concluded that there is no effect on springback of duty cycle and other parameters refer Fig. 4.12.

Interaction between tool radius and feed rate and dwell time are also observed and concluded that these parameters are effective if current is not one of the active parameter refer Fig. 4.13.

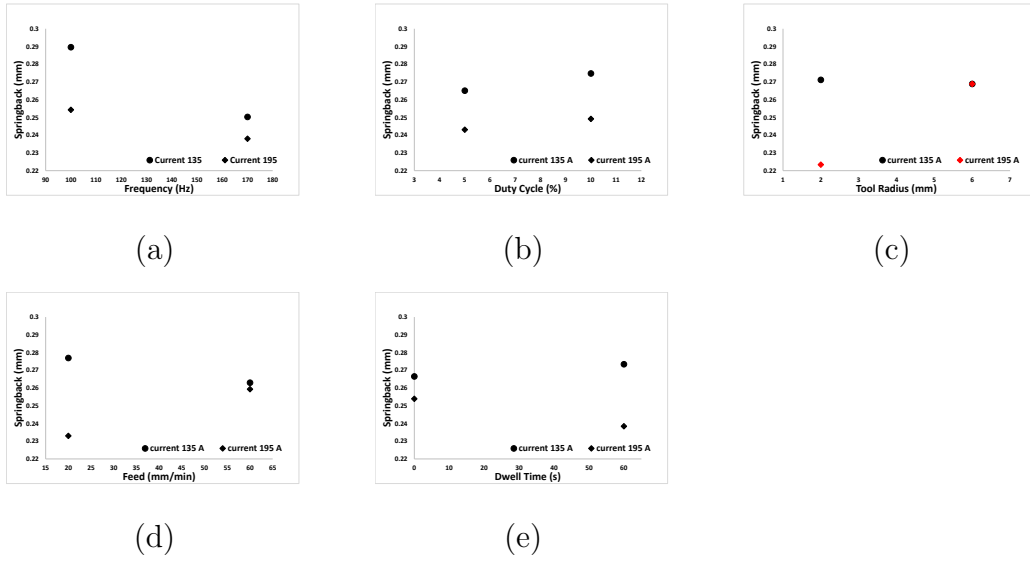


Figure 4.10: Interaction plots for current and other parameters

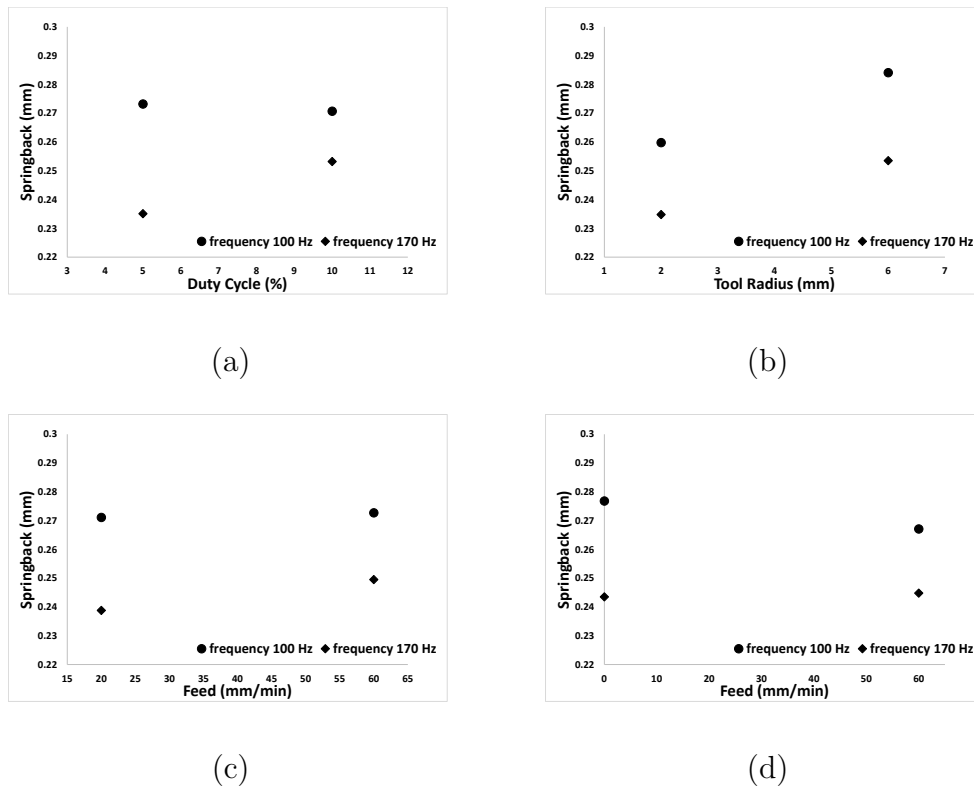


Figure 4.11: Interaction plots for Frequency and other parameters

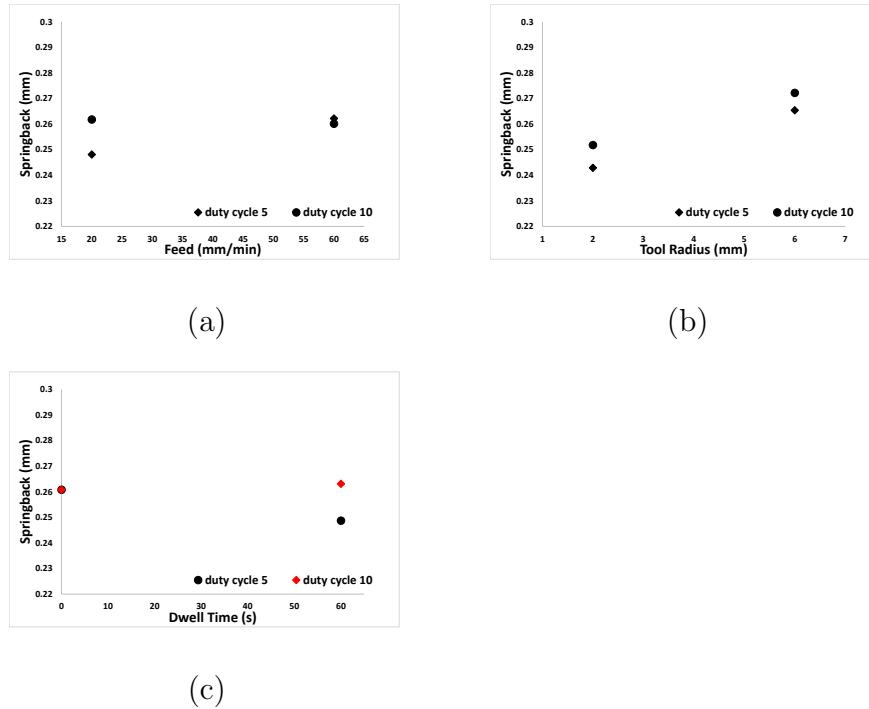


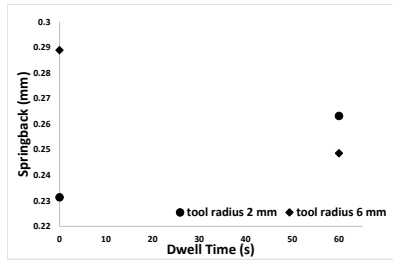
Figure 4.12: Interaction plots for duty cycle and other parameters

#### 4.4.2 Effect of parameters on bend profile

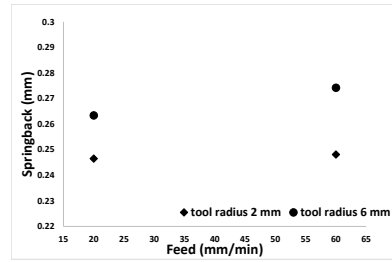
Bend profiles were also compared to see the effect of process parameters. As it was observed that electrical parameters are not having any effect on bend angles but at region where tool and sheet make contact, were showing different behavior with different electrical parameters.

#### Current effect

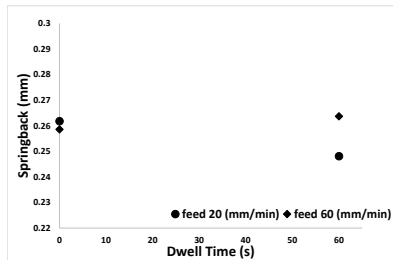
Effect of current on bend profiles are observed by comparing bend profiles for experiments with and without current refer Fig. 4.14. It is observed that with increase in tool radius springback is decreasing. Also bend profiles are not same even after deformation due to application of electric current. The difference in bend profiles before unloading indicates that application of electric current, reduces flow stress which in turn changes the material flow.



(a)



(b)

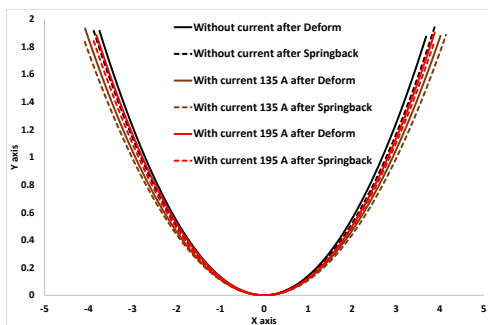


(c)

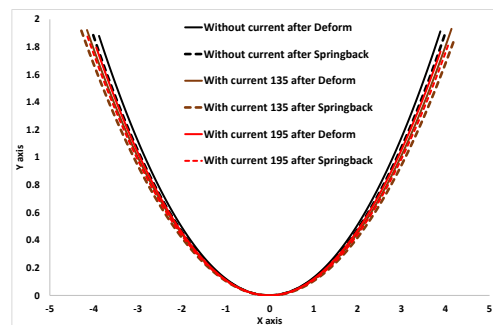
Figure 4.13: Interaction plots for remaining parameters

### Frequency Effect

Effect of frequency on bend profile indicates that with increase in frequency springback decreases. This effect is only visible for tool radius 2 mm, not for 6 mm tool radius.

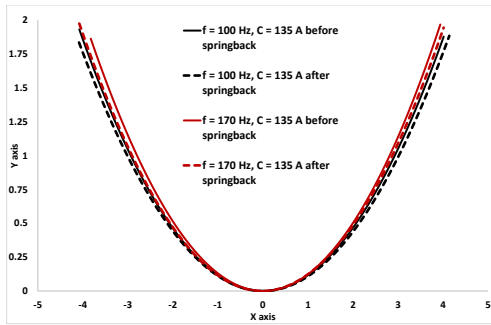


(a)

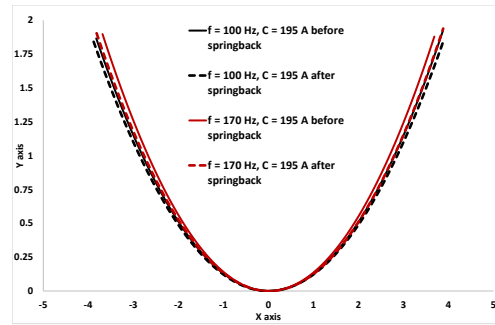


(b)

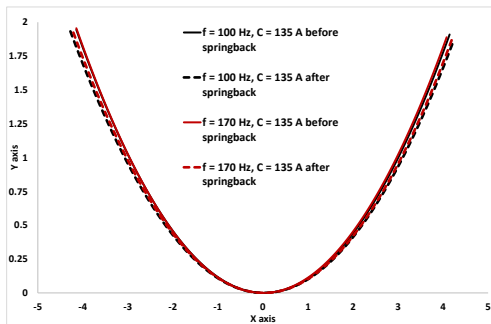
Figure 4.14: Variation in bend profiles in Deformation zone with and without electric current and other parameters same (Freq. = 100 Hz, Duty cycle = 5%, Feed = 20 mm/min and Dwell = 0 s), (a) Tool radius 2 mm and (b) Tool radius 6 mm.



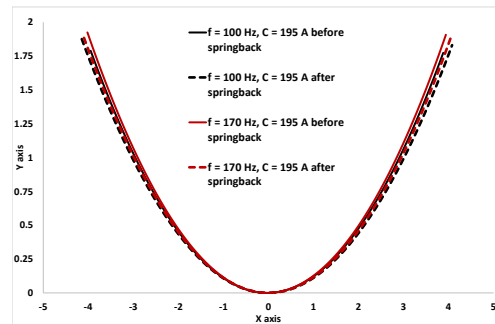
(a)



(b)



(c)



(d)

Figure 4.15: Effect of frequency on springback at (duty cycle 5%, Feed 20mm/min, and dwell 0 s) (a) Tool radius 2 and Current 135 A, (b) Tool radius 2 and Current 195 A, (c) Tool radius 6 and Current 135 A and (d) Tool radius 6 and Current 195 A

### Duty cycle effect

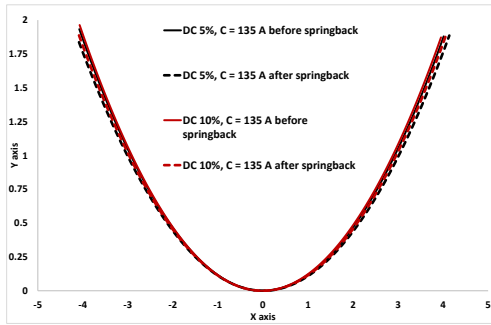
There is no duty cycle effect is observed on bend profiles as both before and after springback profiles are exactly matching refer Fig 4.16.

### Feed effect

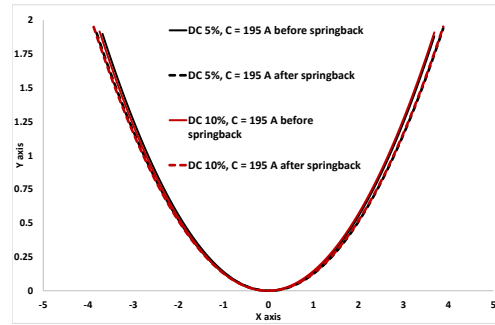
Bend profiles for different feed values are plotted and is observed that profiles are not showing any significant effect on springback refer Fig. 4.17.

### Dwell time effect

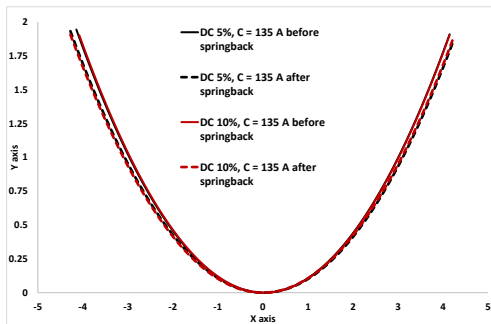
Bend profiles for dwell time effect indicates that the dwell time is not having any significant effect on springback refer Fig. 4.18.



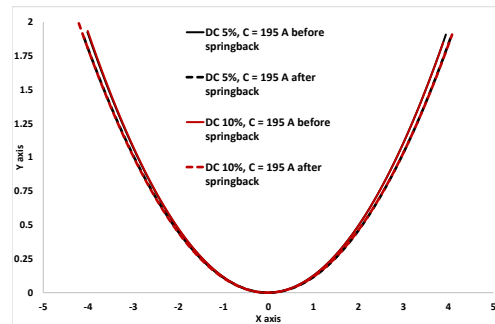
(a) Frequency = 100 Hz.



(b) Frequency = 170 Hz.

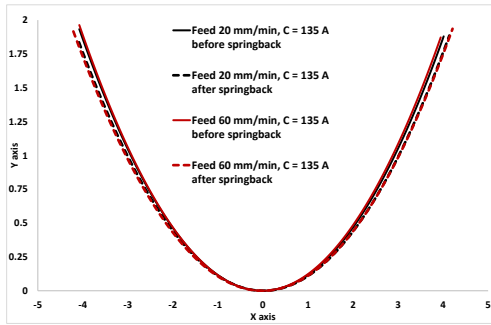


(c) Frequency = 100 Hz.

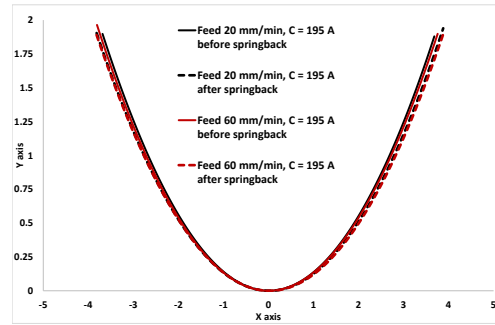


(d) Frequency = 170 Hz.

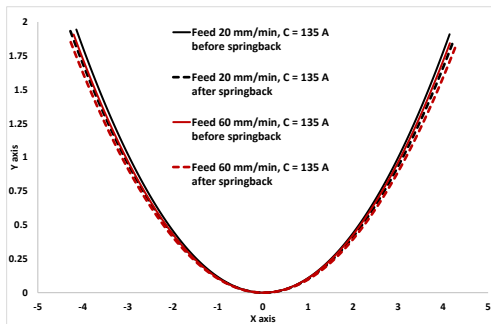
Figure 4.16: Effect of duty cycle on springback at (Feed 20mm/min, and dwell 0 s)  
 (a) Tool radius 2 and Current 135 A, (b) Tool radius 2 and Current 195 A, (c) Tool radius 6 and Current 135 A and (d) Tool radius 6 and Current 195 A.



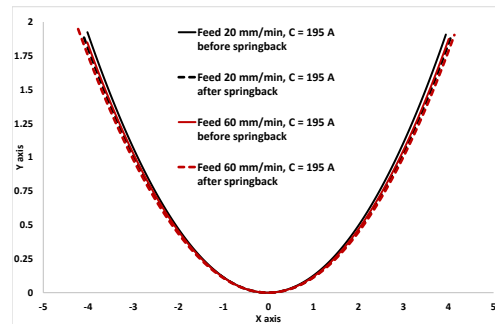
(a) Frequency = 100 Hz.



(b) Frequency = 170 Hz.

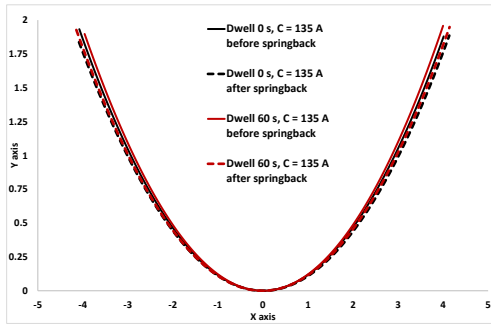


(c) Frequency = 100 Hz.

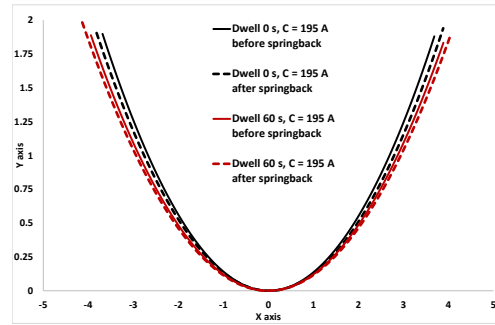


(d) Frequency = 170 Hz.

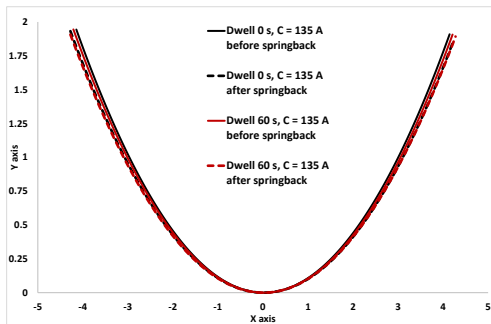
Figure 4.17: Effect of feed on springback at (duty cycle 5%, and dwell 0 s) (a) Tool radius 2 and Current 135 A, (b) Tool radius 2 and Current 195 A, (c) Tool radius 6 and Current 135 A and (d) Tool radius 6 and Current 195 A.



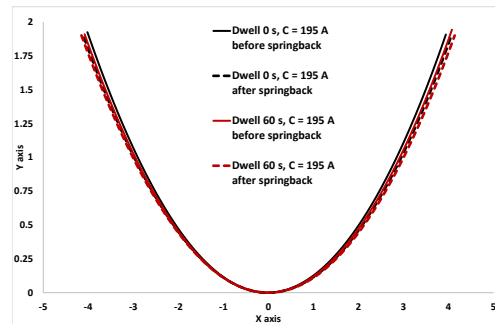
(a) Frequency = 100 Hz.



(b) Frequency = 170 Hz.



(c) Frequency = 100 Hz.



(d) Frequency = 170 Hz.

Figure 4.18: Effect of dwell on springback at (duty cycle 5% and Feed 20mm/min) (a) Tool radius 2 and Current 135 A, (b) Tool radius 2 and Current 195 A, (c) Tool radius 6 and Current 135 A and (d) Tool radius 6 and Current 195 A.



# Chapter 5

## Conclusions and Scope for Future Work

With the application of electric current pulses to the sheet metal bending process of HSQ steel, the bending forces and springback reduces. The parameters, having significant effect on springback are current, frequency and tool radius. Whereas duty cycle, feed and dwell time are not showing any significant effect on springback. The temperature increase (less than 200°C) during electrical assisted bending process indicates that thermal resistive heating effect is not high enough to make any changes in crystal structure.

### 5.1 Scope for Future Work

- Determination of springback effect at a higher rating of current density values.
- Simulate the process of electroplasticity using FEA packages.
- Study the effect of current flow through the material at microstructure level.
- Development of a model to predict springback at different process parameters.

# Appendices

# Appendix A

## Investigation of Electroplastic Effect in Bending for Various Materials

Different materials like stainless steel, spring-steel, and titanium were selected to see the effect of electric current. In following sections effect of electroplasticity on these materials are studied.

### Commercially Available Stainless Steel Scale

Initial trials were carried out to see the effects of electric current on stainless steel. Experiments were conducted with tool radius 2 mm and feed rate 60 mm/min. These experiments were carried out with dwell time 60 s. During this dwell time, current flow was kept on, to increase the pulsed current effect on springback. It was observed also that with dwell time springback decreases by  $4.45^\circ$  refer Fig. A.1.

Experiments were conducted with and without current for both dwell period of 60 s. Electric current was set at 195 A and frequency at 170 Hz. To see the effect of resistive heating temperature was measured by using pyrometer. The maximum temperature reached during deformation was only  $170^\circ$  C, which is too low for recrystallization to happen in steels. Hence it can be considered during these experiments any heat treatment is not happening.

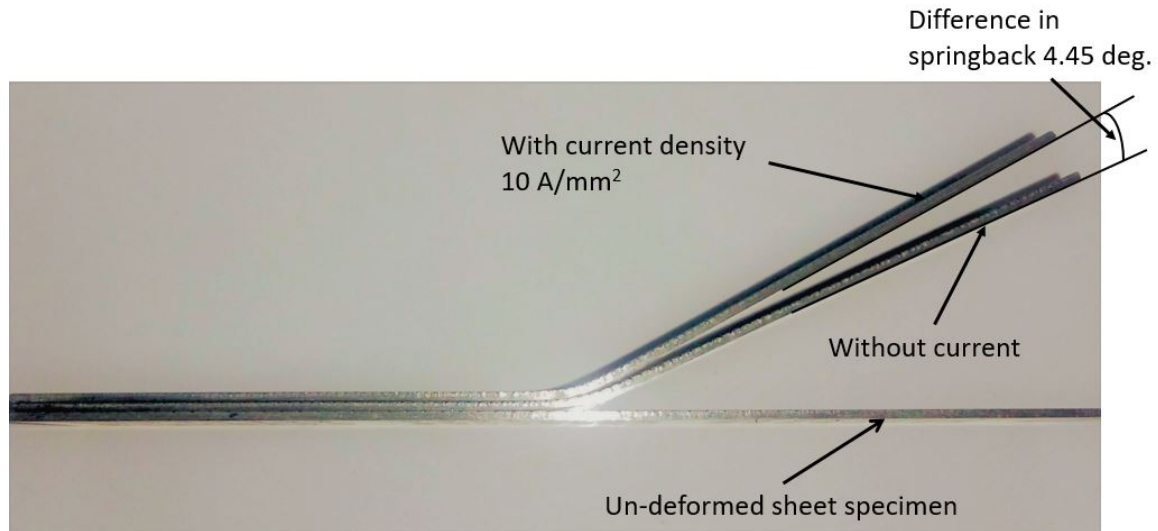


Figure A.1: Electroplasticity effect on commercially available stainless steel scale

## High Strength Spring Steel

As with increase in yield strength springback also increases. Hence higher strength than stainless steel was selected to see the electroplastic effect in V bending process. For spring steel thickness of 1.2 mm and width of 10 mm selected for experiments to increase the current density by decreasing contact area.

Four factors such as electric current, tool radius, feed and dwell time were considered to see the electroplastic effect for this material. To see the repetition each experiment was repeated twice and if both results were not matching the third experiment was also conducted.

Table A.1: Process parameters used for spring steel experiments

Factors	Levels	
Current (A)	100	300
Tool radius (mm)	2	6
Feed (mm/min)	20	60
Dwell time (s)	20	60

## Results

Springback was measured for each specimen and the results were analyzed using Minitab (statistical software). DOE helped to see the individual effect of each pa-

parameter on springback. Also, the interaction of parameters was observed to have significant effect on springback.

### Significant terms

Normal plot obtained after analyzing results in Minitab shows which factor is significant and which one is not refer Fig. A.2.

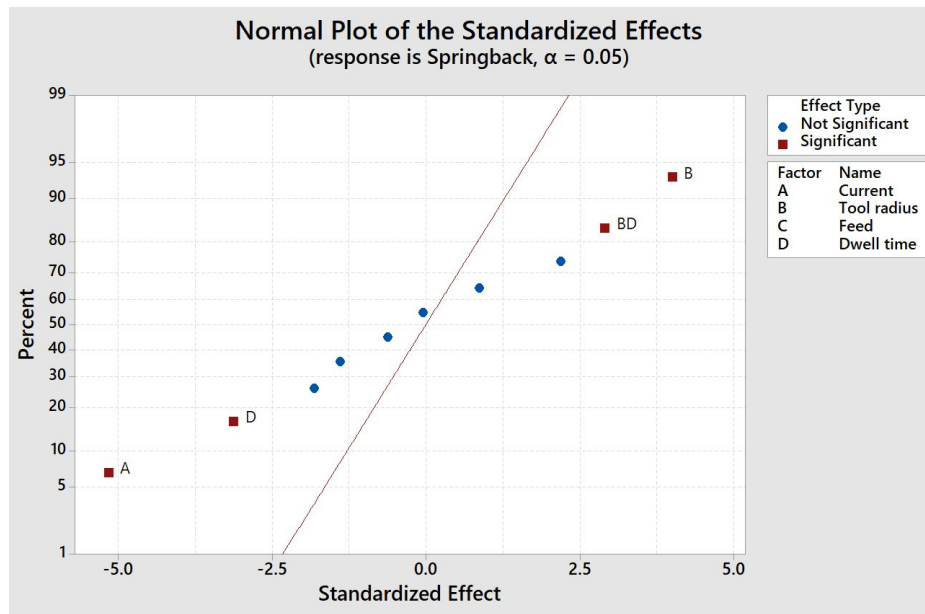


Figure A.2: Normal plot

It was observed that all parameters except feed rate have significant effect on springback. The interaction between tool radius and dwell time is also significant. Results show that effect of current on springback is more than all other parameters.

### Main effect against mean of Springback

The main effect plots are important to study the effect of process parameters on springback. The main effect for each parameter are shown in Fig. A.3.

- Current effect - Effect of current is clearly observed in main effect plots. It can be concluded that springback decreases with increase in current as main plot is showing negative slope for current graph.
- Tool radius effect - With increase in tool radius, the contact area between tool and sheet specimen increase. Because of increase in contact area current density decrease hence effect of current on springback decreases. Increase in

tool radius shows exactly same behavior as expected. Springback got increased with increase in tool radius.

- Feed effect - There was slight variation in springback with increase in feed, which suggest that feed effect was not present on springback.
- Dwell time - Springback decreases with increase in dwell time. Decrease in springback suggest stress relaxation during this period of time.

### Interaction effects between the parameters

Interaction effects between the parameters are shown in Fig. A.4.

It was observed that with the increase in current and dwell time, springback decreases. But for tool radius, the effect is opposite as with the increase in tool radius springback increases. It was observed that feed is not affecting significantly to springback. The interaction between all parameters except feed and dwell time are

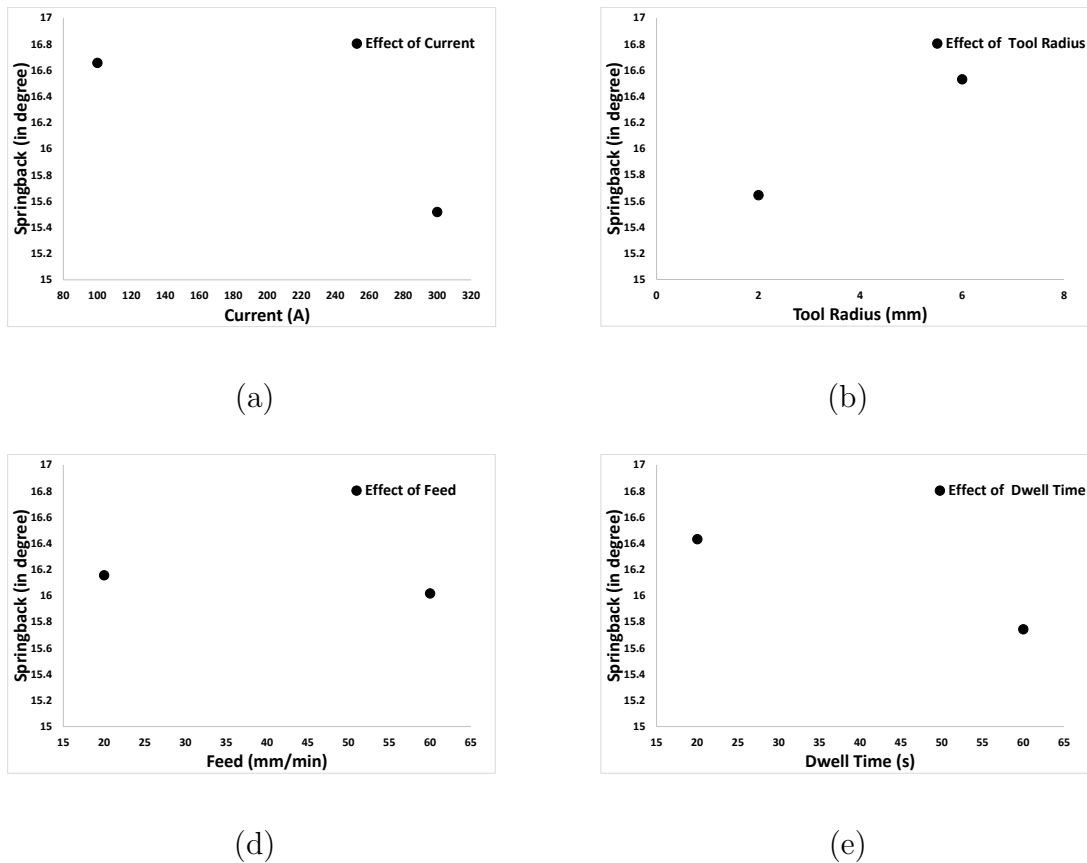


Figure A.3: Main effects of process parameters on springback

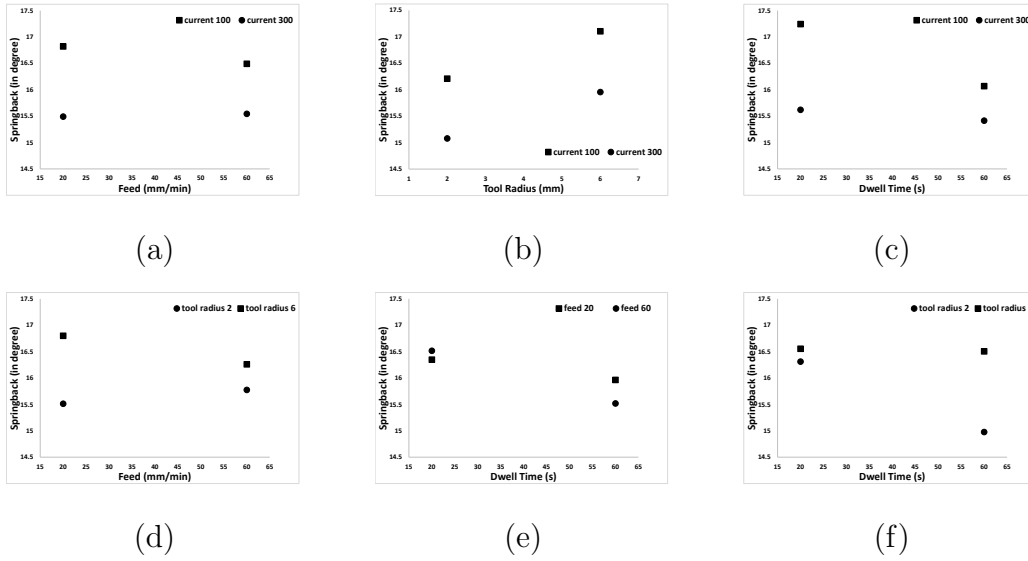


Figure A.4: Interaction effects on springback between parameters

showing a significant effect on springback. For feed and dwell time interaction plots are showing approximately horizontal lines which suggest that interaction between these parameters are not significant.

## EDD (Extra Deep Drawing) and IF (Interstitial Free) Steel

Experiments were conducted on EDD (Extra Deep Drawing) and IF (Interstitial free) steel to see the effect of electric current. It was observed that these steels do not show any effect of electric current on springback, but there was reduction in flow stress was observed.

Experiments shows that with application of electric current force decrease approximately by 10% for each material refer Fig. A.5.

Figure A.6 shows there is no significant effect of electric current on springback. As current density used for these experiments was only  $10.75 \text{ A/mm}^2$  which shows no effect on springback, hence it can be concluded that the current density level is not reaching the threshold value to show any interaction effect between electrons and moving dislocations for these materials.

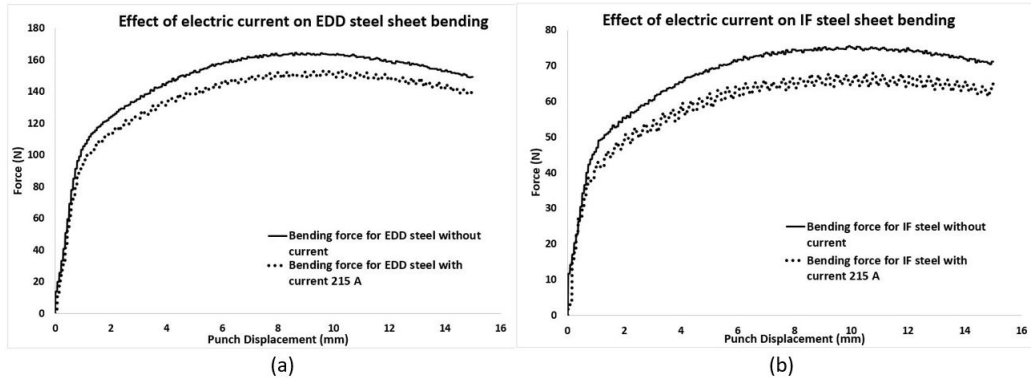


Figure A.5: Effect of electric current on bending force for (a) EDD Steel and (b) IF Steel

## Ti-6Al-4V alloy

Materials with higher strength shows greater springback and also they requires high mechanical energy input for deformation. Titanium alloys belong to same high strength material category also their strength to weight ratio is greater than other ferrous alloys.

Experiments with and without electric current were conducted for Ti-6Al-4V alloy and was observed that this material is very sensitive to electric pulsed current. Reduction in springback and force reduction was observed for this material. Experiments were performed for two different current value at 150 A and 300 A also experiment without current was performed to compare the reduction in springback. Because of higher electrical resistivity, slight increase in temperature was recorded and maximum temperature reached during process was noted. Maximum temperature read by pyrometer was  $200^{\circ}\text{C}$ . This temperature level is also very low compared to its melting point (approx.  $1600^{\circ}\text{C}$ ). Hence in this process also Joule heating effect was neglected.



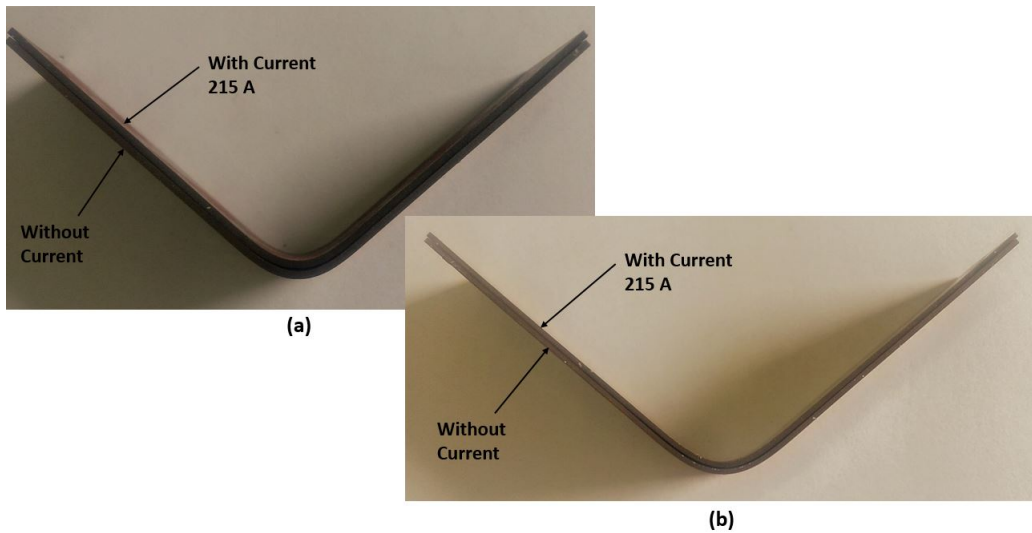


Figure A.6: Effect of current on springback (a) EDD Steel and (b) IF Steel

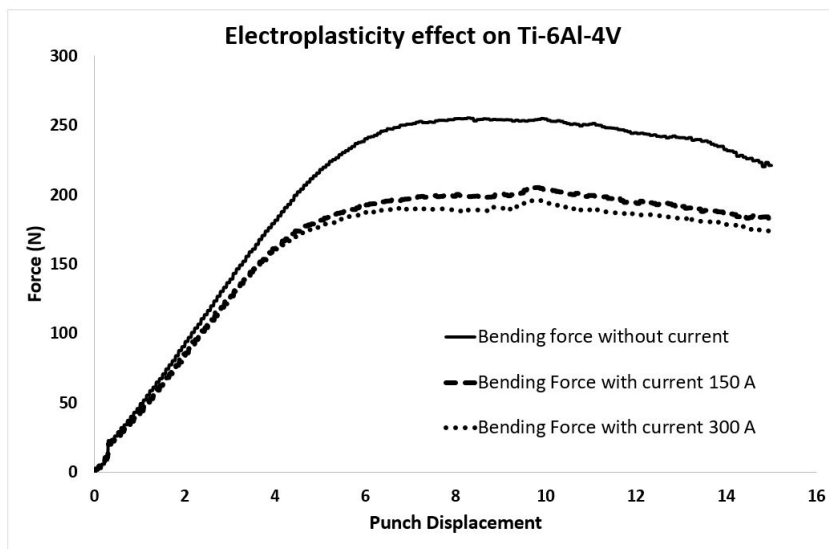


Figure A.7: Effect of electric current on bending force for Ti-6Al-4V

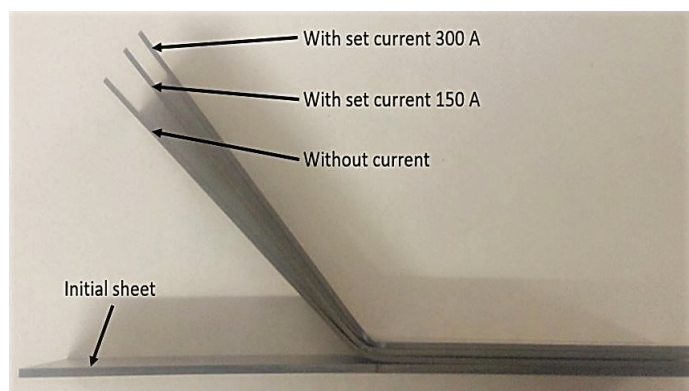


Figure A.8: Effect of current on springback for Ti-6Al-4V

# References

- [1] O. Troitskii. Electromechanical effect in metals. *ZhETF Pisma Redaktsiiu* 10, (1969) 18.
- [2] O. Troitskii. Electroplastic deformation of metal. *Strength of Materials* 8, (1976) 1466–1471.
- [3] K. Okazaki, M. Kagawa, and H. Conrad. A study of the electroplastic effect in metals. *Scripta Metallurgica* 12, (1978) 1063–1068.
- [4] V. Stashenko, O. Troitskii, and V. Spitsyn. Action of current pulses on zinc single crystals during creep. *physica status solidi (a)* 79, (1983) 549–557.
- [5] O. Troitskii. The electroplastic effect in metals. *Strength of Materials* 16, (1984) 277–281.
- [6] H. Conrad. Electroplasticity in metals and ceramics. *Materials Science and Engineering: A* 287, (2000) 276–287.
- [7] G. Tang, J. Zhang, Y. Yan, H. Zhou, and W. Fang. The engineering application of the electroplastic effect in the cold-drawing of stainless steel wire. *Journal of Materials Processing Technology* 137, (2003) 96–99.
- [8] Y. Zhou, S. Xiao, and J. Guo. Recrystallized microstructure in cold worked brass produced by electropulsing treatment. *Materials Letters* 58, (2004) 1948–1951.
- [9] T. A. Perkins, T. J. Kronenberger, and J. T. Roth. Metallic forging using electrical flow as an alternative to warm/hot working. *Journal of manufacturing science and engineering* 129, (2007) 84–94.
- [10] G. Fan, L. Gao, G. Hussain, and Z. Wu. Electric hot incremental forming: a novel technique. *International Journal of Machine Tools and Manufacture* 48, (2008) 1688–1692.

- [11] C. D. Ross, T. J. Kronenberger, and J. T. Roth. Effect of dc on the Formability of Ti-6Al-4V. *Journal of engineering materials and technology* 131, (2009) 031,004.
- [12] J. J. Jones and L. Mears. A process comparison of simple stretch forming using both conventional and electrically-assisted forming techniques. In Proc. of ASME International Manufacturing Science and Engineering Conference. 2010 623–631.
- [13] W. A. Salandro, C. Bunget, and L. Mears. Modeling and quantification of the electroplastic effect when bending stainless steel sheet metal. In 2010 ASME International Manufacturing Science and Engineering Conference, Erie, PA, Paper No. MSEC2010-34043. 2010 581–590.
- [14] J. J. Jones and L. Mears. Constant Current Density Compression Behavior of 304 Stainless Steel and Ti-6Al-4V During Electrically-Assisted Forming. In ASME Conference Proceedings, volume 44304. 2011 629–637.
- [15] J. Asghar and N. Reddy. Importance of tool configuration in incremental sheet metal forming of difficult to form materials using electro-plasticity .
- [16] T. Meinders, A. Konter, S. Meijers, E. Atzema, and H. Kappert. A sensitivity analysis on the springback behavior of the unconstrained bending problem. *International Journal of Forming Processes* 9, (2006) 365–402.
- [17] F. Micari, A. Forcellese, L. Fratini, F. Gabrielli, and N. Alberti. Springback evaluation in fully 3-D sheet metal forming processes. *CIRP Annals-Manufacturing Technology* 46, (1997) 167–170.
- [18] V. Vorkov, R. Aereens, D. Vandepitte, and J. R. Dufflou. Springback prediction of high-strength steels in large radius air bending using finite element modeling approach. *Procedia Engineering* 81, (2014) 1005–1010.
- [19] S. Jiang. Springback investigations. Ph.D. thesis, The Ohio State University 1997.